UNIVERSITY OF PADOVA

DEPARTMENT OF MEDICINE – DIMED

In collaboration with **Medical University Gdansk**

PhD Program: ARTERIAL HYPERTENSION AND VASCULAR BIOLOGY

(XXVII CYCLE)

GLYCOGEN SYNTHASE KINASE-3 (GSK-3) IN THE PATHOGENESIS OF PULMONARY FIBROSIS: WHAT WE KNOW FROM THE MOUSE MODEL

Coordinator: Ch.mo Prof. Gian Paolo ROSSI, MD

Supervisore: Ch.mo Prof. Carlo AGOSTINI, MD

PhD Student : Francesco CINETTO, MD

ACADEMIC YEAR 2013/2014

INDEX

ABBREVIATIONS

AMs	Alveolar Macrophages
APC	*Adenomatous polyposis coli* protein
APC	Antigen Presenting Cell
BLM	Bleomycin
CBP	CREB Binding Protein
CI	Confidence Interval
CK2	Casein Kinase 2
CCR	Chemokine Receptor
COPD	Chronic Obstructive Pulmonary Disease
CTGF	Connective Tissue Growth Factor
CXCL	CXC chemokine
CXCR	Chemokine CXC Receptor
CXR	Chest X Radiograph
DLCO	Diffusing capacity of the Lung for Carbon Monoxide
ECM	Extracellular Matrix
EMT	Epithelial–Mesenchymal Transition
FGF-2	Fibroblast Growth Factor 2
FRAT/GBP	Frequently Rearranged in advanced T-cell lymphomas/GSK-3 binding protein
FVC	Forced Vital Capacity
FXA	Activated Factor X
GSK-3	Glycogen Synthase Kinase 3
HP-NAP	Neutrophil-activating protein of *Helicobacter pylori*

HRCT	High Resolution Chest Radiography
IFN-γ	Interferon γ
i.p.	Intraperitoneally
i.v.	Intravenously
IIPs	Idiopathic Interstitial Pneumonias
ILDs	Interstitial Lung Diseases
IPF	Idiopathic Pulmonary Fibrosis
MAPK	Mitogen-Activated Protein kinase
MMPs	Matrix Metallo Proteinases
LPS	bacterial Lipopolysaccharides
PAH	Pulmonary Arterial Hypertension
PAI-1, PAI-2	Plasminogen Activator
PH	Pulmonary hypertension
P(I)3K/Akt	Phosphatidylinositol 3-Kinase
PGE_2	Prostaglandin E2
PDGF	Platelet-Derived Growth Factor
PKA	Protein Kinase A
PKC	Protein Kinase C
STAT	Signal Transducer and Activator of Transcription protein
TGF- β	Transforming Growth Factor- β
TLRs	Toll like receptors
TDZD	Thiadiazolidinones
TIMPs	Tissue Inhibitors of Metallo Proteinases;
TNF-α	Tumor Necrosis Factor-α
VEGF	Vascular Endothelial Growth Factor

ABSTRACT

***Introduction**:* Idiopathic pulmonary fibrosis (IPF) is a fatal disease characterized by an aberrant interstitial deposition of collagen in the lung parenchyma, leading to progressive lung function impairment. Repeated injuries to the alveolar epithelium are believed to lead to an imbalance of the extracellular matrix (ECM) turnover supported by metalloproteinases (MMPs) and their tissue inhibitors (TIMPs). The kinase GSK-3 is a mediator of the cytokine homeostasis and favors the production of pro-inflammatory mediators. Its specific inhibitor, SB216763, displayed anti-inflammatory and anti-fibrotic properties of in a mouse model of Bleomycine (BLM)-induced pulmonary fibrosis. Furthermore, GSK-3 seems to be involved in the epithelial to mesenchimal transition (EMT). The purpose of this study was to assess the expression of MMP9, TIMP1, MMP2 and and TIMP2 in the early inflammatory response and in the late fibrosis induced by BLM in a mouse model of pulmonary fibrosis. Next goal was to elucidate whether the *in vivo* treatment with SB216763 could modulate MMPs activity and their balance with TIMPs. Moreover, *in vitro* experiments were aimed to identify the signal pathways through which GSK-3 can modulate MMPs and TIMPs.

***Methods**:* Cohorts of C57BL6 mice (12 weeks old) were randomized to receive intratracheal instillation of either saline (PBS), or BLM alone, or BLM in association with SB216763. The inhibitor was administered intraperitoneally the day after BLM and every 48 hours up to the sacrifice on day 7 (inflammatory phase) or 28 (fibrotic phase), when bronchoalveolar lavage (BAL) was performed and lungs harvested. MMP9 and MMP2 activity was measured by gel zymography in BAL fluid (BALF). MMPs and TIMPs expression levels were evaluated by Real Time-PCR and Western Blotting. Their tissue localization was evaluated by IHC analysis. *In vitro* experiments were performed using A549 cells as epithelial model, assessing expression and activity of MMPs downstream of TNFα, with and without GSK-3 silencing by siRNA.

***Results**:* MMP9 and MMP2 levels were elevated in BALF from BLM-treated mice at day 7. At this time point, the inflammatory cells recruited in the intra-alveolar spaces were alveolar macrophages (AMs), lymphocytes and neutrophils. Furthermore, the lung IHC staining indicated a strong positivity for MMP9, MMP2, TIMP1 and TIMP2 in interstitial AM (iAM) and, specifically, in injured and cuboidalized epithelium. BLM-treated mice sacrificed at day 28 presented high levels of MMP2 and TIMP1 and low levels of MMP9 in the BALF. Interestingly, i*n vivo* GSK-3 inhibition reduced MMP9, MMP2 and TIMP1 levels in the BALF and their positivity in iAMs and in epithelium. Moreover, *in vitro* experiments performed with A549 cells, as epithelial model, demonstrated that GSK-3α and GSK-3β silencing increased MMP9 expression after stimulation with the pro-inflammatory cytokine TNFα. This effect was achieved by the interaction of GSK-3 with NF-kB and ERK signalling transduction pathway.

***Conclusions**:* Our mouse model of BLM-induced pulmonary fibrosis clearly showed an imbalance between MMPs and TIMPs during inflammation and fibrosis. Importantly, we proposed GSK-3 as a crucial mediator of their expression in AMs and in damaged epithelium. Next, i*n vitro* results with A549 cells suggested that GSK-3 silencing induce MMP-9 secretion, downstream of TNFα, in a p65-mediated and ERK1,2 dependent manner.

RIASSUNTO

Introduzione: La fibrosi polmonare idiopatica (IPF) è un'interstiziopatia caratterizzata da un decorso fatalmente progressivo, che conduce alla completa compromissione della funzione polmonare. Pur essendo la sua patogenesi non pienamente compresa, il primum movens sembra essere un danno epiteliale ripetuto che induce l'aberrante deposizione di matrice extracellulare (ECM), il cui turnover non viene più garantito da metalloproteasi (MMPs) e loro inibitori tissutali (TIMPs). La chinasi GSK-3 è nota per il suo ruolo cardine nella modulazione di citochine pro-infiammatorie ed in diverse vie del segnale e processi cellulari verosimilmente coinvolti nella patogenesi della IPF. La sua inibizione in vivo, in un modello murino di fibrosi polmonare indotta da bleomicina (BLM), si è dimostrata in grado di modulare sia la risposta infiammatoria precoce che la fase fibrotica tardiva. Il ruolo della chinasi nella modulazione dell'equilibrio fra MMPs e TIMPs nella fibrogenesi polmonare non è ad oggi chiarito.

Metodi: Diverse coorti di topi C57BL6 sono state sottoposte all'instillazione endotracheale di BLM o PBS e trattate o meno, per via intraperitoneale, con l'inibitore di GSK-3 SB216763. Per misurare attività, espressione proteica e genica delle MMPs sono stati utilizzati, rispettivamente, zimografia, WB analysis e RT-PCR del liquido di lavaggio bronco alveolare (BALF) di topi sacrificati a 7 o 28 giorni dalla somministrazione di BLM. L'espressione proteica e genica delle TIMPs è stata valutata con WB e RT-PCR. E' stata inoltre eseguita l'analisi istologica ed immunoistochimica dei polmoni, ai due intervalli di tempo. L'effetto in vitro del silenziamento di GSK-3 è stato infine studiato su una linea di cellule epiteliali alveolari umane (A549).

Risultati: Il trattamento con BLM ha dimostrato di aumentare la cellularità ed i livelli di MMP2 e MMP9 nel BALF al giorno +7. Si è inoltre registrato un significativo aumento dell'espressione di MMP2, MMP9, TIMP1 e TIMP2, all'analisi immunoistochimica, a livello di macrofagi alveolari (iAMs) e cellule epiteliali alveolari cuboidalizzate (CEACs). I topi sacrificati al giorno +28 hanno mostrato un incremento dei livelli di MMP2 e TIMP1, ma non di MMP9, nel BALF. L'inibizione in vivo di GSK-3 mediante SB216763 si è dimostra in grado di ridurre il reclutamento di cellule infiammatorie e la secrezione di MMPs al giorno +7, a livello del BALF; ha inoltre ridotto i livelli di MMP2 al giorno +28. Anche l'espressione di MMPs e TIMPs è stata modulata dall'inibizione di GSK-3, a livello di iAMs e CEACs, ad entrambi gli intervalli di tempo. Gli esperimenti in vitro su A549 hanno invece dimostrato che il silenziamento di GSK-3 è in grado di potenziare la secrezione di MMP9 indotta dallo stimolo proinflammatorio con TNFa, che attiva la via di NF-kB.

Conclusioni: Il nostro lavoro dimostra un ruolo di GSK-3 nella modulazione dell'espressione di MMPs e TIMPs in un modello murino di fibrosi polmonare indotta da BLM, che interessa sia la fase infiammatoria precoce che quella fibrotica tardiva. L'effetto dell'inibizione di GSK-3 sembra esplicarsi, in particolare, a livello di iAMs e CEACs. I dati in vitro, pur preliminari, indicano un effetto opposto del silenziamento di GSK-3 sulla secrezione di MMP9 in una linea di cellule epiteliali alveolari (A549); il silenziamento di GSK-3 potenzia l'effetto di TNFα sulla secrezione di MMP-9, tramite un meccanismo che coinvolge p65 ed è ERK1,2-dipendente

1. INTRODUCTION

1.1 Idiopathic Pulmonary Fibrosis

Idiopathic pulmonary fibrosis (IPF) is a progressive lung disease characterized by an extensive lung parenchyma remodelling involving the abnormal deposition of the extracellular matrix (ECM) by fibroblasts and the migration of epithelial cells and myofibroblasts through the disrupted basement membrane (BM) into the alveolar spaces [1]. The incidence and prevalence of IPF are difficult to determine because diagnostic criteria are evolving over time [2] (Table 1). The available data demonstrate that IPF favours no particular race, ethnic group or social environment. It is estimated that IPF effects at least 5 million persons worldwide, with an incidence of approximately 10.7 *per* 100,000 persons for men and 7.4 *per* 100,000 persons for women [3, 4]. The incidence increases with age. Most commonly the symptoms appear between the fifth and the seventh decades of life, with two-thirds of all cases arising in patients over 60 years of age; mean age at presentation is 66 [5]. Due to the last update of diagnostic criteria, allowing diagnosis based on High Resolution Computed Tomography (HRCT) pattern and clinical feature, even without a lung biopsy showing a Usual Interstitial Pneumonia (UIP) pattern, IPF incidence is likely to increase over the next few years.

Although idiopathic pulmonary fibrosis is, by definition, a disease of unknown etiology, a number of potential risk factors have been described. Smoking is strongly associated with IPF, particularly for individuals with a smoking history of more than 20 pack-years. Environmental exposure to metal dusts, chemicals, stonecutting, vegetable and animal dusts (e.g. farming) have been associated with IPF, as long as microbial agents and gastro-esophageal reflux. Genetic factors have also been implied in the pathogenesis or at least associated to the disease, both in sporadic and familial forms of IPF. Genetic susceptibility involves, for example, mutations expressed in the alveolar epithelial cells including mutations in surfactant proteins A and C [6] and the genes encoding the components of telomerase (*TERT*/*TERC*), leading to shortened telomeres [7].

Familial cohorts of IPF (two or more verified cases within a group of relatives belonging to a primary family unit) are described, though sporadic cases constitute the majority of disease. Clinical features of familial IPF are indistinguishable from those of sporadic form, excepting for an earlier age of onset and the appearance of different patterns of gene transcription[8]. Familial IPF accounts for less than 5% of all cases of IPF; notably, IIPs other than IPF have been identified in unaffected members of those families[9].

According to the last ATS/ERS guidelines [2], the diagnosis of IPF requires the following:

1. Exclusion of other known causes of ILD (e.g., domestic and occupational environmental exposures, connective tissue disease, and drug toxicity).

2. The presence of a UIP pattern on HRCT in patients not subjected to surgical lung biopsy (see Table 1).

3. Specific combinations of HRCT and surgical lung biopsy pattern in patients subjected to surgical lung biopsy (Table 2 and 3).

UIP Pattern (All Four Features)	Possible UIP Pattern (All Three Features)	Inconsistent with UIP Pattern (Any of the Seven Features)
• Subpleural, basal predominance • Reticular abnormality • Honeycombing with or without traction bronchiectasis • Absence of features listed as inconsistent with UIP pattern (*see* third column)	• Subpleural, basal predominance • Reticular abnormality • Absence of features listed as inconsistent with UIP pattern (*see* third column)	• Upper or mid-lung predominance • Peribronchovascular predominance • Extensive ground glass abnormality (extent > reticular abnormality) • Profuse micronodules (bilateral, predominantly upper lobes) • Discrete cysts (multiple, bilateral, away from areas of honeycombing) • Diffuse mosaic attenuation/air-trapping (bilateral, in three or more lobes) • Consolidation in bronchopulmonary segment(s)/lobe(s)

Table 1. High-Resolution Computed Tomography criteria for UIP pattern. Modified from [2]

UIP Pattern (All Four Criteria)	Probable UIP Pattern	Possible UIP Pattern (All Three Criteria)	Not UIP Pattern (Any of the Six Criteria)
• Evidence of marked fibrosis/ architectural distortion, ± honeycombing in a predominantly subpleural/ paraseptal distribution • Presence of patchy involvement of lung parenchyma by fibrosis • Presence of fibroblast foci • Absence of features against a diagnosis of UIP suggesting an alternate diagnosis (see fourth column)	• Evidence of marked fibrosis / architectural distortion, ± honeycombing • Absence of either patchy involvement or fibroblastic foci, but not both • Absence of features against a diagnosis of UIP suggesting an alternate diagnosis (*see* fourth column) OR • Honeycomb changes only‡	• Patchy or diffuse involvement of lung parenchyma by fibrosis, with or without interstitial inflammation • Absence of other criteria for UIP (*see* UIP Pattern column) • Absence of features against a diagnosis of UIP suggesting an alternate diagnosis (*see* fourth column)	• Hyaline membranes* • Organizing pneumonia*† • Granulomas† • Marked interstitial inflammatory cell infiltrate away from honeycombing • Predominant airway centered changes • Other features suggestive of an alternate diagnosis

Table 2. Histopathological criteria for UIP pattern (*) Can be associated with acute exacerbation of idiopathic pulmonary fibrosis. (†) An isolated or occasional granuloma and/or a mild component of organizing pneumonia pattern may rarely be coexisting in lung biopsies with an otherwise UIP pattern. (‡) This scenario usually represents end-stage fibrotic lung disease where honeycombed segments have been sampled but where a UIP pattern might be present in other areas. Such areas are usually represented by overt honeycombing on HRCT and can be avoided by pre-operative targeting of biopsy sites away from these areas using HRCT. Modified from [2].

HRCT Pattern*	Surgical Lung Biopsy Pattern* (When Performed)	Diagnosis of IPF?†
UIP	**UIP** **Probable UIP** **Possible UIP** **Nonclassifiable fibrosis‡**	**YES**
	Not UIP	No
Possible UIP	**UIP** **Probable UIP**	**YES**
	Possible UIP Nonclassifiable fibrosis	Probable§
	Not UIP	No
Inconsistent with UIP	UIP	Possible§
	Probable UIP Possible UIP Nonclassifiable fibrosis Not UIP	No

Table 3. Combination of HRCT and surgical lung biopsy for the diagnosis of IPF (requires multidisciplinary discussion). Bold type indicates combinations of HRCT and surgical lung biopsy patterns that correspond with a diagnosis of IPF. (*) Patterns as described in Tables 1 and 2. (‡) Nonclassifiable fibrosis: some biopsies may reveal a pattern of fibrosis that does not meet the criteria for UIP pattern and the other IIPs. These biopsies may be termed ''nonclassifiable fibrosis.'' (†) The accuracy of the diagnosis of IPF increases with multidisciplinary discussion (MDD). This is particularly relevant in cases in which the radiologic and histopathologic patterns are discordant. Data suggest that the accuracy of diagnosis is improved with MDD among interstitial lung disease experts; timely referral to interstitial lung disease experts is encouraged. MDD include discussions of the potential for sampling error and a re-evaluation of adequacy of technique of HRCT. Modified from [2].

1.1.1 Definition of UIP pattern

UIP Pattern: HRCT Features

HRCT is an essential component of the diagnostic pathway in IPF (Table 4, Figure 1). UIP is characterized on HRCT by the presence of reticular opacities, often associated with traction bronchiectasis. Honeycombing is common, and is critical for making a definite diagnosis. Honeycombing is manifested on HRCT as clustered cystic airspaces, typically of comparable diameters on the order of 3–10 mm but occasionally as large as 2.5 cm. It is usually subpleural and is characterized by well-defined walls. Ground glass opacities are common, but usually less extensive than the reticulation. The distribution of UIP on HRCT is characteristically basal and peripheral, though often patchy. The presence of coexistent pleural abnormalities (e.g., pleural plaques, calcifications, significant pleural effusion) suggests an alternative etiology for UIP pattern. Micronodules, air trapping, nonhoneycomb cysts, extensive ground glass opacities, consolidation, or a peribronchovascular-predominant distribution should lead to consideration of an alternative diagnosis. Mild mediastinal lymph node enlargement (usually 1.5 cm in short axis) can be seen. The chest radiograph is less useful than HRCT in evaluating patients with suspected IPF.

Several studies have documented a great positive predictive value of a HRCT diagnosis of UIP. Thus, an UIP pattern on HRCT is highly accurate for the presence of UIP pattern on surgical lung biopsy. If honeycombing is absent, but the imaging features otherwise meet criteria for UIP,

the imaging features are regarded as representing possible UIP, and surgical lung biopsy is necessary to make a definitive diagnosis. In patients whose HRCT does not demonstrate a UIP pattern, the surgical lung biopsy may still demonstrate UIP pattern on histopathology.

UIP Pattern: Histopathology Features

The histopathologic hallmark and chief diagnostic criterion is a heterogeneous appearance at low magnification in which areas of fibrosis with scarring and honeycomb change alternate with areas of less affected or normal parenchyma (1, 12) (Table 5, Figure 2). These histopathologic changes often affect the subpleural and paraseptal parenchyma most severely. Inflammation is usually mild and consists of a patchy interstitial infiltrate of lymphocytes and plasma cells associated with hyperplasia of type 2 pneumocytes and bronchiolar epithelium. The fibrotic zones are composed mainly of dense collagen, although scattered convex subepithelial foci of proliferating fibroblasts and myofibroblasts (so-called **fibroblast foci**) are a consistent finding. Areas of honeycomb change are composed of cystic fibrotic airspaces that are frequently lined by bronchiolar epithelium and filled with mucus and inflammatory cells. Smooth muscle metaplasia in the *interstitium* is commonly seen in areas of fibrosis and honeycomb change.

The differential diagnosis for UIP pattern on pathology is relatively short, especially when strict criteria for UIP are maintained. The major differential diagnostic considerations include UIP in other clinical settings such as connective tissue diseases, chronic hypersensitivity pneumonitis (extrinsic allergic alveolitis), and pneumoconioses (especially asbestosis). Some biopsies may reveal a pattern of fibrosis that does not meet the above criteria for UIP pattern. These biopsies may be termed ‘‘nonclassifiable fibrosis.’’ In the absence of histologic features diagnostic of an alternative condition (e.g., hypersensitivity pneumonitis, sarcoidosis, etc.), such biopsies may be consistent with the diagnosis of IPF (Tables 2 and 3) in the appropriate clinical and radiologic setting and after careful multidisciplinary discussion.

1.1.2 Clinical picture

The natural course of IPF is characterized by a progressive decline in subjective and objective pulmonary function until eventual death from respiratory failure or complicating comorbidity. Available longitudinal studies do not allow a clear assessment of median survival. Retrospective longitudinal studies suggest a median survival time from 2 to 3 years since diagnosis but recent data from prospective studies suggest that this may be an underestimate [10].

Symptoms such as weight loss, fever, and athralgias are unusual in IPF, whereas gastro-oesophageal acid reflux is present in close to 90% of patients, but often occurs without symptoms [11]. Auscultation of the lungs reveals early bibasal inspiratory crackles, known as *Velcro* crackles. Clubbing is found in approximately 50% of patients. There are no other physical manifestations, unless cor pulmonale has developed in association with end-stage disease. There are no specific laboratory abnormalities. Noteworthy pulmonary hypertension has been reported

to occur in 32 to 84% of patients with IPF. The exact prevalence remains unclear because triggers for the evaluation of pulmonary pressures and the best method to detect pulmonary hypertension in IPF remain unsettled [12]. Diffusion capacity is strongly correlated with pulmonary hypertension, being inversely related [13, 14]. However, the severity of restrictive physiology has little bearing on the prevalence or degree of pulmonary hypertension. Several studies have demonstrated a lack of correlation between pulmonary artery pressure and forced vital capacity (FVC) [13-15]. Right-heart catheterization is the best diagnostic test for pulmonary hypertension but the implementation of such invasive testing is difficult to justify in the absence of data demonstrating a benefit to treatment of pulmonary hypertension in IPF. Still it is clear that the presence of pulmonary hypertension in IPF adversely affects survival [16].

There appear to be several possible natural histories for patients with IPF (Figure 1). For a single patient, the natural history is unpredictable at the time of the diagnosis. The majority of patients demonstrate a slow, gradual progression over years. Some patients remain stable while others have an accelerated decline. Some may experience episodes of acute respiratory worsening. It is unknown if these different natural histories represent distinct phenotypes of IPF or if the natural history is influenced by geographic, ethnic, cultural, racial, or other factors. Other comorbid conditions such as emphysema and pulmonary hypertension may impact the disease course [13].

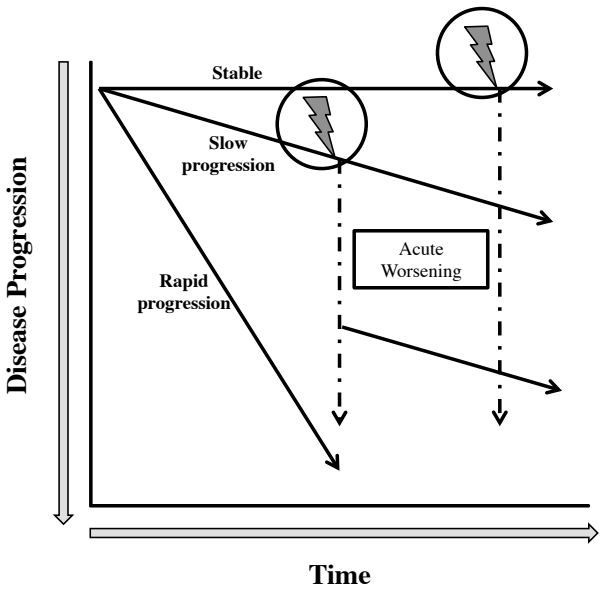

Figure 1. Natural history of IPF. Modified from **[2]**

1.1.3 Treatment

In terms of disease management, steroids, N-acetylcysteine (NAC), Azathioprine have been used for many years without any evidence of efficacy, whilst lung transplantation have been the only effective treatment until 2012. Over the last 3 year 2 different drugs, Pirfenidone [17] and Nintedanib [18], have been shown to slower disease progression in multicentric placebo controlled clinical trials and another trial showed an increased risk of mortality associated with

triple therapy (NAC + Azathioprine + Prednisone), if compared to placebo [19]. Currently, Pirfenidone and Nintedanib are the only drugs approved for IPF treatment and lung transplantation is still the unique strategy that has been shown to improve survival in IPF patients.

1.1.4 Pathogenesis

Although IPF etiology is, by definition, still unknown, many different mechanisms and pathways have been shown to be involved, with different degree of evidence, in the pathogenesis of this disease.

The *primum movens* is believed to be a persistent epithelial injury which, in genetically susceptible individuals, turns into extensive epithelial regeneration, reactivation of developmental pathways and uncontrolled fibroproliferation due to disturbed epithelial–mesenchymal crosstalk; this results in progressive scarring of the lung [6, 20, 21]. The disturbed epithelial–mesenchymal crosstalk involves: increased generation of fibrogenic mediators by the epithelium, including the tissue factor/factor VIIa–factor X complex, transforming growth factor (TGF)-β, platelet-derived growth factor (PDGF) and connective tissue growth factor [20, 22]; the loss of control of fibroblasts *via* reduced epithelial prostaglandin E2/urokinase plasminogen activator [23]; and the upregulation of developmental pathways such as Wnt and Notch [20, 21, 24], which may act in a paracrine fashion on the parenchyma [25].

IPF is characterized by an extensive lung parenchyma remodeling involving the abnormal deposition of the extracellular matrix (ECM) by fibroblasts and the migration of epithelial cells and myofibroblasts through the disrupted basement membrane (BM) into the alveolar spaces [1]. Within the histologic picture of UIP, fibroblastic foci are areas of myofibroblast proliferation thought to be the main site of ECM deposition. ECM-producing lung fibroblasts are the key source of this deposition; however, these cells are heterogeneous in a number of phenotypic features [26].

Recent investigations have provided support for the hypothesis that they arise from several sources, including:

- resident pulmonary fibroblasts,
- bone marrow-derived circulating fibrocytes that infiltrate the lungs, *via* the gradient formed by the chemokine stromal cell-derived factor-1–CXCR4 axis [20];
- alveolar epithelial cells through a process called epithelial-mesenchymal transition (EMT) [27];
- transcription factor Foxd1 progenitor-derived pericytes, whcich may be an important precursor of lung myofibroblasts [28].

Several growth factors are suggested to be pivotal in the development of IPF, including platelet-derived growth factor (PDGF), basic fibroblast growth factor (bFGF), and vascular endothelial

growth factor (VEGF). PDGF is a fibrogenic mediator [29], and was increased in a murine IPF-animal model [30]. The inhibition of PDGF signalling reduced bleomycin-induced pulmonary fibrosis in mice [31]. bFGF is a potent mitogenic factor and high levels of bFGF were found in lung tissue derived from patients with IPF [32]. And finally, blocking VEGF signalling reduced lung fibrosis in a mouse model [33].

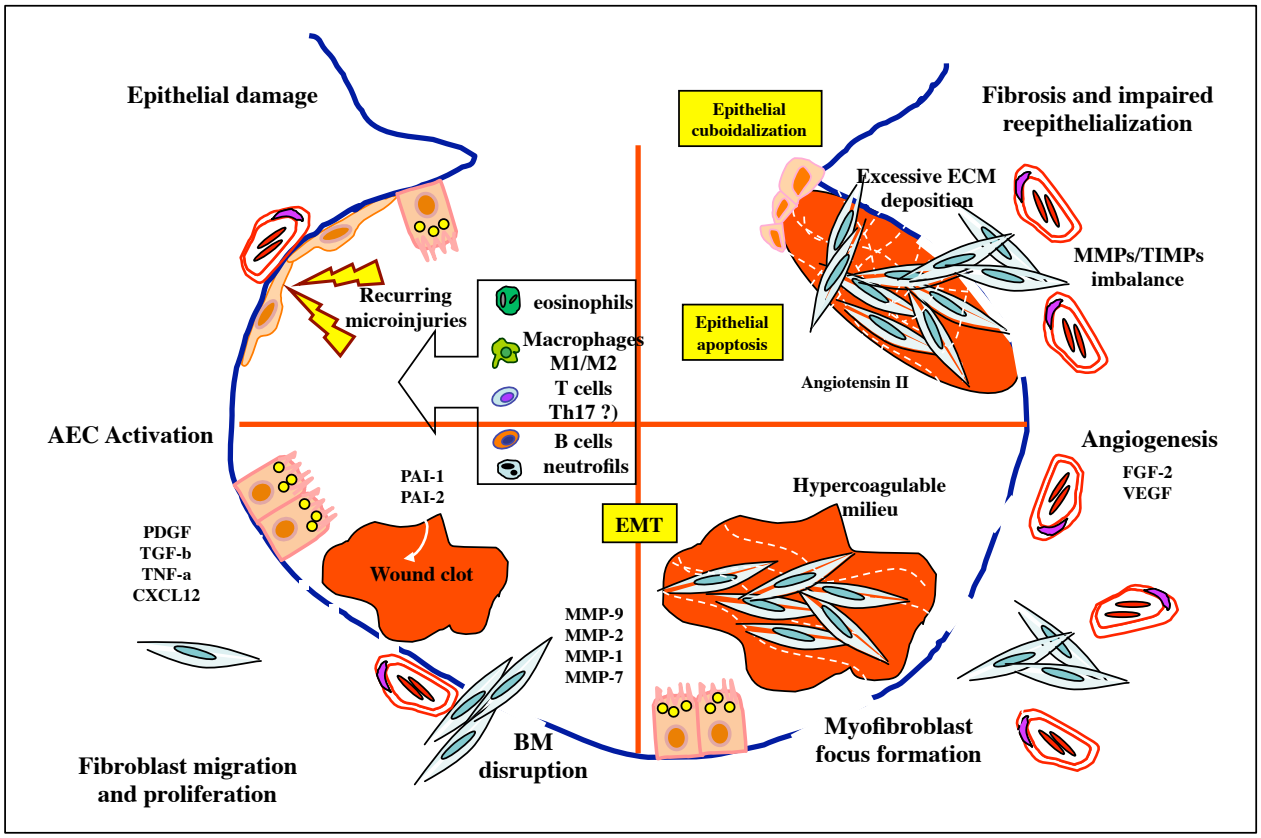

Figure 2. **Pathogenesis of IPF.** Chronic apithelial injury is believed to induce impaired ECM turnover and aberrant finrotic response, sustained by many different pathways. Balance between MMPs and TIMPs seems to play a crucial role in this process.

Nintedanib is an orally available indolinone derivate that competitively binds to the ATP-binding sites within the kinase domains of VEGF receptor (VEGFR)1, VEGFR2, VEGFR3, FGF receptor (FGFR)1, FGFR3, and PDGF receptor (PDGFR)α and PDGFRβ [34].

Pirfenidone is an orally available drug that exhibits anti-fibrotic and anti-inflammatory properties *in vitro* and *in vivo*. There is evidence to show that pirfenidone diminishes fibroblast proliferation, secretion of the fibrosis-associated proteins and cytokines, biosynthesis and accumulation of extracellular matrix as well as accumulation of inflammatory cells and tumour necrosis factor-α synthesis [35].

The exact anti-fibrotic mechanism of action is less characterized, for pirfenidone if compared with Nintedanib. However, further *in vitro* and *in vivo* studies are ongoing for both drugs, in order to better understand their full anti-fibrotic potential and their specific effect on each pro-fibrotic pathway, this way improving the comprehension of IPF pathogenesis.

1.1.5 Matrix Metalloproteases (MMPs) and their Tissue Inhibitors (TIMPs)

The aberrant deposition of ECM is a hallmark of IPF. In this context, matrix metalloproteinases (MMPs), a family of extracellular and Zinc-dependent enzymes, play a crucial role because of their proteolytic activity against many components of ECM, including interstitial collagens, BM collagen (type IV), fibronectin, laminin and various proteoglycans (J.F. Woessner, FASEB, 1991). MMPs activity is regulated at multiple levels including gene transcription, compartimentalization, extracellular activation of the zymogen and inactivation by specific inhibitors referred to as tissue inhibitors of metalloproteinases (TIMPs) [36]. Accumulating evidence indicates that an imbalance between MMPs and TIMPs may lead to the alteration of the ECM metabolism in a variety of pulmonary disorders including IPF [37, 38], emphysema [39], asthma [40, 41] and lung carcinoma [42]. Moreover, MMPs activity in ECM remodeling has been shown to be crucial in local and metastatic cancer invasiveness [43].

Studies from different groups have shown that some MMPs such as MMP-1, MMP-2, MMP-3, MMP-7, MMP-9, and MMP-13 are highly expressed in IPF, playing diverse roles in the fibrotic response; however, the exact mechanisms are not well characterized [38, 44-46]. Recently, it has been identified the overexpression of MMP-19 in the hyperplastic alveolar epithelium of IPF lungs and demonstrated that, surprisingly, mice lacking this MMP developed an exacerbated bleomycin-induced lung fibrosis [47]. The gelatinases (MMP-2 and -9) and, in particular, MMP-7, have already been suggested to play a role in human and experimental lung fibrosis, thus underscoring the dynamic regulation of the ECM and of remodelling processes in the lung [48]; MMP-1 is lacking in rodents, and, hence, MMP-13 (also known as collagenase-3) is the principal interstitial collagenase in this species and has a high specificity for degrading insoluble fibrillar collagens, especially type II and I collagens [49-51]. The expression of MMP-8 and -13 was shown to be down-regulated in a model of pulmonary fibrosis induced in rats with paraquat and hyperoxia [52]. A recent study performed on human lung tissues from patients with sporadic IPF identified MMP-7 and the collagenases MMP-1 and MMP-13 as key MMPs upregulated in human IPF. In a murine model of bleomycin-induced lung fibrosis, in response to bleomycin challenge and compared with wild-type (WT) mice, MMP-13$^{-/-}$ mice exhibited an increased inflammatory reaction and a greater extent of fibrosis, thus pointing at MMP-13 as a key factor in the regulation of ECM turnover and collagen deposition in both mice and man [38].
We focused our study on two gelatinases, MMP-9 (gelatinase B) and MMP-2 (gelatinase A) that are able to degrade the common substrates type IV collagen, the major constituent of the BM, type V collagen and gelatin. MMPs are secreted as inactive precursors which have to be activated in the extracellular space. MMP-2 can be activated by type I collagen and thrombin [53, 54], but also by a membrane-type MMP-dependent pathway involving TIMP-2 [55]. An imbalance between MMPs and TIMPs might be involved in the accumulation of ECM in fibrogenesis [56]. Accordingly, a greater increase in the levels of TIMP than levels of MMP-2 was reported and such an imbalance would favour the enhanced deposition of ECM proteins [45]. Interestingly, TGF-β induced lung fibrosis in mice was primarily due to TIMP up-regulation [57], and a recent study demonstrated that over expression of MMP-9 by alveolar macrophages in mice attenuated the fibrotic reaction after bleomycin instillation [58]. Interestingly, it has been showed that

Nintedanib can up-regulate pro-MMP-2 secretion, but down-regulated its inhibitor TIMP-2 in primary lung fibroblasts from IPF patients. Only minor amounts of pro-MMP-9 were detected in those cells [34].

These two gelatinases, MMP-2 and MMP-9, differ greatly in transcription control being MMP-2 constitutively expressed and MMP-9 induced by soluble factors such as cytokines and growth factors and by integrin-mediated signalling through cell-matrix or cell-cell interactions [36]. The property of being induced has made MMP-9 an interesting target of study in many pathological conditions including IPF [59]. In healthy lung, indeed, MMP-9 secretion is usually low or absent but, under stimulation, bronchial epithelial cells, Clara cells, alveolar type II cells, fibroblasts, smooth muscle cells and endothelial cells can produce it. Among inflammatory cells, alveolar macrophages, eosinophils, mast cells, lymphocytes, NK cells and dendritic cells, all can produce MMP-9 but, the neutrophil represents the main source of MMP-9 which is synthesized during cell maturation in the bone marrow and then, stored in specific granules from which it is readily released. Moreover, the neutrophil does not secrete MMP-9 in complex with TIMP-1 as many cells do, but can secrete it either alone or in a covalent complex with NGAL [60]. Despite the large number of studies, the role of MMP-9 in the lung is still not completely understood. In vitro studies of wound repair of human respiratory epithelium demonstrated that MMP-9 is implicated in epithelial cell migration [61]. Another study employing mouse model of lung injury carried out with intratracheal instillation of bleomycin (BLM) demonstrated that MMP-9 is required for alveolar bronchiolization, by facilitating migration of Clara cells and other bronchiolar cells into the region of alveolar injury [39].

1.2 GSK-3

The serine-threonine kinase GSK-3 was initially considered an unconventional and interesting kinase because it is constitutively active, its substrates usually need to be pre-phosphorylated by another kinase, and it is inhibited, rather than activated, in response to stimulation of the two main signalling pathways known to impinge on GSK-3, the insulin and Wnt pathways [62, 63]. However, two key developments in particular transformed this perspective to the current state of widespread interest:

- the discovery that GSK-3 is a key kinase contributing to abnormal phosphorylation of the microtubule-binding protein tau in the process thought to cause neurofibrillary tangles in Alzheimer's disease [64]; this finding underlined GSK-3 as a potential therapeutic target in this disease;
- the finding that GSK-3 is inhibited by lithium [65], the classical mood stabilizer used in the treatment of bipolar disorder This finding not only raised the prospect that GSK-3 may have a central role this disorder, but also provided a relatively selective and well tolerated inhibitor of GSK-3 that opened the door for discoveries of other targets of GSK-3. Thus, starting from a single disorder, the interest in GSK-3 and its actions became widespread, and it now seems like GSK-3 touches almost every aspect of cellular signalling and is involved in an unparalleled number of disease processes.

Following these discoveries and the increasing awareness of new actions of GSK-3, many additional inhibitors of GSK-3 were developed, as GSK-3 began to be seriously considered as a therapeutic target [66]. Potential therapeutic applications include many prevalent conditions, such as cancer, cardiovascular diseases, diabetes, inflammatory conditions, neurodegenerative diseases, and psychiatric diseases, as well as other less prevalent conditions. Such an expansive influence on cellular signalling and association with multiple disease processes has stimulated to inquire how GSK-3 can manage all of its tasks in an organized fashion, and how such a pervasive kinase can reasonably be thought of as a feasible therapeutic target. Recent progresses are leading to a more complete understanding of this enigmatic kinase and its potential as a therapeutic target. Moreover, substantial evidence supports the conclusion that inhibition of GSK-3 is an important action contributing to the mood stabilizing action of lithium in bipolar disease, demonstrating that in vivo inhibition of GSK-3 is, in fact, feasible for safe therapeutic interventions.

1.2.1 Regulation of glycogen synthase kinase-3-mediated substrate phosphorylation

GSK-3 exists in two paralogs (homologous proteins derived from different genes) **GSK-3α** and **GSK-3β** that are commonly referred to as isoforms. A theoretical analysis found that GSK-3β has more predicted substrates than any other kinase [67]; about 100 proteins phosphorylated by GSK-3 have already been reported [68], and this high number of substrates raises the question of how GSK-3 can phosphorylate so many proteins in a cell with any discretion. There must be certain characteristics of GSK-3 that are particularly useful and versatile which outweigh the functional constraints and complexities required to provide discretion among many substrates. Since GSK-3's activity as a kinase is not particularly different from other kinases, there has been a suggestion that the mechanisms regulating GSK-3 might be particularly adaptable for incorporation into new signalling pathways without perturbing those already existent. Thus, a key to GSK-3's actions may be the multiple regulatory mechanisms available to orchestrate its substrate-specific actions. However, this promiscuity also appears to have provided multiple interactions that can be disrupted to result in unbridled actions of GSK-3 contributing to multiple types of diseases. These crucial mechanisms that confer specificity for signalling pathways and for substrates have originally been categorized to include the regulatory phosphorylation of GSK-3 itself, the regulation of substrate availability, the subcellular localization of GSK-3 and its substrates, and the incorporation of GSK-3 into protein complexes, categories that remain the primary mechanisms known to regulate GSK-3 [69].

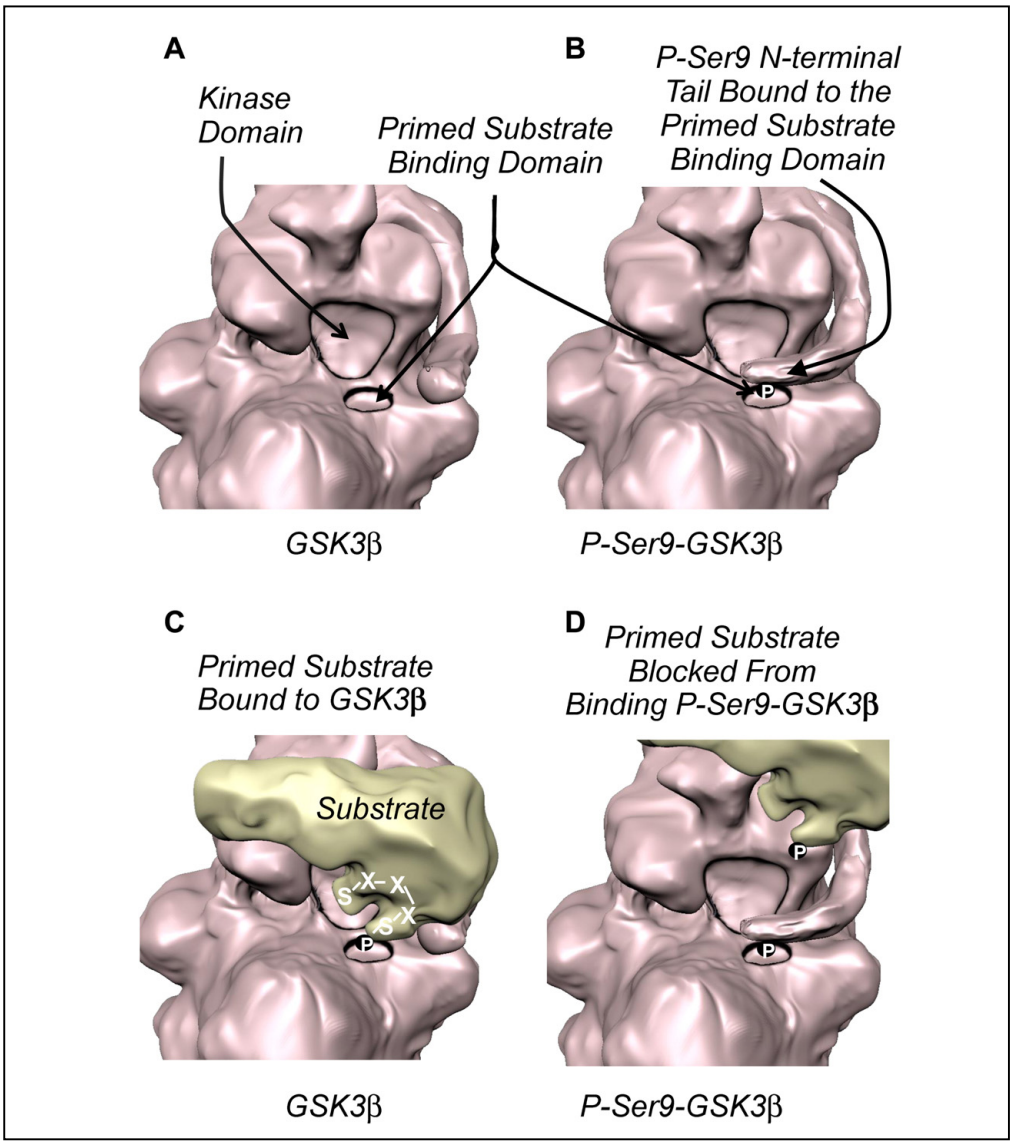

Figure 3. Serine9-phosphorylation of GSK-3β inhibits its phosphorylation of primed substrates. (A) Representation of GSK-3β based on a recently reported crystal structure showing the adjacent kinase domain and primed-substrate binding domain [70]. (B) Phosphorylated serine-9 in the N-terminal tail of GSK-3β binds the primed substrate-binding domain. (C) Primed substrates first associate with the primed substrate-binding domain of GSK-3β, which places a Ser/Thr four residues N-terminal to the primed phosphorylated Ser/Thr adjacent to the kinase domain of GSK-3β to facilitate substrate phosphorylation. (D) Phosphorylated serine-9 in the N-terminal tail of GSK-3β inhibits the association of primed substrates with the primed substrate binding domain of GSK-3β. From (Beurel et al. / Pharmacology & Therapeutics 148, 2015) [71].

1.2.2 Regulatory post-translational modifications of GSK-3

Inhibitory serine-phosphorylation is the most frequently examined mechanism that regulates the activity of GSK-3. Two key functional domains of GSK-3 have been identified (Figure 3), a primed-substrate binding domain that recruits substrates to GSK-3, and a kinase domain that phosphorylates the substrate [72]. The former domain provides a binding site for most GSK-3 substrates, those that are primed by being pre-phosphorylated. Although GSK-3 can phosphorylate a few non-primed substrates at Ser-Pro sites, the most common target for

phosphorylation by GSK-3 is the pre-phosphorylated sequence, S/T-X-X-X-S/T(P), where GSK-3 phosphorylates a serine/threonine four residues N-terminal to a pre-phosphorylated serine/threonine. However, the three-dimensional structure of the substrate also influences its interactions with GSK-3. The priming phosphorylation allows the substrate to bind the primed-substrate binding domain, placing the target serine/threonine adjacent to the kinase domain of GSK-3 to facilitate its phosphorylation (Figure 3). In some cases, non-primed substrates may contain an acidic residue four amino acids C-terminal from the GSK-3 target site in place of the primed phosphorylated residue, such that the acidic residue can interact with the primed substrate binding site, but this is not always the case.

The frequent requirement for a primed substrate is central to two mechanisms that regulate GSK-3's actions: inhibitory serine phosphorylation of GSK-3, and control of substrate availability. Phosphorylation of serine-21 in GSK-3α or of serine-9 in GSK-3β causes the N-terminal tail of GSK-3 to act as a pre-phosphorylated substrate, or pseudosubstrate. This phosphorylated serine tail self-associates in the primed-substrate binding pocket, hindering the binding of primed substrates, and thus diminishing primed-substrate phosphorylation by GSK-3 (Figure 3). Multiple signalling pathways feed into this site to increase the serine phosphorylation of GSK-3, which can be mediated by Akt, protein kinase A (PKA), protein kinase C, p70 S6 kinase, and other kinases. Thus, many signalling pathways that activate these kinases can inhibit GSK-3 by phosphorylating the inhibitory serines on GSK-3. An intriguing exception is the recent discovery that GSK-3 phosphorylates AMP-activated kinase (AMPK) to inhibit its activity [73]. Remarkably, Akt, which usually inhibits GSK-3 by serine-9/21 phosphorylation, promotes AMPK phosphorylation by GSK-3, showing that in some circumstances Akt and GSK-3 cooperatively modulate signalling pathways.

In general, measuring the serine-9/21 phosphorylation of GSK-3 provides a valuable assessment of conditions that regulate the activity of GSK-3 via this mechanism, but it is useful to consider four caveats to this conclusion.

1. Not all substrates of GSK-3 are primed, so these non-primed substrates may not require binding to the primed substrate-binding domain to be phosphorylated by GSK-3. Thus, the serine-phosphorylation inhibitory mechanism does not necessarily regulate the phosphorylation of non-primed substrates by GSK-3.
2. The activity of GSK-3 in certain protein complexes is not affected by serine-phosphorylation of GSK-3. This has been most well-established, and most often misinterpreted, for Wnt signalling, which is impervious to the serine-phosphorylation status of GSK-3 bound to Axin,
3. The serine-phosphorylation status of GSK-3 is probably most often undergoing oscillations, thus influencing the basal level of GSK-3 phosphorylation and responsiveness to experimental manipulations.
4. The serine-phosphorylation inhibitory mechanism does not cause absolute inhibition of GSK-3 activity. In contrast, the phospho-Ser9/21 domain is inhibitory by a mechanism that is competitive with primed substrates. As the primed substrate concentration increases it displaces phospho-Ser9/21 and once again can be phosphorylated by GSK-3. Thus, the

mechanism allows an accumulation of the primed substrate that reaches a new steady-state level at which it re-emerges as a substrate of GSK-3.

Taken altogether, there are many intricacies associated with the serine-phosphorylation mechanism of regulating GSK-3, which provide important clues about the regulation of signalling systems [71].

Phosphorylation of ser21-GSK-3α and ser9-GSK-3β can be mediated by a large number of different kinases. This allows multiple signalling pathways to impinge on GSK-3, and for GSK-3 to act as an integrator of signals. It seems likely that the formation of protein complexes has an important role in allowing multiple signals and their particular kinases to regulate GSK-3. It is also intriguing to note that these are not one-way interactions, but there are clearly bi-directional interactions between GSK-3 and kinases that phosphorylate GSK-3, which are likely driven by specific signalling pathways in a cell type-specific manner, and there are mechanisms by which active GSK-3 can perpetuate its own activity. This bi-directionality has been studied, for instance, with the Akt–GSK-3 interaction, in which Akt not only inhibits GSK-3 but GSK-3 can also regulate Akt.

GSK-3 is also phosphorylated at other sites besides serine9/21, but their regulatory outcomes remain unclear. Phosphorylation on Tyr216-GSK-3β and Tyr279-GSK-3α, for example, is required for maximal activity [72]. During translation, GSK-3 phosphorylates itself on these residues so that an active kinase is immediately synthesized. This is another fascinating characteristic of GSK-3, during synthesis it can be a tyrosine kinase, but mature GSK-3 is a serine/threonine kinase [71].

Investigators have long thought that GSK-3 must be regulated by additional post-translational mechanisms because it seemed that more control is necessary for it to distinguish among numerous substrates and to be uniquely regulated by specific signalling pathways. Such modifications are finally beginning to be identified. GSK-3 has been reported to be cleaved to activated fragments by calpain and by matrix metalloproteinase-2 [74], which may affect its selection of substrates to phosphorylate. A regulatory effect of acetylation on GSK-3 activity was recently reported. Furthermore, GSK-3β was recently found to be inhibited by mono-ADP-ribosylation and to be regulated by citrullination [71].

1.2.3 Substrate pre-phosphorylation and availability

As previously explained, GSK-3 need for substrate pre-phosphorilation requires temporal and spatial coincidence of two signals: induction of the priming substrate phosphorylation and GSK-3 activation. This means that GSK-3 does not recognize the substrate unless another signalling pathway is activated that primes the substrate: signals must be generated to activate a kinase to pre-phosphorylate the substrate, GSK-3 must be co-localized with the primed substrate, and the timing of signals that activate GSK-3 all must be coordinated to determine if and when GSK-3 phosphorylates the substrate. This prevents spurious actions of GSK-3 and temporally limits the lifetime of primed substrates.

For example, the transcription factor cyclic AMP response element binding protein (CREB) is not recognized by GSK-3 unless a CREB-activating pathway is turned on that induces phosphorylation of CREB on serine-133, which activates CREB. This creates a primed phosphorylation site for GSK-3, and in this way intracellular signalling pathways direct GSK-3 to its target. However, since GSK-3 is constitutively partially serine-phosphorylated, and thus partially inhibited from recognizing primed substrates, another signal coinciding in time and intracellular location is required to reduce serine-phosphorylation of GSK-3 to allow it to recognize phosphoserine133-CREB. In other words, for nuclear CREB, a signal must cause serine-dephosphorylation of GSK-3 in the nucleus at a time when CREB is phosphorylated on serine-133. Since phosphorylation of CREB on serine-129 by GSK-3 inactivates CREB, this is likely to be the mechanism ensuring that the activation of CREB is transient, an outcome that may be employed in transient learning events that require active CREB for a short time. Thus, this provides an exquisite mechanism for cycling the actions of GSK-3 substrates.

1.2.4 Other regulatory Mechanisms

Subcellular localization

GSK-3 has traditionally been considered to be largely a cytosolic protein. However, it is also present within the mitochondria and nucleus, as well as other subcellular compartments, where its levels and/or activation state can be regulated by localized signalling activities. Little is known about mechanisms regulating the mitochondrial level and activity of GSK-3, or the mitochondrial substrates of GSK-3. In contrast, many nuclear effects of GSK-3 have been identified, particularly those involving the regulation of gene expression. GSK-3 enters the nucleus via an intrinsic nuclear localization sequence in GSK-3β, and the nuclear levels of GSK-3β rapidly increase in response to some apoptotic stimuli. Conversely, the GSK-3-binding protein Frat promotes nuclear export of GSK-3. The distinct N-terminal region of GSK-3α causes nuclear exclusion that can be counter-activated by calcium signalling [71]

Actions of GSK-3 affecting nuclear functions, specifically gene expression, include indirect effects via its regulation of many transcription factors, and more direct effects resulting from the regulation of recently identified epigenetic mechanisms. Among the many transcription factors regulated by GSK-3 are Fos/Jun AP-1, CREB, heat shock factor 1, nuclear factor of activated T cells (NFAT), myc, C/EBP, NF-ϰB, p53, signal transducer and activator of transcription-3 (STAT3), as well as many others. More recently, evidence has begun to reveal significant modulatory effects of GSK-3 on proteins involved in epigenetics. Epigenetic regulation by GSK-3 has been especially well-characterized in the **regulation of expression of a subset of NF-ϰB-regulated genes** [75]. Thus, by regulating numerous transcription factors and proteins involved in epigenetic regulation, GSK-3 has widespread modulatory effects on gene expression [71].

Besides these classical nuclear and mitochondrial compartments, GSK-3 is also compartmentalized in other subcellular structures and in protein complexes. **The localization of GSK-3 obviously is important in regulating its actions**, but much remains to be learned about mechanisms regulating GSK-3 trafficking within cells and the functional consequences.

Association in protein complexes

A major mechanism that has evolved for targeting GSK-3 towards specific substrates is by its incorporation into protein complexes that recruit substrates for GSK-3 to phosphorylate. These include both preassembled complexes and signal-induced complexes. The classical example of a GSK-3-containing preassembled complex is the β-catenin destruction complex in the Wnt signalling pathway (Figure 4). In this complex, the scaffold protein Axin, with the assistance of the associated protein APC (Adenomatous Polyposis Coli), brings β-catenin into close proximity to GSK-3. GSK-3 phosphorylates β-catenin on residues 41, 37, and 33 after priming phosphorylation by casein kinase 1, which targets β-catenin to the proteasomal degradation machinery. Wnt ligands induce disruption of the complex, which prevents GSK-3 from phosphorylating β-catenin, allowing the accumulation and nuclear import of β-catenin. Several Axin-binding proteins have been identified that modulate the phosphorylation of β-catenin in the Axin–GSK-3 complex, suggesting that much remains to be learned about how signalling pathways are integrated at this locus. It is interesting to note that:

1. As reviewed by Woodgett and colleagues [76], the activity of GSK-3 coupled to Axin is not controlled by the GSK-3 serine- phosphorylation mechanism. This independence of regulation by GSK-3 serine-phosphorylation may be due to structural constraints that make Axin-bound GSK-3 inaccessible to kinases that would otherwise phosphorylate the inhibitory serine, or it may be due to the proximity of its primed substrate β-catenin. Taken together with the fact that only a very small portion of cellular GSK-3 is bound to Axin, it is evident that most phosphoserine-GSK-3 measured in cells is not the GSK-3 that is associated with Axin. Thus, it is important to be wary of the often-stated conclusion after an experimental treatment that there is a direct relationship between increases in the serine-phosphorylation of GSK-3 and increases in the level of β-catenin; these outcomes can occur in parallel but **increased serine-phosphorylation of GSK-3 does not inhibit GSK-3 in the β-catenin destruction complex**. This mechanism of insulating Wnt signalling from other pathways that regulate serine-phosphorylation of GSK-3 is critical to avoid disastrous activation of Wnt signalling by insulin and by every other signal that increases serine-phosphorylated GSK-3.
2. In many cells, if not all, only a small portion of β-catenin is associated with the Axin destruction complex, while much of the β-catenin is intead associated in other protein complexes at the plasma membrane. Therefore, it is more informative to measure changes in nuclear β-catenin rather than total cellular levels to assess the activity of the Axin-linked β-catenin destruction complex
3. β-Catenin is not the only GSK-3 substrate that binds to Axin. Axin also brings other substrates into close proximity for phosphorylation by Axin-bound GSK-3, such as Smad3. Largely unaddressed are the regulatory consequences of the existence of multiple Axin-bound GSK-3 substrates in terms of regulation by serine-phosphorylation or competition between β-catenin and other GSK-3 substrates for the limited amount of Axin. However, there must be some important regulatory interactions between different signalling pathways that utilize the Axin–GSK-3-substrate route. For example, cooperative actions of Axin and p53, and several p53-regulating proteins, have been demonstrated to regulate both p53 and β-catenin actions

and may contribute to the promotion of p53 actions by GSK-3.

4. The Axin–β-catenin destruction complex has a variety of interactions with Axin-independent actions of GSK-3.

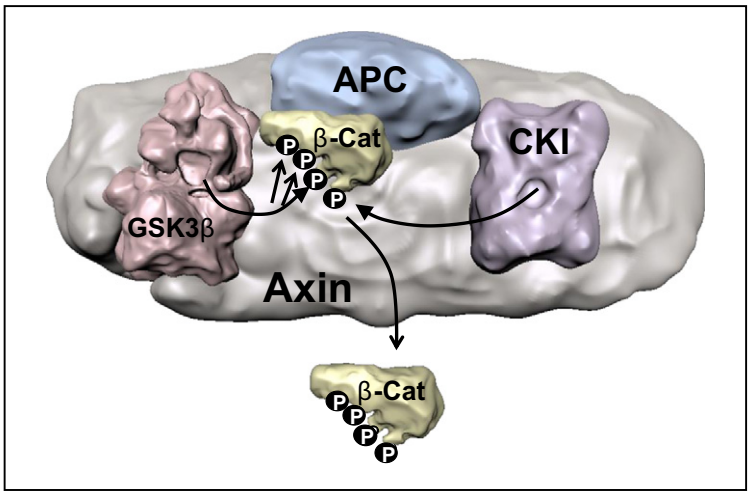

Figure 4. The Axin–β-catenin destruction complex (simplified scheme): the pre-assembled complex of Axin, Adenomatous Polyposis Coli (APC), casein kinase 1 (CK1), GSK-3β, and β-catenin allows GSK-3 to phosphorylate β-catenin sequentially on residues 41, 37, and 33. Phosphorylation leads to the release of β-catenin from the complex and targets it for proteasomal degradation. Activation of Wnt signalling disrupts the complex (not shown), blocking phosphorylation of β-catenin by GSK-3, resulting in β-catenin stabilization. From [71].

.

In addition to Axin, a growing number of GSK-3-binding proteins, have been identified that appear to direct GSK-3 phosphorylation for specific functions, including cell structure and adhesion reflecting the importance of protein complexes in allowing signals to regulate the action of GSK-3 in a substrate-selective manner. The actions of GSK-3 in protein complexes also extend to receptors and receptor-coupled signal transduction systems. It is not known which of these protein binding interactions, like Axin, also insulate the activity of GSK-3 from being regulated by serine- phosphorylation [71].

GSK-3 interactions with receptors and receptor-coupled signal transduction events

It is now evident that GSK-3 is intimately involved in numerous receptor-coupled signalling mechanisms, not only the commonly recognized signalling induced by insulin and Wnt. These interactions include regulation of receptor-coupled signal transduction proteins, direct interactions with receptors, and regulation of receptor trafficking. G-protein coupled receptors (e.g. Dopaminergic D2 receptor, which induces the association of β-arrestin, Akt, GSK-3, and protein phosphatase 2A), hormone receptors (e.g. Estrogen Receptor α and β, glucocorticoid receptor, androgen and progesterone) and ionotropic neurotransmitter receptors have been shown to involve GSK-3 downstream of their activation. These accumulating findings indicate that many receptor-mediated signals are regulated by GSK-3, with undoubtedly many more to be identified in the near future.

Other mechanisms regulating the actions of glycogen synthase kinase-3

GSK-3 seldom appears to be regulated by changes in expression, as only a few conditions have been reported in which the expression or levels of GSK-3 are markedly altered. However, large changes in GSK-3 levels can occur; for example there is a large, ~10-fold increase in GSK-3β in the Th17 subtype of T cells, relative to other T cells [77].

Single nucleotide polymorphisms (SNPs) have been identified in the GSK-3β gene that may be linked to disease susceptibility or responses to therapeutic drugs. Alternative splicing can give rise to forms of GSK-3β with altered functions.

Altogether, in contrast to the common notion that GSK-3 is only regulated by serine-phosphorylation and by binding to Axin, there is a plethora of mechanisms that guide the actions of GSK-3. These mechanisms apparently provide the underpinnings for GSK-3 to select among its many substrates in response to each signalling pathway that impinges upon GSK-3.

1.2.5 Differential actions and regulation of GSK-3α and GSK-3β

An emerging topic is the identification of differential regulation and actions of GSK-3α and GSK-3β. The catalytic domains of GSK-3α and GSK-3β are nearly identical, but their C-terminal sequences diverge and GSK-3α contains a large glycine-rich N-terminal region that is absent in GSK-3β [76]. Surprisingly, little is known about mechanisms that differentially regulate their expressions, except for the novel discovery that the GSK-3α gene is absent in birds. Reported expression differences include the selective up-regulation of GSK-3β expression in the Th17 subtype of T cells, which are pathogenic in autoimmune diseases [77], and differences in the expression of GSK-3α and GSK-3β in mouse brain regions during development and in the suprachiasmatic nucleus during the circadian rhythm. Studies of mechanisms that differentially regulate the expression of GSK-3α and GSK-3β are needed to identify signals that control the expression of each isoform.

For many years GSK-3α and GSK-3β were often considered as identical twins, in part because all known GSK-3 inhibitors inhibit both isoforms so it was difficult to identify differential effects of the two isoforms. Unfortunately, many studies have attributed the outcomes of treatments with GSK-3 inhibitors specifically to GSK-3β, leading to incorrect conclusions that GSK-3β selectively mediates the processes under investigation. There is also a widely held misconception that certain commercially available GSK-3 inhibitors are specific for one isoform, but there is not a commercially available GSK-3 inhibitor that is selective for either isoform, although there is some progress in the development of GSK-3 isoform-selective inhibitors [78]. Recently, different actions of the GSK-3 isoforms have begun to be identified, primarily due to the advent of knockout and knockdown methods. Identifying individual actions of GSK-3α and GSK-3β was particularly stimulated by the finding that GSK-3β knockout mice are embryonically lethal, whereas GSK-3α knockout mice are viable, which provided an important demonstration that the two isoforms are not interchangeable. Studies in GSK-3α knockout mice, GSK-3β+/– heterozygote knockout mice, and with partial suppression of GSK-3β expression in mouse brain,

have demonstrated functions regulated by each isoform. However, in most cases this approach does not prove isoform-specific actions, as it may be unclear if the outcomes of isoform reduction are due to lower total levels of GSK-3, or to isoform-specific effects, unless outcomes of individually knocking down GSK-3α and GSK-3β are compared.

Although many substrates appear to be phosphorylated by both GSK-3 isoforms, there is a growing recognition that certain substrates are preferentially linked to one isoform and that the two isoforms differ in certain regulatory functions. As might be expected, since GSK-3α and GSK-3β have differences in their functional effects, there is also evidence of differences in signalling mechanisms that regulate the two isoforms. Since further identification of mechanisms that differentially regulate GSK-3α and GSK-3β may lead the way towards the development of interventions that can predominantly affect one isoform more than the other, this topic is likely to receive much attention in the near future [71].

1.2.6 Targeting glycogen synthase kinase-3 therapeutically

GSK-3 takes part into many signalling pathways associated with pathogenesis of different diseases, so it is not surprising that it is under investigation as a therapeutic target in multiple disorders. On the other hand, the great number of substrates that are phosphorylated by GSK-3 raises the question of whether this limits its feasibility as a therapeutic target, due to the potential disruption of many cellular processes. Based on over 60 years of safe and successful treatment of bipolar disorder with lithium, it is evident that a GSK-3 inhibitor can be tolerated and effective for many years, regardless of whether or not lithium's inhibition of GSK-3 contributes to its mood stabilization effects, which is still a matter of debate. Another important consideration is the extent to which GSK-3 should be inhibited therapeutically. As discussed previously, therapeutic levels of lithium only partially inhibit GSK-3, and this may be optimal for dampening GSK-3's self-activating mechanisms in disease processes while allowing GSK-3 to fulfil, unhindered, its many other cellular actions. In addition to the potential benefit of only partial inhibition of GSK-3, developing disease-selective inhibitors of GSK-3 should be possible based on the many previously listed mechanisms that regulate GSK-3. For example, it has already been developed an effective GSK-3 inhibitor peptide derived from the sequence of the GSK-3 primed substrate CREB, and a peptide inhibitor of GSK-3 that is primed by Akt-dependent phosphorylation was shown to be effective after insulin treatment. As more is learned about the mechanistic involvement of GSK-3 in individual diseases, it may be possible to develop inhibitors that predominantly block the actions of GSK-3 that are involved in pathological mechanisms. Thus, one goal for future development of therapeutic GSK-3 inhibitors will be to target specific cells or signalling pathways. Even as we await these developments, GSK-3 is already being considered as a therapeutic target in multiple conditions, as discussed below.

Psychiatric diseases

Psychiatric diseases are likely to be one of the major classes that are amenable to GSK-3 inhibitor

therapeutics. Patients with bipolar disorder, are already being effectively treated with lithium and there is no doubt that lithium is a GSK-3 inhibitor. Although the therapeutic mechanism of action of lithium remains to be definitively determined, substantial evidence indicates that inhibition of GSK-3 is an important component of lithium's mood stabilizing capacity. Lithium directly binds and inhibits GSK-3 by competing for a Mg^{2+} binding site. Besides directly inhibiting GSK-3, lithium administration at therapeutically relevant levels (i.e., near 1 mM lithium in the serum) also increases the inhibitory serine-phosphorylation of GSK-3 in rodent brain in vivo and in many other cell types, which can result from those amplification mechanisms previously discussed. Peripheral blood mononuclear cells from patients treated with lithium display increased serine-phosphorylated GSK-3, confirming that therapeutic levels of lithium inhibit GSK-3 and increase its inhibitory serine-phosphorylation in humans [71].

It is worthy to underline some of the implications of the increased serine-phosphorylation of GSK-3 induced by lithium. **First**, this induction only occurs with pools of GSK-3 that are subject to GSK-3's self-regulation via modulating phosphatases or other mechanisms previously discussed. Thus, the serine-phosphorylation of all cellular GSK-3 may not be equally affected by lithium. **Second**, this serine-phosphorylation of GSK-3 mechanism of action leaves untouched the activity of GSK-3 in the Wnt signalling pathway, and perhaps in other protein complexes. However, the direct inhibitory effect of lithium on GSK-3 is often sufficient to impede β-catenin degradation. **Third**, serine-phosphorylation of GSK-3 only inhibits its phosphorylation of primed substrates. **Furthermore**, accumulated primed substrates eventually can out-compete the phosphoserine of GSK-3 for binding to the primed substrate-binding pocket. Thus, the lithium-induced increase of serine-phosphorylated GSK-3 does not completely block its phosphorylation of primed substrates, but instead leads to a new increased steady state level of the primed substrate. It can be speculated that this may be crucial for allowing lithium to be therapeutic without completely blocking all of GSK-3's actions.

In addition to the substantial evidence that GSK-3 inhibition is therapeutic for bipolar disorder, there is evidence that GSK-3 inhibitors may contribute to therapies for depression, anxiety (, and schizophrenia.

Neurological diseases

There is abundant evidence that inhibition of GSK-3 is likely to be therapeutic for a number of neurological disorders. The evidence is particularly strong for Alzheimer's disease [79], where, GSK-3 has been demonstrated to promote every major pathological process, including amyloid β peptide production and tau phosphorylation, which lead to the two hallmark pathologies of Alzheimer's disease, amyloid plaques and neurofibrillary tangles, respectively. Much evidence also demonstrates that GSK-3 inhibitors improve many cognitive functions in rodent models of Alzheimer's disease. Encouraging findings for targeting GSK-3 have been identified in examinations of dementia development in bipolar patients that have been treated with lithium for long periods of time, as these patients often have a lower prevalence of dementia than the general population. Clinical trials of lithium in Alzheimer's disease have demonstrated some beneficial effects [80], although not in all studies.

Studies in rodent models have also demonstrated evidence of therapeutic effects of GSK-3 inhibitors in several other neurological disorders, e.g. Fragile X syndrome. There is also exceptionally strong evidence from mouse models that GSK-3 inhibitors are able to ameliorate the autoimmune disease multiple sclerosis, whose onset and progression are thought to be due to a combination of the effects of inflammation and pathogenic T cells, particularly Th17. Studies also have underlined the potential therapeutic benefits of GSK-3 inhibitors in several models of Parkinson's disease, Huntington's disease, stroke, traumatic brain injury and spinocerebellar ataxia type 1.

Most of the above mentioned diseases involve inflammation and neurodegeneration, and GSK-3 inhibitors are strong anti-inflammatory agents and neuroprotectants, reducing apoptosis after a wide range of insults. In addition to apoptosis, GSK-3 inhibitors also provide neuroprotection by other mechanisms, in particular multiple regulatory influences on dendrite and axon growth and repair. In some conditions, regulation of several components of the circadian rhythm by GSK-3 may also make a significant contribution. Thus, there are multiple mechanisms by which inhibition of GSK-3 may contribute to therapies of neurological and psychiatric disorders.

Inflammatory diseases

Diseases involving inflammation in the periphery have also been shown to benefit from the anti-inflammatory effects of GSK-3 inhibitors [81]. Remarkably, administration of GSK-3 inhibitors was sufficient to afford mice protection (survival) from an otherwise lethal dose of the inflammatory stimulant lipopolysaccharide used to model sepsis [82]. Administration of GSK-3 inhibitors also reduced inflammation and pathology in rodent models of asthma, arthritis, colitis, and peritonitis. Thus, GSK-3 inhibitors provide an effective intervention for all inflammatory diseases in which they have been tested in rodent models.

The strong pro-inflammatory action of GSK-3 in multiple peripheral and CNS diseases raises the question of why evolutionary mechanisms did not provide the means to more adequately down-regulate the activity of GSK-3 in inflammatory conditions. It could be hypothesized that a significant survival benefit is achieved by GSK-3 promoting responses to infection and stress, both of which activate inflammatory responses. Thus, survival may have benefited from GSK-3 promoting both innate and adaptive immune responses, increasing the production of multiple inflammatory cytokines and promoting the production of Th1 and Th17 inflammatory T cells, which should increase resistance to injury and infection. However, these same innate and adaptive immune responses can exacerbate chronic conditions that have become more prevalent in modern societies, such as neurodegenerative diseases, mood disorders, asthma, arthritis, and diabetes. Therefore, GSK-3 inhibitors provide feasible means to counteract excessive inflammation that is involved in a diverse number of chronic conditions.

Cancer

There is much interest in GSK-3 as a potential therapeutic target in many types of cancer. However, this application is complicated by findings that GSK-3 can act as a tumor suppressor or

it can promote cell proliferation in different types of cancer. The tumor suppressor action is exemplified by GSK-3-mediated phosphorylation of β-catenin and its subsequent degradation, a transcriptional co-activator that often promotes cellular proliferation. There is evidence that GSK-3 acts as a tumor suppressor in some skin and breast cancers. On the other hand, the tumor promoting actions of GSK-3 are indicated by the elevated levels of GSK-3 present in certain types of tumors and/or by the anti-proliferative effects of GSK-3 inhibitors, such as in colon and pancreatic cancers, in Non Small Cell Lung Cancer [83] and in mixed lineage leukemia.

These differences in the actions of GSK-3 in various types of cancer may have obstructed the development of GSK-3 inhibitors for cancer. Examination of the mechanisms underlying the opposite actions of GSK-3 in different types of cancer may provide opportunities to better understand the mechanistic cellular changes and to identify those that may safely benefit from GSK-3 inhibitor administration. In fact the type of apoptosis (GSK-3 has opposite actions on the intrinsic and extrinsic apoptotic signalling pathways), the role of β-catenin, and the actions of NF-κB are likely important in the actions of GSK-3 and its inhibitors in specific cancers, making it difficult to harness potential therapeutic interventions.

Other conditions

In addition to the diseases discussed here, potential therapeutic applications of GSK-3 inhibitors have been explored in other prevalent conditions, including cardiovascular diseases [84], AIDS, bone disorders, and diabetes.

1.2.7 GSK-3 inhibitors

Apart from Lithium, several GSK-3 inhibitors have been recently developed and more than 30 are currently available, most of which acting with a ATP competitor mechanism[85]. Among ATP competitor GSK-3 inhibitors it is worthy to mention Aloisines, Hymenialdisines, Indirubins, and Maleimides, among not ATP competitor the Tiadiozolidinoni (TDZD), including Tideglusib which is currently involved in phase II-III trials. As previously explained, there is not a commercially available inhibitor that is selective for either GSK-3 isoform, although there is some progress in the development of GSK-3 isoform-selective inhibitors [78]. SB216763 and SB415286 are two structural distinct maleimides (Figure 1.12), able to travel across the plasma membrane, acting as ATP competitors selectively on GSK-3α and GSK-3β. These two compounds have been shown to drastically reduce the GSK-3 activity; indeed they were able to induce all the answers induced by GSK-3 inhibition and resulted useful drugs in the study the role of GSK-3 in different signal pathways [86].

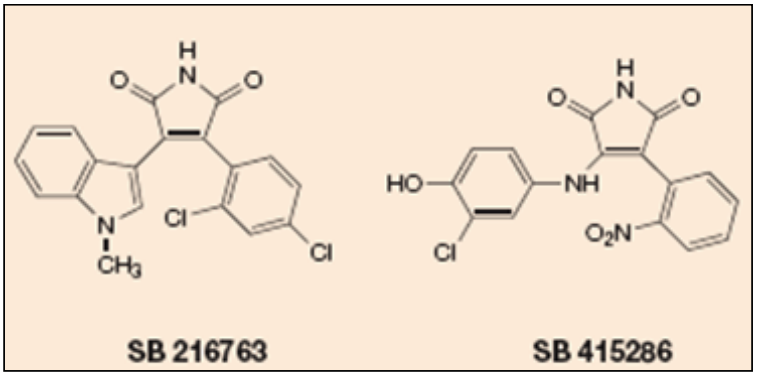

Figure 5. Structure of GSK-3 inhibitors SB216763 and SB415286

1.2.8 GSK-3 in the context of fibrosis

The role of GSK-3 in the context of fibrosis has been studied in different tissues, including liver, heart and lung. Only few data are available on the role of GSK-3 in the context of pulmonary fibrosis

It is believed that distinct intracellular pools of GSK-3 can simultaneously regulate divergent signalling pathways within the same cell, and the large number of putative substrates suggest that GSK-3 act as a key regulator of cellular processes in fibroblasts (Ding et al., 2000; Götschel et al., 2008). However, the role of GSK-3 signalling in human lung fibroblasts function is still largely unknown. Previous studies have tried to assess the contribution of GSK-3 signalling to myofibroblast differentiation of human primary lung fibroblasts. It has been reported a critical involvement of the GSK-3 signalling in the TGF-β1-induced myofibroblast differentiation, pointing either on his negative role by inhibiting β-catenin nuclear translocation or on its positive role by regulating CREB-dependent signalling. Thus, GSK-3 inhibition has been suggested either as a pro-fibrotic strengthening of TGFβ1-dependent differentiation to myofibrobasts, due to β-catenin accumulation [87], or as a possible anti-fibrotic strategy, due to the consequent phospho-CREB-mediated antagonism of TGFβ/SMAD signalling [88] (Figure 6).

In epithelial alveolar type 2 cells and in other epithelial cell types GSK-3 has been shown to negatively regulate epithelial to mesenchymal transition (EMT) [89].

We previously demonstrated the in vivo anti-inflammatory and anti-fibrotic properties of the specific inhibitor of the kinase GSK-3, SB216763, in a mouse model of BLM-induced lung fibrosis [90].

Therefore it seems that GSK-3 role is context and cell type-dependent and, in the still poorly understood pathogenesis of pulmonary fibrosis, more investigation is needed to assess the exact role of GSK-3. It is likely that cell to cell interaction and in vivo pro-fibrotic microenvironment (including ECM) can significantly influence the consequences of GSK-3 inhibition.

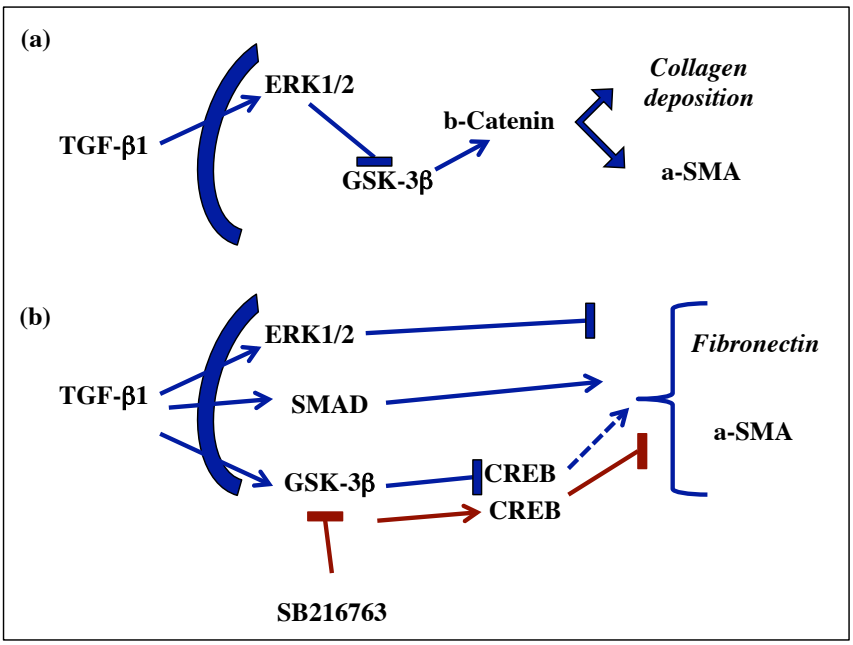

Figure 6. Two different GSK-3 roles in myofibroblast differentiation. (a) GSK-3 pharmacologic inhibition increases availability of β-Catenin, due to its reduced degradation, which moves into the nucleus and drive myofibroblast differentiation [87]. **(b)** Pharmacologic inhibition of GSK-3 allows the phosphorilaiton of CREB, which in turn acts as an antagonist of the TGF-β/smad signalling [88].

1.3 Pulmonary fibrosis mouse model

A universally trusted in vivo or in vitro model of IPF is still lacking. Nonetheless, experimental lung fibrosis models are routinely used for the identification of relevant underlying pathogenic mechanisms and assessment of drug efficacy. Unfortunately, IPF research is hampered by animal models that do not recapitulate all the features of the human disease, and whose ability to predict future clinical outcomes has been questioned. From the plethora of pathways/targets that show anti-fibrotic potential in these experimental models, few have gone on to show benefit in clinical trials [91]. Several different models exist [92], of which lung fibrosis induced by bleomycin application is probably the best characterised and most widely utilised, although there is no accepted standardised version of this model [93]. A variety of factors will affect the nature of the fibrotic response, including the route of administration, the bleomycin preparation, dose, mouse strain, age and so on. Prophylactic dosing schedules and nonconditional genetically deficient mouse studies often report beneficial effects, but potentially not through a direct antifibrotic response, but instead by dampening the early inflammatory reaction to bleomycin [94].

However, the BLM-induced mouse model of pulmonary fibrosis is still considered, by many researchers, the gold standard in the field of IPF and evidence deriving from this mouse model are still required before moving to phase I clinical trials for possible new IPF-targeted drugs.

1.3.1 Bleomycin

Bleomycin (Figure 7) is a glycopeptide of 1.5 kDa produced by *Streptomyces verticillus[95]*. This molecule has antitumor and antiviral activity and acts mostly by blocking the cell cycle in G2 phase. The bleomycin stimulates the lung damage through its ability to interlayer the DNA every 5 base pairs, inducing a site specific nick (between G-C and G-T bases) and a non-specific nick both in the single and in double helix. Moreover bleomycin is able to inhibit the DNA repair enzymes such as DNA ligase. This compound is usually degraded by bleomycin-hydrolyse enzymes, that are expressed in several tissues, except skin and lung. In the extremities this molecule presents a DNA and Fe^{2+} binding regions. The Fe^{2+} binding region is necessary because acts like co-factor able of damaging the DNA with the consequent cytotoxic effect.

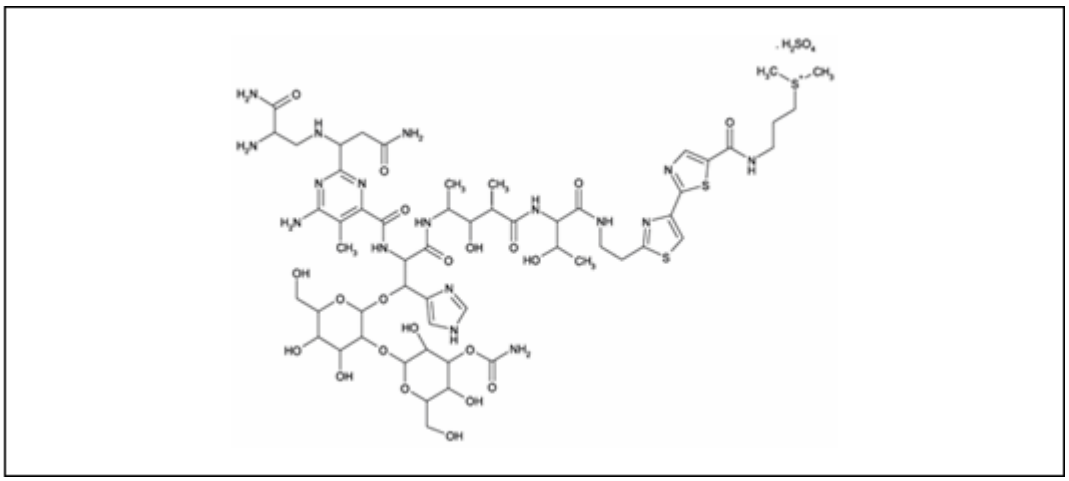

Figure 7. Chemical structure of bleomycin

This drug is in clinical use for chemotherapy of neoplasms such as squamous cell carcinoma of the cervix, oesophagus, skin, lung, neoplasms of testis germ cells, Hodgkin and non-Hodgkin lymphomas. Unfortunately, 10% of patients treated with a cumulative dose of bleomycin upper than 200U/m^2 develops interstitial pneumonia, that progresses to fibrosis. In terms of pathogenesis of lung inflammation, it has been demonstrated that the stimulation of Toll-like receptor 2 (TLR2) by bleomycin itself induces the activation of monocytes and pro-inflammatory chemokine release[96]. The ability of innate immune system to recognize and replay to exogenous agents is largely attributed to the Toll-like receptors family (TLRs). These receptors are mostly expressed on the surface of antigen presenting cells (APC) such as monocytes, macrophages and dendritic cells, and are able of discriminating among separate molecular patterns associated to microbial elements. The recognition by these receptors of products of pathogens stimulates several transduction signalling pathways that regulate the type, the scope and the duration of inflammatory response. In this context the inability of host itself to

regulate the type or duration of inflammatory response is critical, as in the case of inflammatory chronic diseases. The stimulation of TLR2 by bleomycin causes the activation of NF-κB, which in turn induces the transcription of genes for pro-inflammatory chemokines such as IL-8, IL-1β e TNF-α [96].

1.3.2 BLM-induced mouse model of Pulmonary Fibrosis

The pulmonary dose-dependent toxicity of bleomycin turned out to be useful to create experimental models of IPF in animals. Though several studies have highlighted the presence of important differences between the acute and the chronic phase in the pulmonary fibrosis of animals, the mouse model represents an evaluable tool in order to verify, *in vivo*, the proteins and the molecules involved in the pathogenesis of pulmonary fibrosis. Moreover the possibility to manipulate genetically the mice, creating knock out models, is useful to demonstrate the involvement of specific genes in pneumonia characterized by fibrosis development. In the mouse model of BLM-induced pulmonary fibrosis, the initial event is represented by the damage to epithelial lung cells, that stimulates the migration of granulocytes and fibroblasts into the injured tissue and the consequent migration of macrophages, lymphocytes and fibroblasts. The development of an acute inflammation is finally followed, within 21-28 days, by interstitial fibrosis. Only in some cases these mechanisms cause a "respiratory distress syndrome" leading to rapid death of animals before the establishment of fibrosis. This mouse model of pulmonary fibrosis draws near some key characteristics of human pulmonary fibrosis, including the damage to alveolar epithelial cells, recruitment of inflammatory cells, proliferation and activation of fibroblasts responsible of extracellular matrix production and deposition in the pulmonary parenchyma. The anatomic-pathologic characteristic of lung lesions, in particular, specifically recall the characteristic pattern of UIP found in IPF human pulmonary biopsies. Nonetheless there are also significant differences between the mouse model and the human IPF. First of all, in human beings, disease is diagnosed when fibrosis is already established and the early natural history of IPF, its causal factors and pathogenetic mechanism, are not anymore comprehensible. Second, the updated pathogenetic hypotheses significantly down-graded the role of inflammation in fibrosis establishment, whilst inflammation is definitely the *primum movens* in BLM-driven lung damage. Third, mouse underwent BLM administration, when surviving after the acute phase and not dying due to respiratory failure around day +28 experience complete spontaneous resolution of fibrotic process. This last point has been partially contradicted by a recent micro-CT based study, showing how the fibrotic lesions did not completely resolve, but instead persisted for several months following a single insult with bleomycin [94]. Thus, lacking a trustable *in vitro* model of disease and given the impossibility to only consider the information obtained by human pulmonary biopsies and to directly test new drugs on human beings, the role of an animal model that can reproduce, as faithfully as possible, the characteristics of IPF [97] is still irreplaceable.

1.3.3 GSK-3 in the mouse model of pulmonary fibrosis

We previously demonstrated the anti-inflammatory and anti-fibrotic properties of the specific inhibitor of the kinase GSK-3, SB216763, in a mouse model of BLM-induced lung fibrosis. In particular, GSK-3 resulted greatly expressed in the sites of inflammation and fibrosis and its inhibition reduced the recruitment of T-lymphocytes, the neutrophil activation and the expression of the macrophagic cytokines TNF-α and MCP-1, evidencing a key role of this Ser-Thr kinase in lung inflammation. Moreover, the late administration of the molecule has been shown to directly affect fibrosis, irrespective of the previous inflammatory phase of the process [90].

2. AIM OF THE PROJECT

In this study, we used the BLM mouse model to investigate the role of the kinase GSK-3 and its SB216763-mediated inhibition in modulating the expression and activity of MMP-9 and MMP-2 and their inhibitors TIMP-1 and TIMP-2 in the development of BLM-induced fibrosing alveolitis. We focused on Brocho-Alveolar Lavage Fluid (BALF) and lung tissue expression of MMPs and TIMPs. We also investigate the impact of GSK-3 silencing or knock-out on A549 and MEF cell lines, respectively, as models of epithelial alveolar type 2 cells and lung fibroblasts. A better understanding of GSK-3 role in pulmonary fibrosis development and, in particular, in modulation of ECM remodelling is the first step to assess the suitability of this kinase as potential therapeutic target in IPF.

3. METHODS

3.1. Drugs

Betadine: povidone-iodine (PVPI) topical antiseptics (B/BRAUN, Milan, Italy).
Zoletil: combination of a dissociative anesthetic agent, tiletamine hypochloride, and a tranquilizer, zolazepam hypochloride (Virbac.srl, Milano, Italy). This drug is used for injection anaesthesia in dogs, cats, wild and zoo animals. It produces dose-dependent sedation to general anaesthesia.
Xilor: xylazine is a muscle relaxant and sedative drug, for veterinary use (bio98 srl, Milano, Italy). It is often used in combination with zolazepam in general anaesthesia.
Bleomycin: glycopeptide antibiotic (Aventis Pharma SpA, Varese, Italy) produced by the bacterium *Streptomyces verticillus*. This drug acts by induction of DNA strand breaks and it is used in the treatment of several diseases, such as Hodgkin lymphoma (as a component of the ABVD regimen), squamous cell carcinomas, testicular cancer, pleurodesis as well as plantar warts.
SB216763: highly selective GSK-3 inhibitor (Sigma-Aldrich, St. Louis, MO, USA). This compound is an arylindolemaleimide that inhibits GSK-3 in an ATP competitive manner [86, 98].
SB203580: MAPK p38 inhibitor (Sigma-Aldrich, St. Louis, MO, USA)
PD98059: ERK inhibitor (Sigma-Aldrich, St. Louis, MO, USA)
TNFa: (Sigma-Aldrich, St. Louis, MO, USA)

3.2 Mouse model

Mice

C57BL/6N mice obtained from Charles River, Jackson Laboratories Inc. (Milan, Italy), were used for this study. Mice were housed under ethical conditions in a pathogen-free animal facility. Mice were used at 12 weeks of age. All procedures were approved by local Animal Care Committee of the University of Padova (Padova, Italy).

Experimental protocol

C57BL/6N mice were randomized into four different subgroups as previously described: (Gurrieri C. et al., JPET, 2010): one treated with saline and another one treated with saline plus SB216763 as control groups, one treated with BLM plus vehicle and the last one treated with BLM plus SB216763. Mice were anesthetized with an intraperitoneal administration of a mixture of ZOLETIL 100 (40-80 mg/Kg) and XILOR. Trachea was surgically exposed and sterile isotonic saline or bleomycin sulfate (3 U/Kg) (Aventis Pharma SpA, Varese, Italy) was instilled into the trachea through a 29-gauge needle. SB216763 (20 mg/Kg) (Sigma-Aldrich, St. Louis, MO) dissolved in dimethhyl sulfoxide and polyethylene glycol was administered

intraperitoneally twice a week. Mice were sacrificed 7 or 28 days after BLM or saline administration by CO_2 narcosis. The lungs from different animals were processed for immunohistochemical and biochemical studies; all lobes underwent histological analysis, separately. At the time of sacrifice, mice underwent broncho-alveolar lavage (BAL).

Bronchoalveolar Lavage (BAL) and cell count in BAL fluid (BALF)

Trachea was exposed and isolated in the site previously sutured and airspaces were lavaged three times with 0.5 ml of sterile saline. BAL was centrifuged and supernatant was stored at -80°C for the zymographic analysis. BAL cells were adjusted to the final concentration of 1 x 10^6 cells/mL in phosphate buffer saline and total cell counts were performed by manual counting under light microscopy with a standard haemocytometer chamber. Finally, 100 mL of BAL cells were smeared on a glass slide and then stained with May-Grünwald Giemsa dyes. Differential counts on 200 cells were made using standard morphological criteria.

3.3 Histology

Lung tissues were fixed in formalin, embedded in paraffin and dissectioned in 4-5μm slices. Subsequently they were stained with Hematoxylin&Eosin (H&E), to evaluate the degree of inflammatory cell infiltration and epithelial alveolar cuboidalization and stained with Masson's trichrome to evaluate the degree of interstitial fibrosis. Then, each section was scanned at 40X magnification to identify at least 5 areas (hot spots) with the largest extension of fibrosis (Trichrome staining). Each hot spot was then examined at X 200 magnification (0.949 mm^2/field) and the fibrosis was quantified by using digital quantitative analysis (Image Pro Plus software version 4.1, Media Cybernetics, Silver Spring MD). The mean value of the five areas was taken as representative of the whole section.

Histochemistry

Lung sections were first washed in 1% H_20_2 PBS and then blocked for 30 minutes in 1% FCC and 0,3% Triton X-100 blocking medium. They were then incubated with primary antibodies (MMP9, MMP2, TIMP1 and TIMP2, 1:500; Santa Cruz Biotechnology, CA). Sections were subsequently washed in PBS and incubated with second stage biotinylated antibodies. After diaminobenzidine (DAB) staining and hematoxylin counter-staining, sections were mounted in Poly-Mount medium (Polysciences, Warrington, PA).

3.4 Gelatin Zymography

Aliquots of BAL fluid were mixed with 4X non reducing sample buffer (1,25M Tris-HCL pH 6.8, 10% (w/v) sodium dodecyl sulfate (SDS), 40% (v/v) glycerol, 1% bromophenol blue) (3:1, v/v) and electrophoresed on 8% SDS-PAGE containing 1% gelatin (Sigma-Aldrich, St. Louis, MO) as MMP-9 and MMP-2 substrate. Following electrophoresis the gels were washed twice with 2.5% Triton X-100 and then incubated overnight at 37°C in developing buffer (50mM Tris-

based, 200mM NaCl, 10mM $CaCl_2$, pH 7.4). The gels were stained with 0.5% (w/v) Comassie Brilliant Blue R-250 (Sigma-Aldrich) in 30% methanol and 10% acetic acid and destained in a solution of 30% methanol and 10% acetic acid. Gelatinases appear as clear bands against blue background. (We used recombinant protein molecular weight markers to estimate the weights of the gelatinolytic bands.) Relative enzyme amounts were quantified by measuring the intensity of the bands with the pixel-based densitometer program Quantity One®, 1-D Analysis Software (Bio-Rad Laboratories, Inc., Hercules CA).

3.5 Western blot analysis

Protein quantitation has been performed using Bradford staining (Sigma-Aldrich) and spectroscopic analysis before running in SDS-page electrophoresis. Primary antibodies: GAPDH monoclonal (Ambion, USA), MMP-9 policlonal (Millipore, MA, USA), TIMP-1 policlonal (Millipore, MA, USA), p38 and phospho-p38 (Tyr180/Tyr182) (Cell Signalling, MA, USA), SAP-JNK and SAP-JNK Thr180/Tyr185 (Cell Signalling), ERK and ERK Thr202/Tyr204 (Cell Signalling), p65 and phospho-p65 (Ser536) (Cell Signalling), IKBα and phospho-IKBα (Ser32/Ser36) (Santa-Cruz) and GSK-3 total (Santa Cruz). Secondary antibodies: rabbit anti-mouse HRP-conjugated and policlonal goat anti-rabbit GE Healthcare (Buckingamshire, UK)

3.6 Quantitative real-time PCR amplification

Total lung RNA was extracted from mouse lungs using TRIzol reagent (Invitrogen Life Technologies, Grand Island, NY) and reversed transcribed into cDNA using Reverse Transcription System (PROMEGA, Madison, WI) according to the manufacturer's instructions. Quantitative real-time PCR amplification was performed on an ABI PRISM 7000 sequence detection system (Applied Biosystems, Foster City, CA). Reactions were carried out with Platinum® SYBR® Green qPCR SuperMix-UDG kit (Invitrogen Life Technologies, Carlsbad, CA). Primer sequences are reported in Table 1.

Gene	*Forward-primer (3' to 5')*	*Reverse-primer (3' to 5')*
β-actin	CTC TCC CTC ACG CCA TCC TG	TCA CGC ACG ATT TCC CTC TCA G
MMP-9	CGA CGG CAA GGA CGG C	GTA AGT GGG GAT CAC GAC GC
MMP-2	CGG TTT ATT TGG CGG ACA GTG AC	ATT CCC TGC GAA GAA CAC AGC
TIMP-1	TGG CAT CCT CTT GTT GCT ATC ACT G	TGA ATT TAG CCC TTA TGA CCA GGT CC
TIMP-2	TGC AGA CGT AGT GAT CAG AGC CAA A	AAC TCG ATG TCT TTG TCA GGT CCT T

Table 1. Primers used for quantitative real-time PCR.

Data analysis

Amplification, detection, and data analysis were performed using the ABI PRISM 7000 sequence detection system (Applied BioSystem, Foster City, CA). The quantification of mRNA levels was obtained by a method of relative quantification, the Delta-Delta Ct method (2-DDCt), following the instructions of the manufacturer (Applied Biosystems). The mice treated with saline or plus SB216763 have been used as internal calibrator of the samples. Once set the threshold line and the baseline, the corrispective Ct values were calculated. For each sample were calculated:

1. $DCt_n = Ct_n(gene) - Ct_n$ (β-actin)
2. $DDCt_n = Ct_n(sample) - Ct_n$ (internal calibrator)
3. Relative Quantification= 2^{-DDCtn}(sample)

In this way for each sample has been calculated a value which represents the relative genic quantification, compared to the sample used as internal calibrator and considered of value 1.

3.7 Cell culture and treatment

A549 cells were cultured at in Dulbecco's modified Eagle's medium (EuroClone; Milano) supplemented with L-glutamine (2 mM), glucosio (4,5 g/L) e Na-pyruvate, penicilline (100 U/ml), streptomycine (100 μg/ml) (Euroclone) and 10% fetal bovine serum (FCS, EuroClone) at 37 °C, in a humidified incubator with an atmosphere of 5% CO_2.

Gene silencing - RNA interference (RNAi)

RNA interference (RNAi) is a process within living cells that moderates the activity of their genes. Two types of small ribonucleic acid (RNA) molecules – microRNA (miRNA) and small interfering RNA (siRNA) – are central to RNA interference. RNAs are the direct products of genes, and these small RNAs can bind to other specific messenger RNA (mRNA) molecules and either increase or decrease their activity, for example by preventing an mRNA from producing a protein. RNA interference has an important role in defending cells against parasitic genes – viruses and transposons – but also in directing development as well as gene expression in general. In this work we used RNAi to down-modulate GSK-3α and GSK-3β expression. In particular we chose siRNA oligos provided by Dharmacon, Thermo Scientific (Waltham, MA): (Table 2), a control oligo without target called SCRAMBLE (SCR), and a siGLO GREEN oligo, used to verify transfection efficiency.
$1.5X10^5$ cells were seeded on 6 wells plates in DMEM medium without antibiotics. Once reached a minimum of 60% confluence, oligonucleotides (140 pmol/well) were diluted in OPTIMEME medium and combined with lipofectamine. Oligonucleotides-Lipofectamine complexes, were then added to each well. Transfection efficiency was monitored 48 hour later through flow cytometry, assessing the percentage of siGLO-GREEN positive cells. Cell were stimulated 48 hours later, after 24 hours of serum starvation.

The down modulation of GSK-3α and GSK-3β genes was verified through western blot and real-time PCR analysis.

Gene	Oligonucleotides sequences
GSK-3α	UCACAAGCUUUAACUGAGA
GSK-3β	GAUCAUUUGGUGUGGUAUA

Table 2: siRNA oligonucleotides sequences

Cell treatment

After transfection and 24 hours of serum starvation, cells were stimulated with TNFa (15 ng/mL) and eventually pre-treated with specific inhibitors. Analysis were then performed 24 or 48 hours after stimulation.

3.8 Statistical analysis

All data are expressed as means ± S.E.M. Statistical differences among groups were determined using Student's test or one-way ANOVA test.. Where needed in the case of failure of the normality tests, analyses were followed by Tukey's test. Significance was defined at the $p < 0.05$ level unless otherwise stated.

4. RESULTS

4.1 In vivo Results (BLM mouse model)

In vivo GSK-3 inhibition has a protective effect on BLM-induced lung inflammation and fibrosis

C57BL/6N mice were randomized into 3 different subgroups: one treated with saline (PBS) a second one treated BLM plus vehicle and the last one treated with BLM plus SB216763. The SB216763-treated group received the inhibitor every 48 hours until sacrifice at day 7 or 28. At the time of sacrifice, mice underwent bronchoalveolar lavage (BAL) and a mean volume of 1.3 mL of BAL fluid (BALF) was obtained. Lungs were then collected and each lobe was separately analyzed by the pathologist. As previously described [90], BLM induced a significant alveolitis at day 7 and lung fibrosis at day 28, while SB21 treatment confirmed his anti-inflammatory and anti-fibrotic potential, as shown in Figure 1 and 2.
In particular, BLM-treated mice presented a significant increase in BALF cell count at day 7, ($5{,}7x10^6$ ± $2{,}1x10^6$ cells/ml); in the BLM+SB216763 group BALF cell count was found significantly reduced ($3{,}2x10^6$ ± $1{,}4x10^6$ cells/ml, $p<0.05$) (Figure 1). PBS treated mice did not present alveolitis at this time point. The same trend was confirmed at day 28 (data not shown). Histologic analysis of lungs collected at day 7 showed a similar behaviour of inflammatory infiltrate.

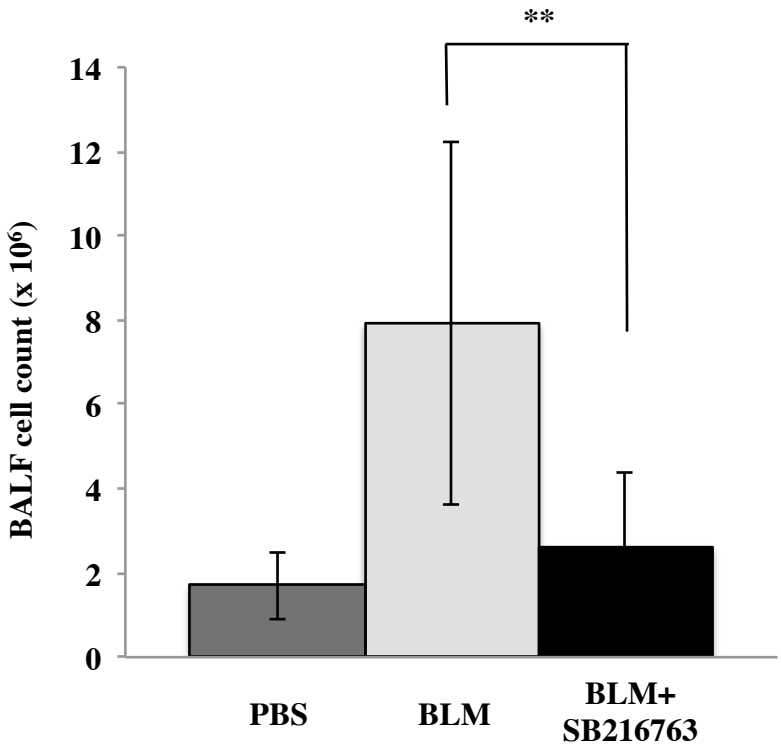

Figure 1. SB216763 reduces BLM-induced alveolitis at day 7 *(**) means p<0.05*

The pathologic score for epithelial alveolar cell cuboidalization (a good index of epithelial damage) and for lung fibrosis resulted consistent with a significant effect of the GSK-3 inhibitor on the late fibrotic phase of the BLM-induced lung damage (Figure 2).

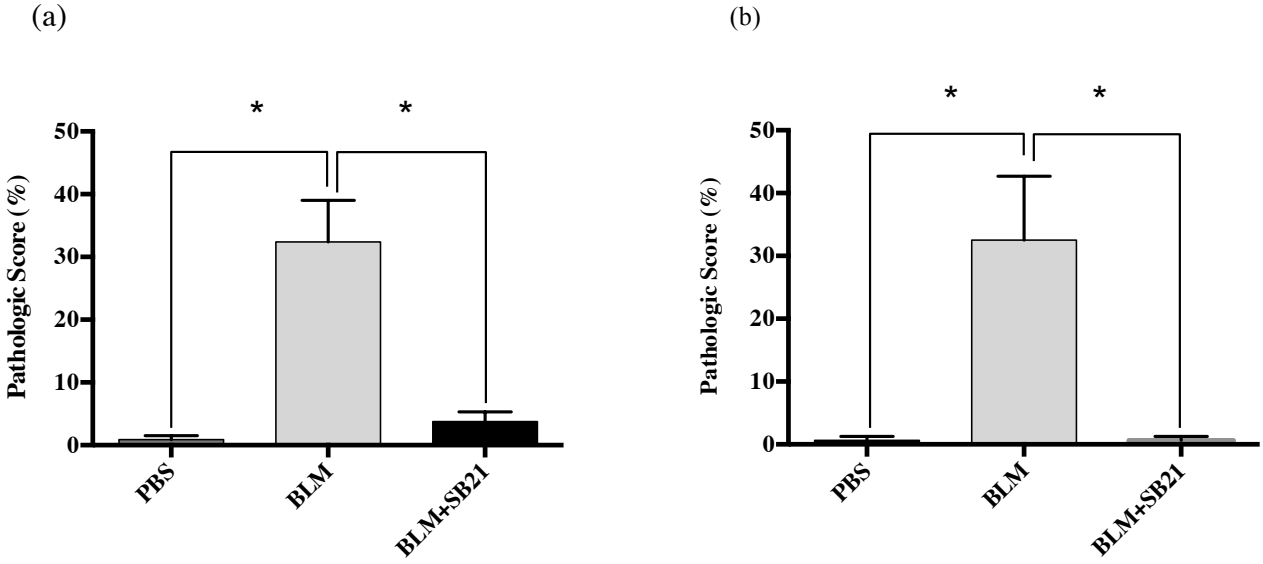

Figure 2. SB216763 reduces BLM-induced epithelial alveolar cell cuboidalization (a) and lung fibrosis (b) at day 28 *(*) p<0.01*

SB216763 reduces alveolar lymphocytosis and neutrophilia induced by BLM at day 7

Differential BALF cell count showed that, in control mice, macrophages represented the main cell population; in contrast, mice exposed to BLM showed a strong increase of lymphocyte percentage as well as the appearance of the two sub-populations of neutrophils and eosinophils. The inhibition of GSK-3 with SB216763 significantly reduced the lymphocytes percentage ($p < 0.01$) which was offset by the growth of macrophages (Table 1). This finding was in accordance with the previously published flow cytometric data, showing how the inhibition of GSK-3 induced a reduction in $CD3^+$ T Lymphocyte percentage at day + 7 after BLM administration [90]. The reduction of neutrophils and eosinophils percentage resulted not statistically significant.

Experimental groups		total cells (x 10^6)	macrophages (%)	lymphocytes (%)	neutrophils (%)	eosinophils (%)
Saline	n=5/experiment	1.7 ± 0.8	96 ± 1.2	4 ± 3.2	0	0
BLM	n=5/experiment	7.9 ± 4.3$^{\Psi}$	62 ± 4.8	26 ± 7.0	10 ± 6.3	2 ± 1.5
BLM + SB216763	n=5/experiment	2.6 ± 1.8**	87 ± 6.4*	11 ± 6.1**	2 ± 1.5	0

Table 1. Influence of GSK-3 inhibitor SB216763 on BALF cell number and composition at day 7. Data are given as mean ± S.D. of three independent animal trials. *($^{\Psi}$) p <0.05 in comparison with saline group; (*) p<0.01 and (**) p <0.05 in comparison with BLM group by Student's t-test*

SB216763 reduces BLM-driven MMP-9 and MMP-2 activity in BALFs

We then performed a zymographic analysis of BALF supernatant, aimed at assessing the gelatinolytic activity of MMP-2 and MMP-9. Both MMP-9 and MMP-2 resulted elevated in the inflammatory phase (day 7) in mice treated with BLM compared to the PBS-instilled mice. Moreover, the *in vivo* treatment with SB216763 strongly reduced the levels of pro-MMP-9 ($p < 0.01$) while it mildly but still significantly reduced both (pro- and active) forms of MMP-2 ($p < 0.05$) as evinced by the densitometric analysis (Figure 3).

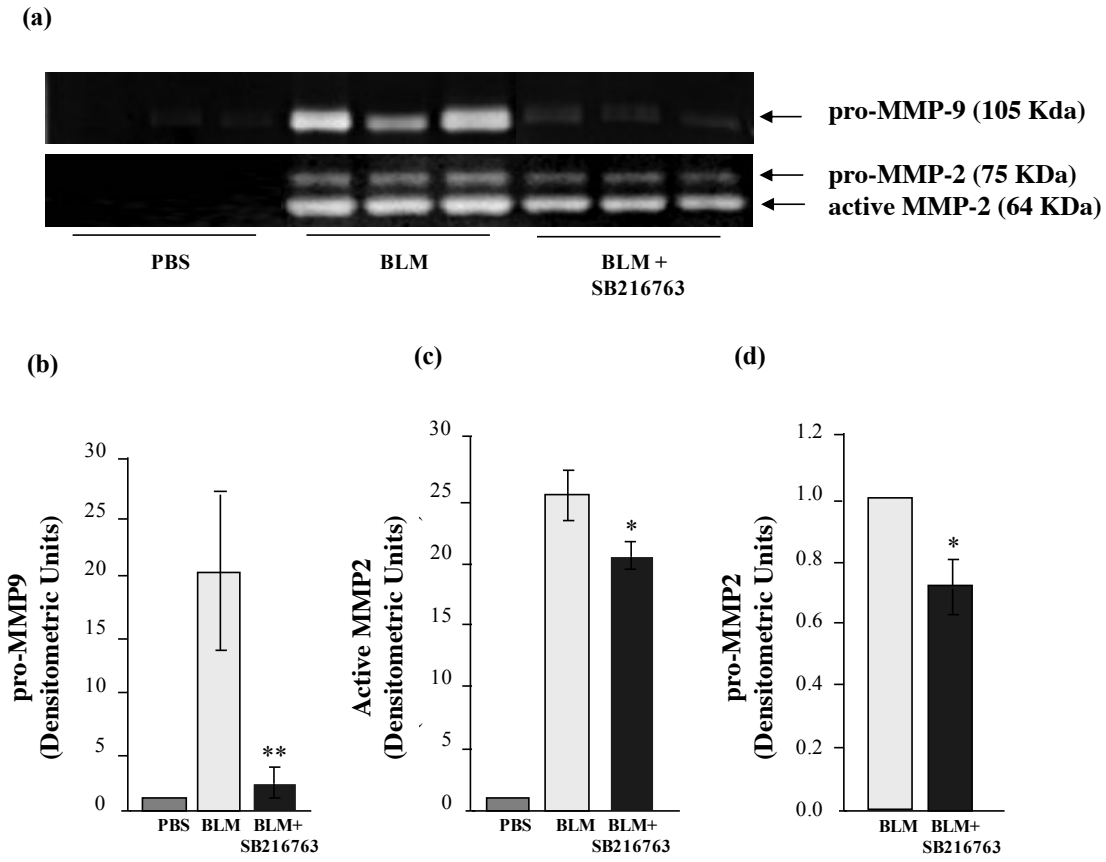

Figure 3. MMP-9 and MMP-2 gelatinolytic activity measured in BALF supernatants by zymographic analysis at day 7 (a) Zymographic analysis for pro-MMP-9, pro- and active MMP-2. Data are confirmed by densitometric analysis of pro-MMP-9 **(b)**, active MMP-2 **(c)** and pro-MMP-2 **(d).** *(*) p <0,05; (**) p< 0.01*

In the late fibrotic phase (day 28) mice treated with BLM showed very high activity of MMP-2 in BALF; GSK-3 inhibition strongly reduced both pro- and active forms of MMP-2 ($p < 0.01$), as showed by the densitometric analysis (Figure 4). MMP-9 activity was almost undetectable at day 28, both in BLM and in BLM + SB21673 group, with no difference compared to the PBS treatment (data not shown).

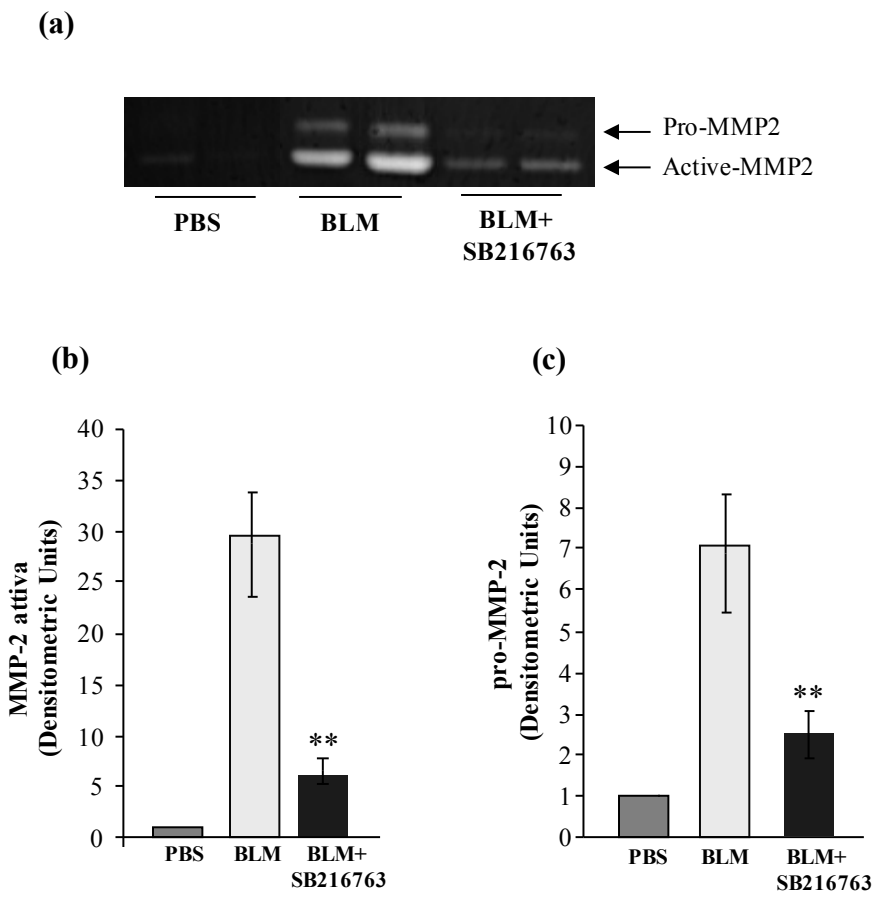

Figure 4. MMP-2 gelatinolytic activity measured in BALF supernatants by zymographic analysis at day 28. **(a)** Zymographic analysis. Densitometric analysis for active MMP-2 **(b)** and pro-MMP-2 **(c)**. *(**) p <0.01*

SB216763 reduces MMP-9, MMP-2 and TIMP-1 secretion induced by BLM in BALFs.

Once assessed the gelanotinolytic activity, we measured by Western Blot analysis the difference of secretion of MMPs and their inhibitors in BALFs between the cohorts of mice. In BLM-treated mice, MMP-9 and TIMP-1 protein levels were increased during inflammation (day 7), if compared to the controls (PBS). As shown in the blot image, the *in vivo* treatment with SB216763 strongly reduced pro-MMP-9 and its tissue inhibitor TIMP-1. On the contrary, as already suggested by zymographic analysis, MMP-2 was constitutively expressed in control mice and its levels were only slightly increased by BLM; SB216763 administration reduced MMP-2 to control levels, but the overall behaviour of this MMP was not relevant at day 7. (Figure 5a). Levels of TIMP-2 were not affected by BLM instillation (data not shown). BLM-treated mice sacrificed at day 28 showed very high protein expression of MMP-2 and only slightly increased levels of MMP-9 compared to the PBS, that was observed also by the zymographic analysis. Moreover, BLM-treated mice also had a greater secretion of TIMP-1 when compared with the controls. Finally, SB216763 down-modulated the protein levels of both MMP-2 and TIMP-1.

The same analysis has been performed on BALF of mice sacrificed at day 28. As expected from zimography, the effect of BLM was much more relevant for MMP-2 than for MMP-9 at this time point. Nonetheless, both MMPs increased after BLM instillation and SB216763 was shown to reduce their levels in the co-treated mice, restoring an almost physiological secretion. Finally, BLM treated mice presented a significant induction of TIMP-1, which was prevented by SB216763 regular administration during the 4 weeks before sacrifice (Figure 5b).

(a)

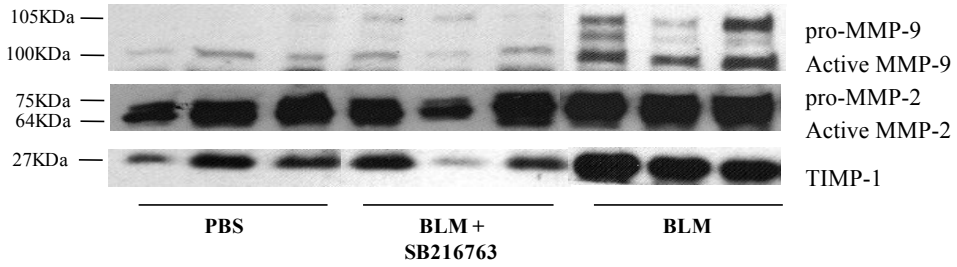

(b)

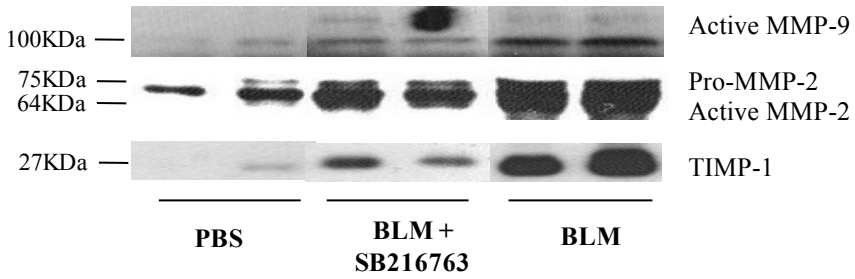

Figure 5. GSK-3 modulates protein expression of MMP-9, MMP-2 and TIMP-1. MMP-9, MMP-2 and TIMP-1 protein levels were assessed in BALF supernatants by Western Blotting at day 7 **(a)** and day 28 **(b).** Images are representative of 3 mice/group of one of three independent experiments. According to molecular weight, it is possible to recognize pro-MMP-9 (105KDa), active MMP-9 (<105KDa), pro-MMP2 (75 KDa), active MMP-2 (64KDa) and TIMP1 (27 KDa).

SB216763 reduces MMP-9, TIMP-1, MMP-2 and TIMP-2 mRNA levels increased by BLM in BALF cells.

After activity and secretion assessment, RNA was extracted from BALF cells and quantitative RT-PCR was performed in order to measure MMPs and TIMPs expression at a cellular level at day 7. BLM was shown to significantly increase MMP-2, MMP-9, TIMP-1 and TIMP-2 levels at this time point, while SB216763 administration was able to keep them comparable to those detected in control mice (Figure 6).

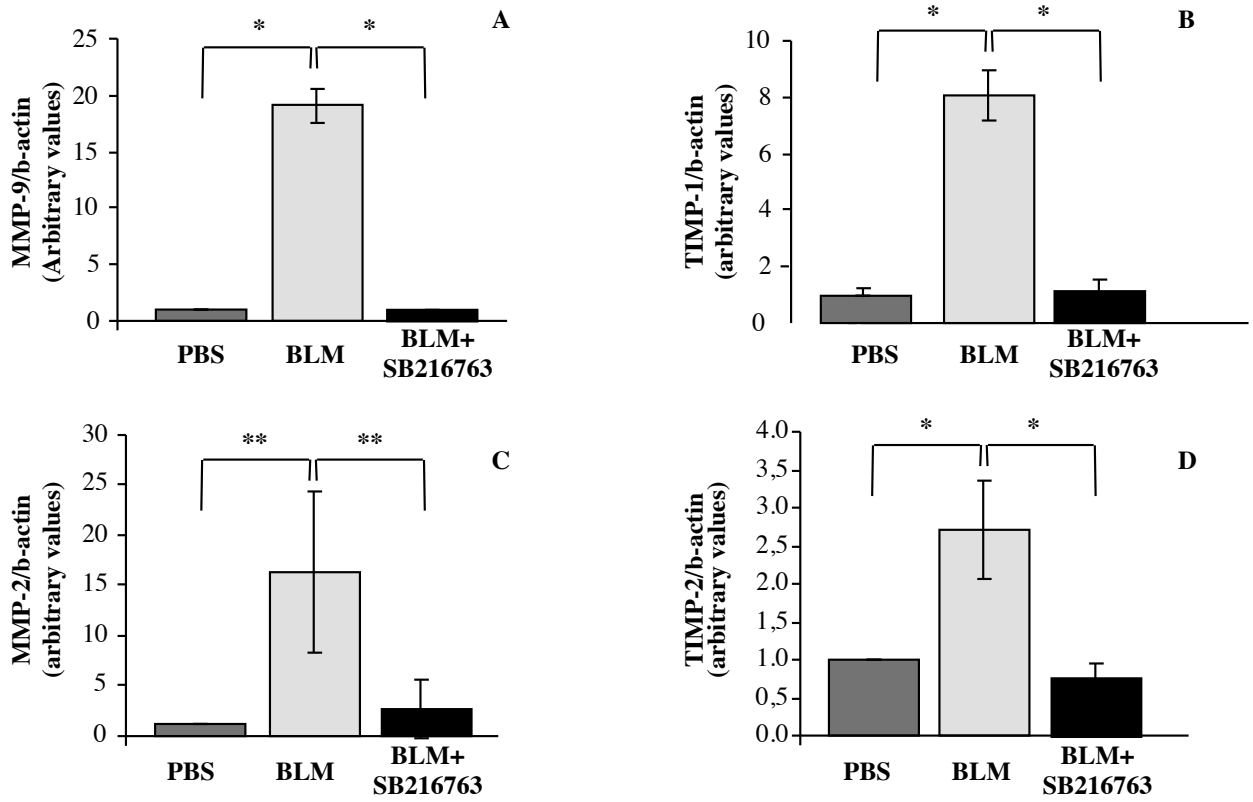

Figure 6. MMP-9 (A), TIMP-1 (B), MMP-2 (C) and TIMP-2 (D) transcript levels were quantified by Real Time PCR in inflammatory cells isolated from BALFs at day 7. Mice treated with BLM showed strong increase of MMP-9 and MMP2 gene expression levels compared to control mice. Also the mRNA levels of the tissue inhibitors, TIMP-1 and TIMP-2, were augmented by BLM treatment. Importantly, GSK-3 inhibition significantly reduced MMP-9, TIMP-1, MMP-2 and TIMP-2 transcript levels. *(n = 6/10/10) (*) p <0.01; (**) p <0.05*

SB216763 downmodulates MMP-9, TIMP-1, MMP-2 and TIMP-2 overexpression induced by BLM in interstitial alveolar macrophages and cuboidalized epithelial alveolar cells.

To correlate BALF-derived data with tissue expression of MMPs and TIMPs, we performed histochemistry staining of formalin-fixed paraffin-embedded lung tissue. Only interstitial alveolar macrophages (iAM) and cuboidalized tipe II epithelial alveolar cells showed a detectable expression of metalloproteases and their inhibitors, at day 7.

iAMs, the main population infiltrating lung interstitium at this time point, showed a strong staining for MMP9 (80±8.7%), TIMP1 (78±4.6%), and MMP2 (66±14%) and were moderately positive for TIMP-2 (55±28%) at day 7 after BLM instillation (Figure 7). *In vivo* SB216763 co-treatment moderately reduced iAM staining for MMP9 (50±24%) and markedly down-modulated TIMP-1 (32±26%) and TIMP-2 (22±18%) positivity. MMP-2 expression, instead, was not significantly affected by GSK-3 inhibition.

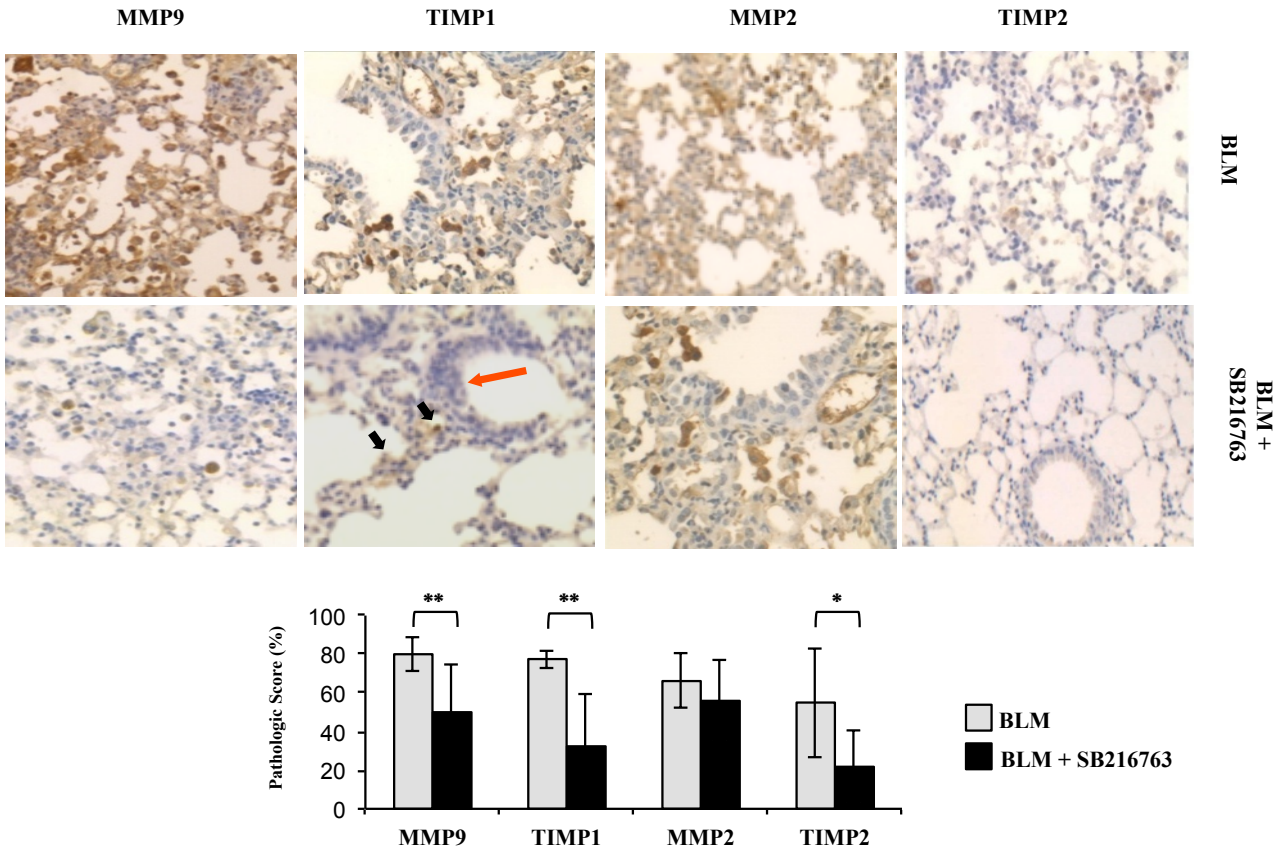

Figure 7. MMP and TIMP tissue expression was measured by the IC analysis of the lungs at day 7. BLM-treated mice showed high positivity for MMP-9, TIMP-1, MMP-2 and TIMP-2 in alveolar macrophages (iAMs). GSK-3 inhibition down-modulated their expression. The pathologic scores in IC analysis represent the percentage of positive cells for each specific markers. Data are given as mean ± S.D. of three independent animal trials. *(*) $p < 0.01$ and (**) $p < 0.05$.*

Moreover, cuboidalized type II epithelial alveolar cells showed an 80% MMP-9 positivity in BLM-treated mice at day 7, strongly reduced to 40% in the BLM + SB216763 group ($p > 0.05$, Figure 8). Cuboidalized type II epithelial alveolar cells also presented a relevant staining for MMP-2 (45%), TIMP-1 (55%) and TIMP-2; no epithelial staining for MMP-2 and TIMPs was detectable in SB216763-treated group (Figure 8). This finding is particularly significant, since cuboidalized type II pneumocytes represent a good marker of alveolar damage at day 7 and, at day 28, the degree of cuboidalization strongly correlate with the extent of fibrosis (Figure 2).

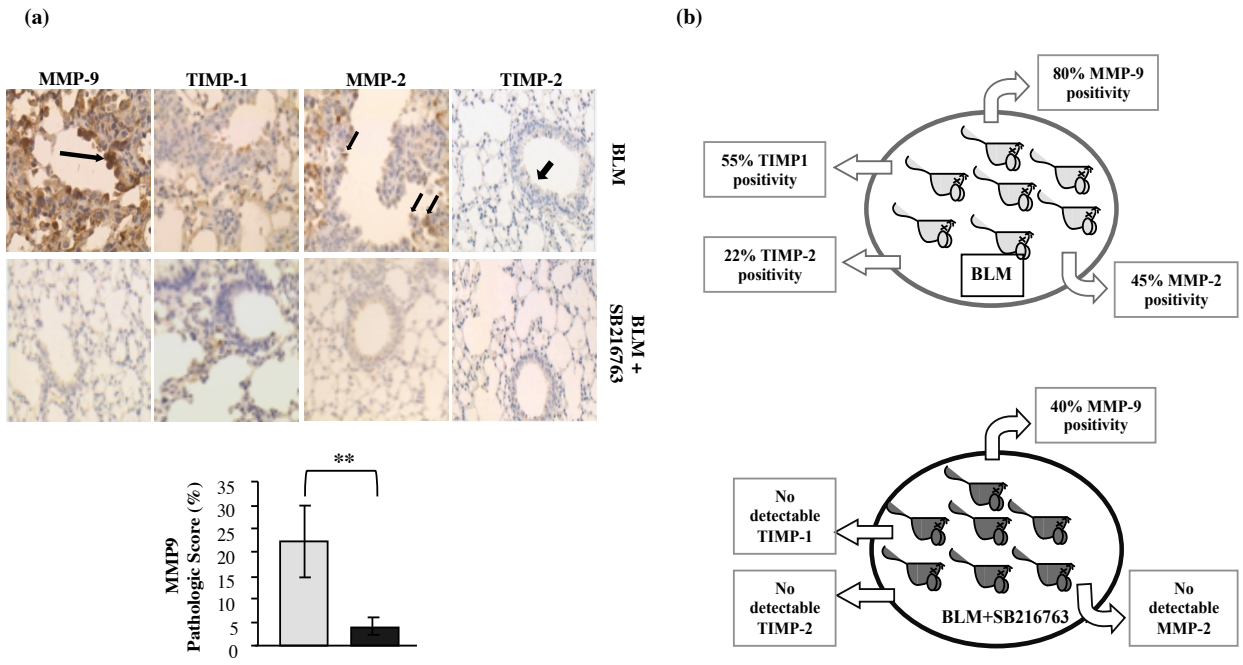

Figure 8. IHC staining of cuboidalized type II epithelial alveolar cells (a) MMP-9, TIMP-1, MMP-2 and TIMP-2 were specifically expressed in injured alveolar cells that underwent cuboidalization (black arrows) and SB216763 selectively reduced their expression. **(b)** The scheme summarizes the effects of GSK-3 inhibition in reducing the BLM-induced epithelial positivity for MMP-9, TIMP-1, MMP-2 and TIMP-2. In particular, BLM treated mice showed a moderate expression of MMP-9 in cuboidalized cells and SB216763 strongly decreased it, as showed in the mean ± S.D of 3 independent animal trials by the histogram. *(**) $p < 0.05$*

Finally, preliminary data from IHC analysis at day 28 showed a virtually absent MMP-9 expression in cuboidalized type II epithelial alveolar cells, while MMP-2 was significantly expressed, together with detectable TIMP-1 and -2. SB216763 treatment did not significantly affect MMP-9 expression, while reducing MMP-2. These results, even if preliminary, seem to confirm what detected in BALF.

4.2 In vitro results (A549 and MEF cells)

GSK-3 silencing induce an increase of MMP-9 activity, downstream of TNFα, in A549 epithelial alveolar cell line.

Since damaged epithelial alveolar cells are currently believed to play the main role in IPF pathogenesis, we decided to further investigate, in vitro, the effect og GSK-3 inhibition on an epithelial alveolar type II cell line, A549. These cells are a NSCLC-derived celle line, but they are the most used type II epithelial alveolar cell model in IPF research. Thus, we reproduced GSK-3α and β inhibition through siRNA and used TNFα as a well known MMPs inducer in A549, via NF-κB pathway. siRNA allowed us to obtain a significant degree of GSK-3 inhibition, which was indeed higher than that obtained in vivo using SB216763. Mean transfection efficiency was 97% after 48 hours in 3 indipendents experiments, as shown in Figure 9; GSK-3 silencing after 48 and 72 hours was significant for both paralogs, α and β, as shown by RT-PCR and Western Blot analysis (GSK-3 half life is 48 hours). Figure 9 shows flow cytometric analysis of transfection efficiency and RT-PCR and WB results for GSK-3 silencing.

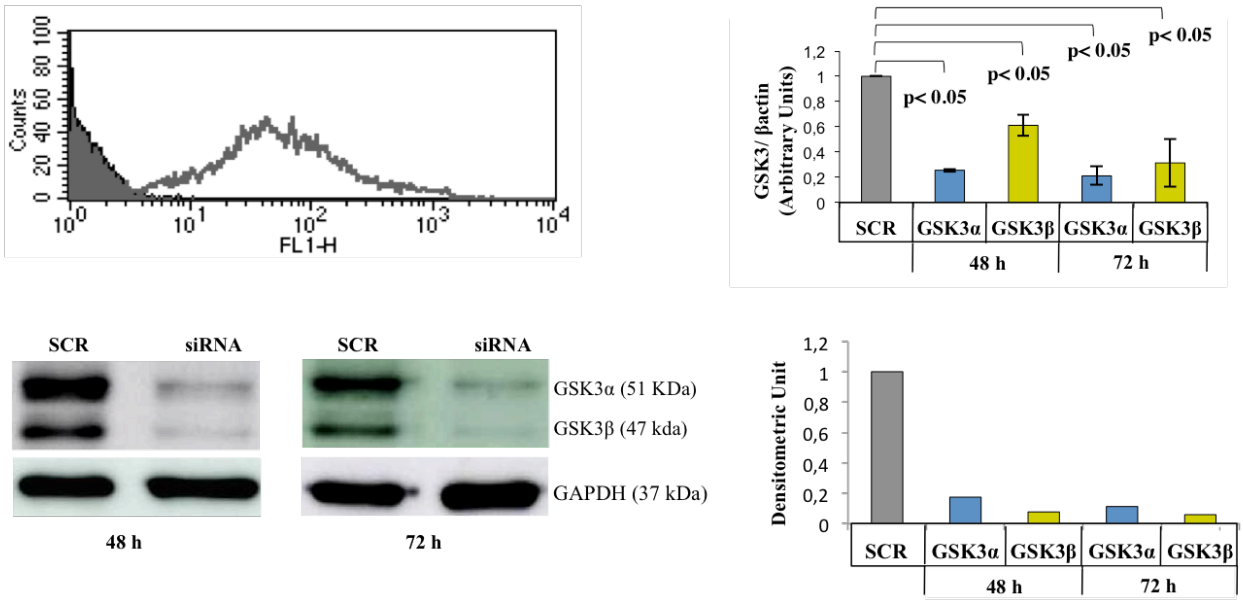

Figure 9. GSK-3 silencing in A549 cells. Mean transfection efficiency was 97% after 48 hours in 3 independent experiments. After 48 and 72 hours RT-PCR showed a degree of silencing of 80 and 85% for GSK-3α and of 40 and 85% for β isoform, respectively. In terms of protein expression. GSK-3α presented a decrease of 85% and 90% while GSK-3β decreased by 90% and 95% at 48 and 72 hours after transfection, respectively.

After tranfection with SCRAMBLE or GSK-3 silencing and 24 hours of serum starvation, A549 cells were stimulated with TNFα 15 ng/mL for 24 or 48 hours. Medium was then collected and used for zymographic analysis. As shown in Figure 10 and as expected on the basis of data available in literature, MMP-9 activity was induced by TNFα stimulation. Moreover, GSK-3 silencing significantly strengthen the TNFa effect on MMP-9 after 24 hours ($p < 0.01$) and 48 hours ($p < 0.05$) (Figure 10). MMP2 resulted constitutively expressed by A549 untreated cells and no treatment affected its activity, as well as its protein and gene expression (data not shown).

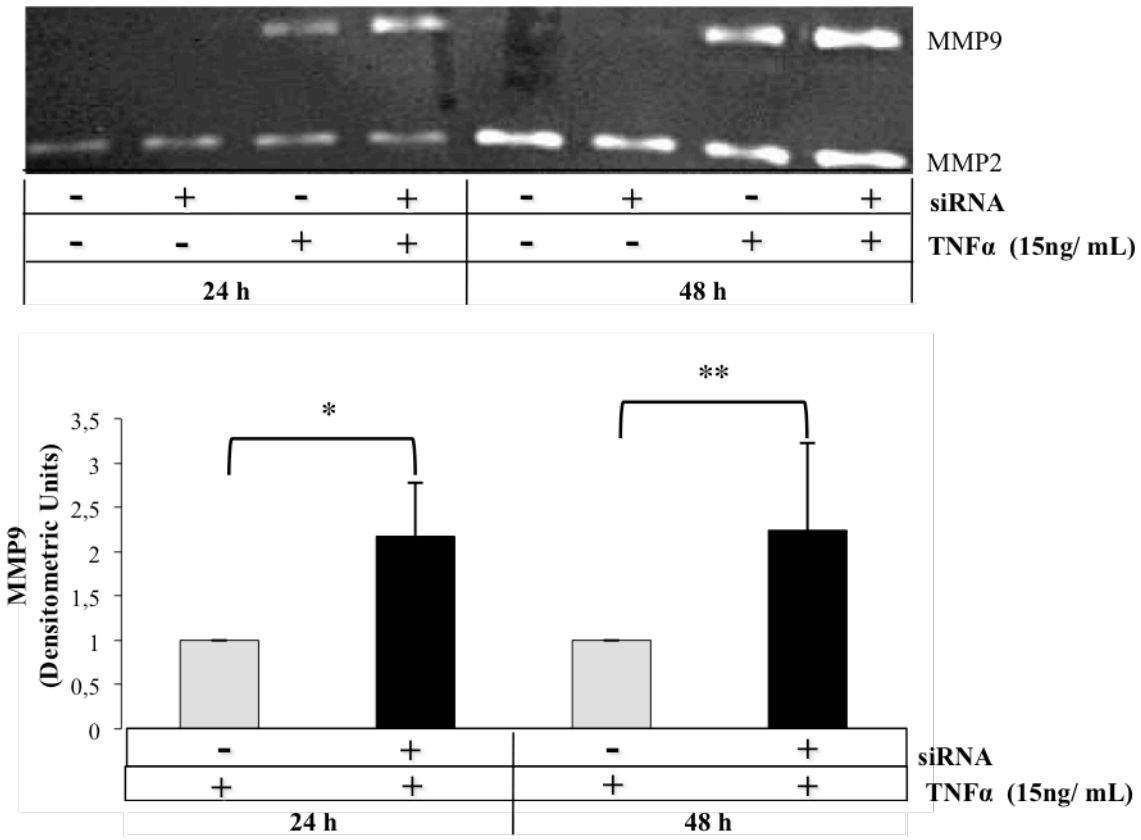

Figure 10. GSK-3 a and b silencing increases TNF-a induced MMP9 secretion in A549 cells. Zymographic analysis No difference was shown in MMP-2 activity. Densitometric results are represented as mean ± SD of 4 independent experiments with A549 cells (*) $p < 0.01$; (**) $p < 0.05$.

GSK-3α and β silencing increase increases TNF-α induced MMP-9 and TIMP-1 expression in A549 cells

Western Blot analysis of cell culture medium at 24 and 48 hours after TNFa stimulation confirmed zymographic data in terms of MMP-9 protein secretion, with a significant strengthening of the stimulus in GSK-3 silenced cells ($p < 0.05$). Moreover, TIMP-1 levels

resulted detectable in untreated A549 culture medium and the protein secretion was significantly increased in those cells underwent GSK-3 silencing ($p < 0.05$). TNFα administration further increased TIMP-1 levels ($p < 0.05$), with no significant difference following GSK-3 silencing (Figure 11)

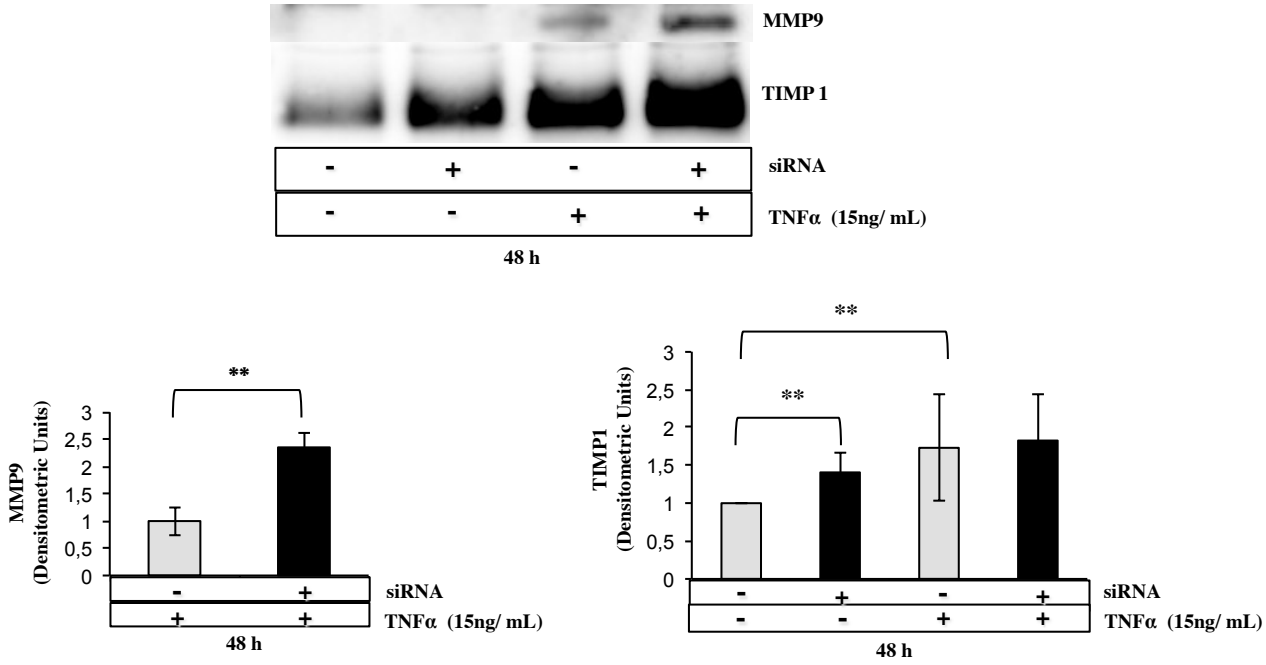

Figure 11. GSK-3α and β silencing in A459 cells induced an increase in MMP9 protein expression 48 hours after stimulation with TNFα. MMP-9 and TIMP-1 levels have been measured at 24 hours (data not shown) and 48 hours after TNFα stimulus. Densitometric analysis shows mean ± SD of 4 independent experiments. *(**) p <0,05 compared to SCR-transfected unstimulated cells*.

Analysis of MMP-9 and TIMP-1 gene expression by RT-PCR analysis confirmed Western Blot results both at 24 hours (Figure 12) and 48 hours (data not shown).

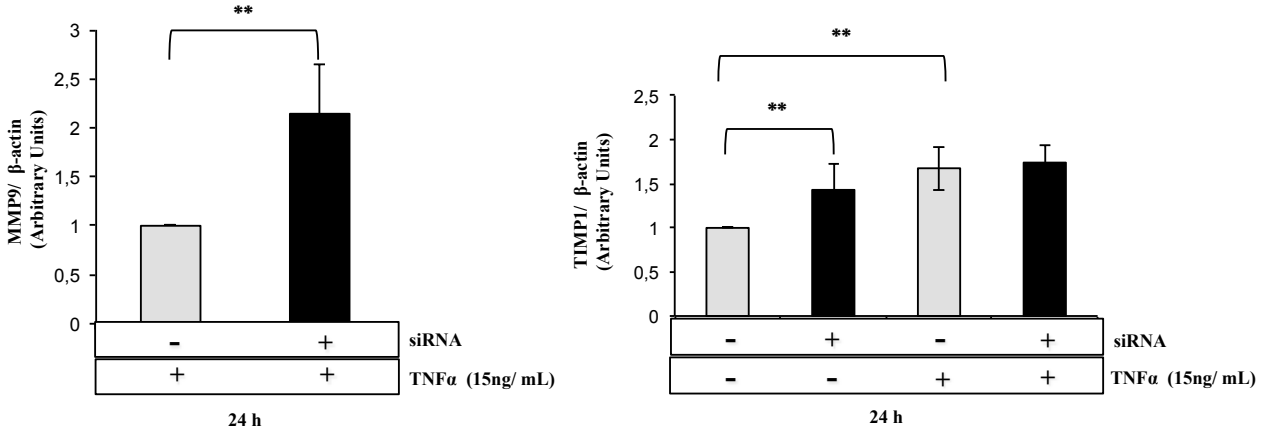

Figure 12. GSK-3α and β silencing in A459 cells induced an increase in MMP9 protein expression 48 hours after stimulation with TNFα. MMP-9 and TIMP-1 mRNA levels have been measured at 24 hours and 48 hours

(data not shown) after TNFα stimulus. Histograms show mean ± SD of 3 independent experiments. *(**) p <0,05 compared to SCR-transfected unstimulated cells*.

GSK-3 silencing modulates phosphorilation of NF-kB p65 and MAPK p38, SAP/JNK and ERK downstream of TNF-a

To deeply explore signalling pathways involved in TNFα-driven MMP-9 production we performed WB analysis to quantitate the phosphorilated (activated) isoforms of MAPK p38, SAP/JNK, ERK and p65. 48 hours after transfection with SCR or GSK-3 siRNA, A549 cells were stimulated with TNFα and collected at 0, 5, 15 and 40 minutes for WB analysis.

As shown in Figure 13, TNFα induced **p65** phosphorilation within the first 5 minutes; at 15 minutes the degreee of phosphorilation was already declining, achieving a complete recovery of basal levels at 40 minutes. GSK-3 silencing increased phospho-p65 levels at 15 minutes after TNFα treatment. Total p65 was not affected by any treatment.

Phosphorilated **JNK2** but not **JNK1** was already detectable at time 0 in control cells; TNFα increased phospho-JNK2 at 5 and 15 minutes, while inducing JNK1 phosphorilation. Phosphorylation degree of both JNK was back to basal level in 40 minutes. Surprisingly, GSK-3 silencing was shown to reduce JNK2 phosphorilation at all time points, including basal levels, while strengthening JNK1 phosphorilation, mainly at 15 minutes. Total JNK1 and 2 were not affected by any treatment.

Phosphorylated **ERK1** and **ERK2** were detectable at time 0 in untreated cells; TNFα induced an increase in phospho-ERK1 and 2, occurring within the first 5 minutes and stable until at least 40 minutes after stimulation. GSK-3 silencing was able to sustain phosphorilation at all time points. Total not-phosphorilated ERK levels were not affected by gene silencing or TNFα stimulation at any time point.

Finally, TNFα induced **p38** phosphorilation within 5 minutes and until 15 minutes after stimulation, with a decrease towards basal levels at 40 minutes. GSK-3 silencing increased phosphor-p38 at all time points, sustaining phosphorilation until at least 40 minute. Once more, levels of unphosphorilated p38 were not affected by any treatment at any time point (Figure 13).

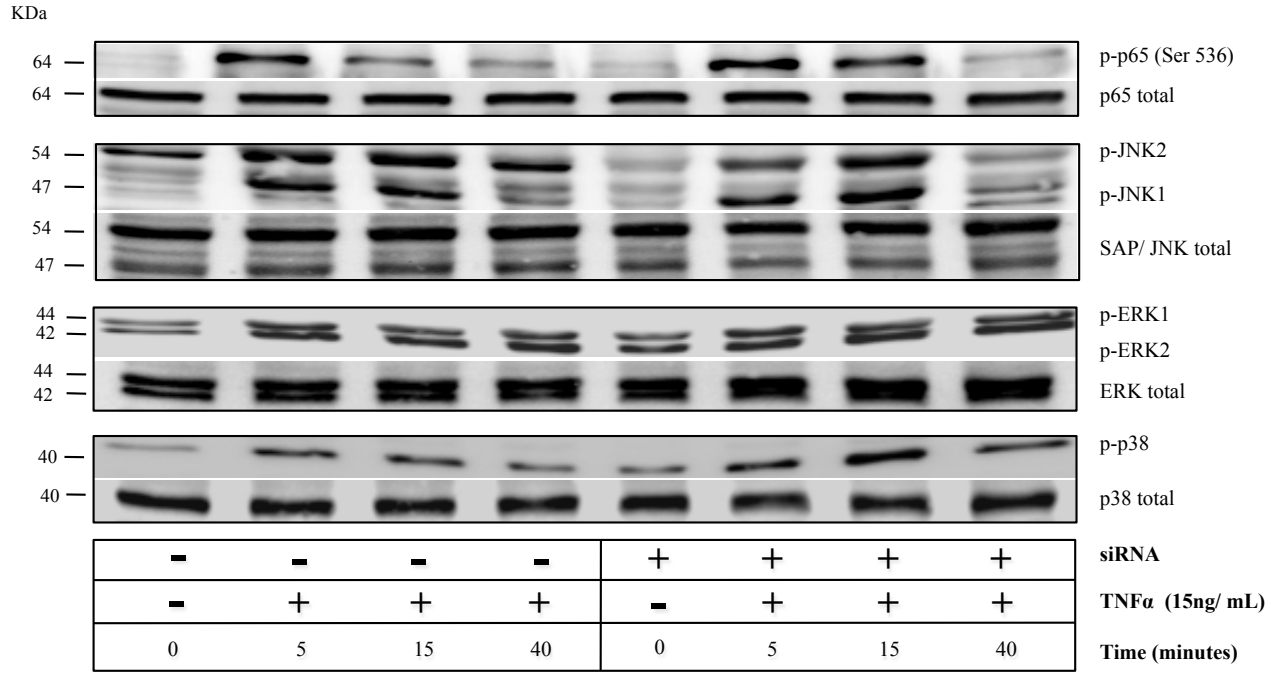

Figure 13. GSK-3 silencing modulates phosphorilation of NF-κB p65 and p38, JNK and ERK downstream of TNF-α. Tranfected A549 (SCR or GSK-3α and β siRNA) were stimulated with TNFα for 0, 5, 15 and 40 minutes. Proteins were extracted for WB analysis. MAPK and NF-κB pathways were investigated by phosphorilation assessment. "Total" forms of the investigated proteins were neither affected by GSK-3 silencing nor by TNFα stimulation.

GSK-3 effect on MMP9 secretion seems to be regulated by interaction with ERK1,2, as demonstrated by using ERK1,2 phosphorilation inhibitor PD98059.

Following phosphorilation data, specific inhibitors of p38 (SB203580) and ERK (PD98059) were used in order to investigate which of the above-mentioned pathways are directly involved in the modulation of MMP-9 secretion, downstream of. Thus, A549 celle underwent or not GSK-3 silencing were pre-treated with each specific inhibitor, simulated with TNFα and collected after 48 hours. Supernatants were used for zymographic analysis. As shown in Figure 14, ERK1,2 phosphorilation inhibitor PD98059 (10μM) induced a decrease of MMP-9 activity, if compared to TNFα stimulated cells not treated with the inhibitor. GSK-3 silencing did not counteract this PD98959-dependent effect. This suggested that GSK-3 could specifically interact with ERK1,2 pathway when modulating MMP-9 activity.
Results were confirmed by Western Blot analysis (data not shown). MMP-2 activity was constitutive and not affected by silencing, stimulation or ERK1,2 inhibition.

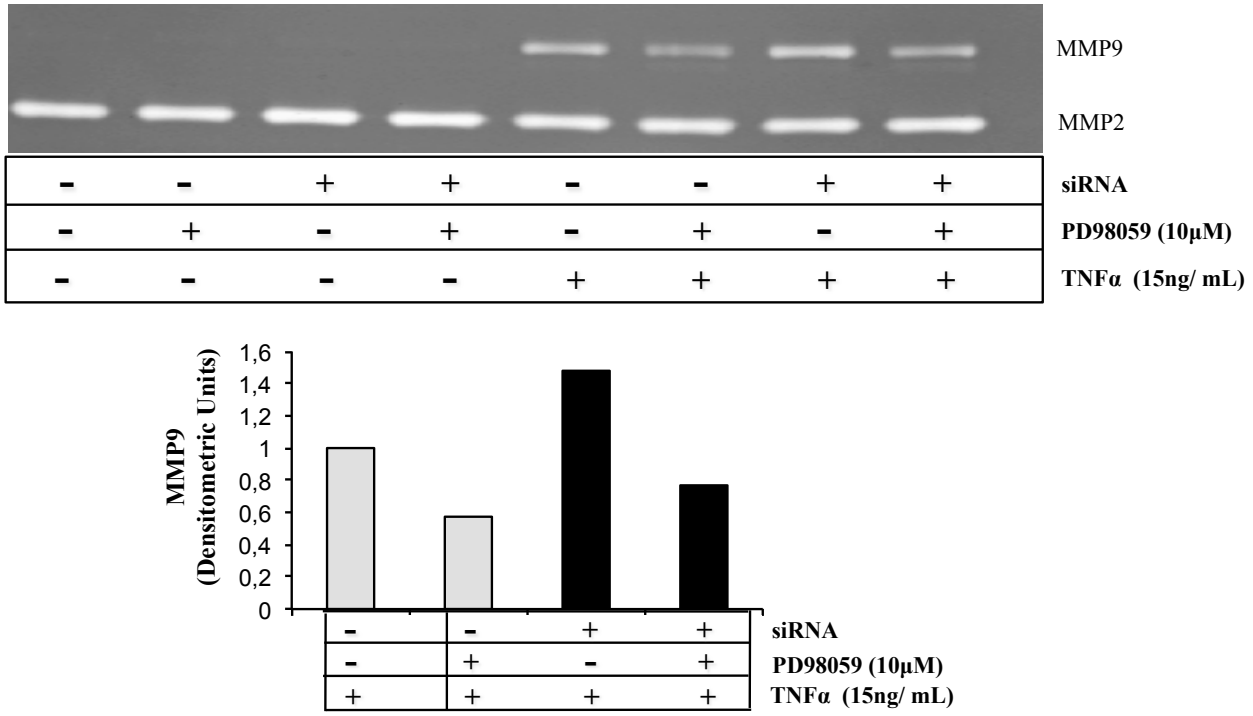

Figure 14. GSK-3 interact with ERK1,2 when modulating MMP-9 activity downstream of TNFα. 48 hours after transfection with SCR or GSK-3α and β siRNA, A549 were pre-treated with PD98059 and underwent TNFα stimulation. Zymographic analysis was performed on supernatants 48 hours after stimulation.

On the other hand, SB203580-mediated inhibition (10µM) of p38 phosphorilation did not affect MMP-9 activity dowstream of TNFα, both in SCR-transfected GSK-3-silenced cells (Figure 15). Results were confirmed by Western Blot analysis (data not shown). MMP-2 activity was constitutive and not affected by silencing, stimulation or inhibition of p38.

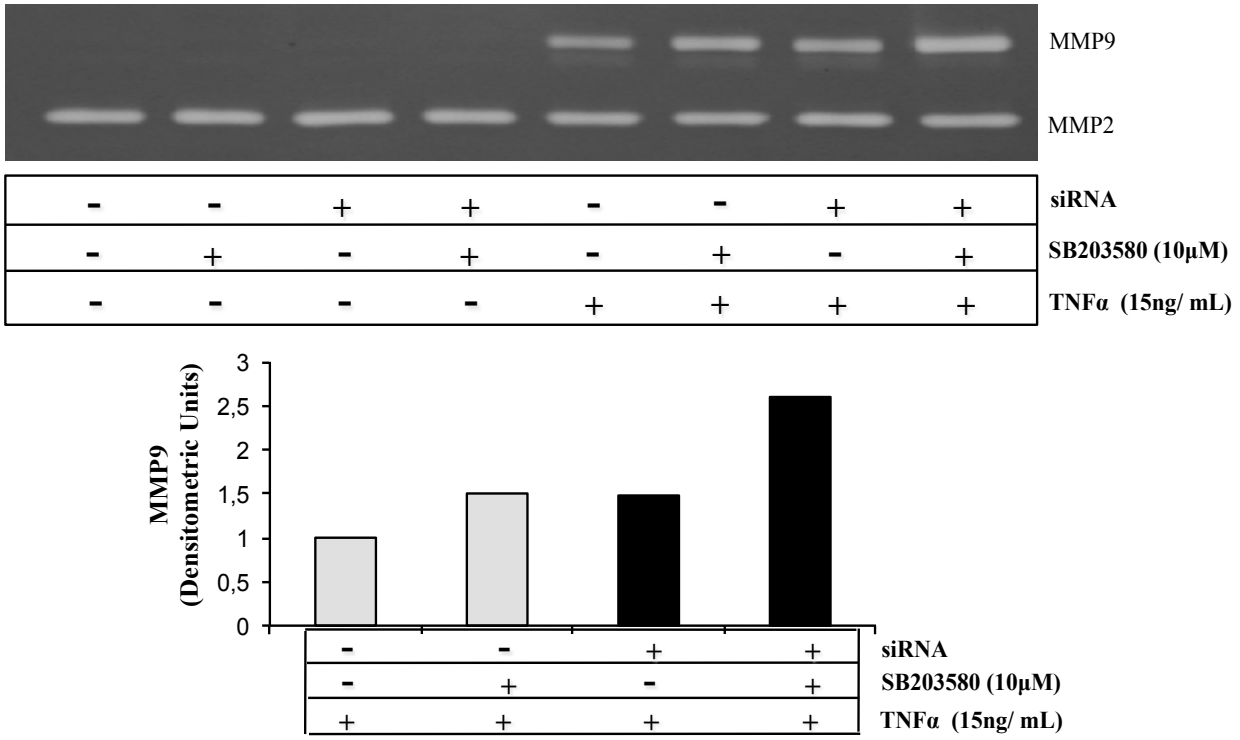

Figure 15. MAPK p38 pathway did not non modulate MMP-9 activity downstream of TNFα. 48 hours after transfection with SCR or GSK-3α and β siRNA, A549 were pre-treated with SB203580 and underwent TNFα stimulation. Zymographic analysis was performed on supernatants 48 hours after stimulation.

TIMP-1 expression is not modulated by MAPK p38 and ERK pathways

Since previous data suggested a TIMP-1 induction consensual with MMP-9 under TNFα stimulation, we wanted to investigate the impact of p38 e ERK pathway inhibition by SB203580 and PD98059, respectively, on TIMP-1 expression.

Thus, 48 hours after transfection with SCR or GSK-3α and β siRNA, A549 were pre-treated with SB203580 or PD98059 and underwent TNFα stimulation. Western Blot analysis was performed on supernatants 48 hours after stimulation

As shown in Figure 16, TIMP1 was consitutively expressed in untreated A549 and induced by TNFα; as previously demonstrated, GSK-3 silencing was able to strengthen TNFα-driven response. PD98059 pre-treatment, however, was unable to affect TIMP-1 expression, thus suggesting that TIMP-1 was not modulated by ERK1,2 phosphorilation in A549 cells (Figure 16).

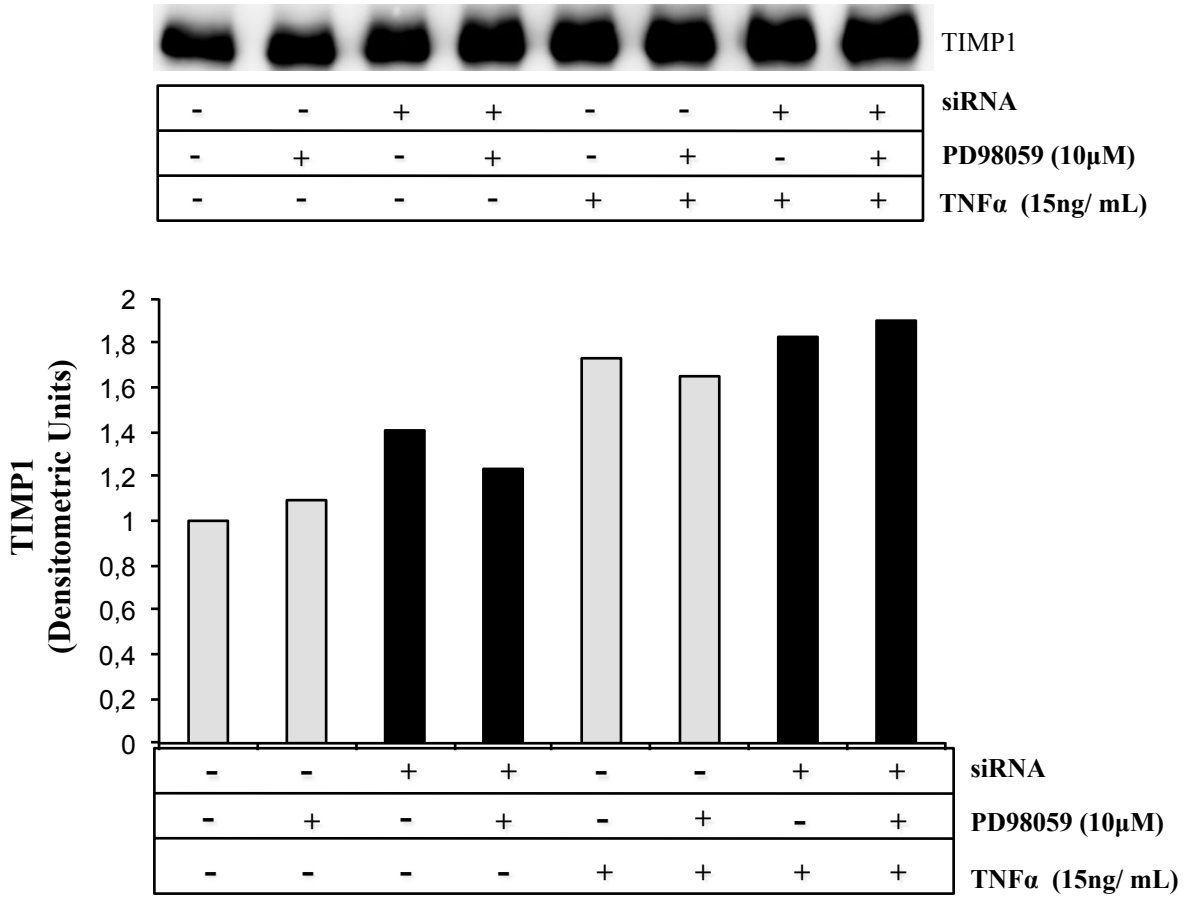

Figure 16. TIMP1 expression was not modulated by ERK1,2 pathway. 48 hours after transfection with SCR or GSK-3α and β siRNA, A549 were pre-treated with PD98059 and underwent TNFα stimulation. Western Blot analysis was performed on supernatants 48 hours after stimulation; TIMP-1 (27 KDa) expression was not influenced by treatment.

Similarly, SB203580 pre-treatment did not influence TIMP-1 expression in any of the experimental conditions, thus suggesting that p38 MAPK pathway was not involved in TIMP-1 modulation in A549 cells (Figure 17).

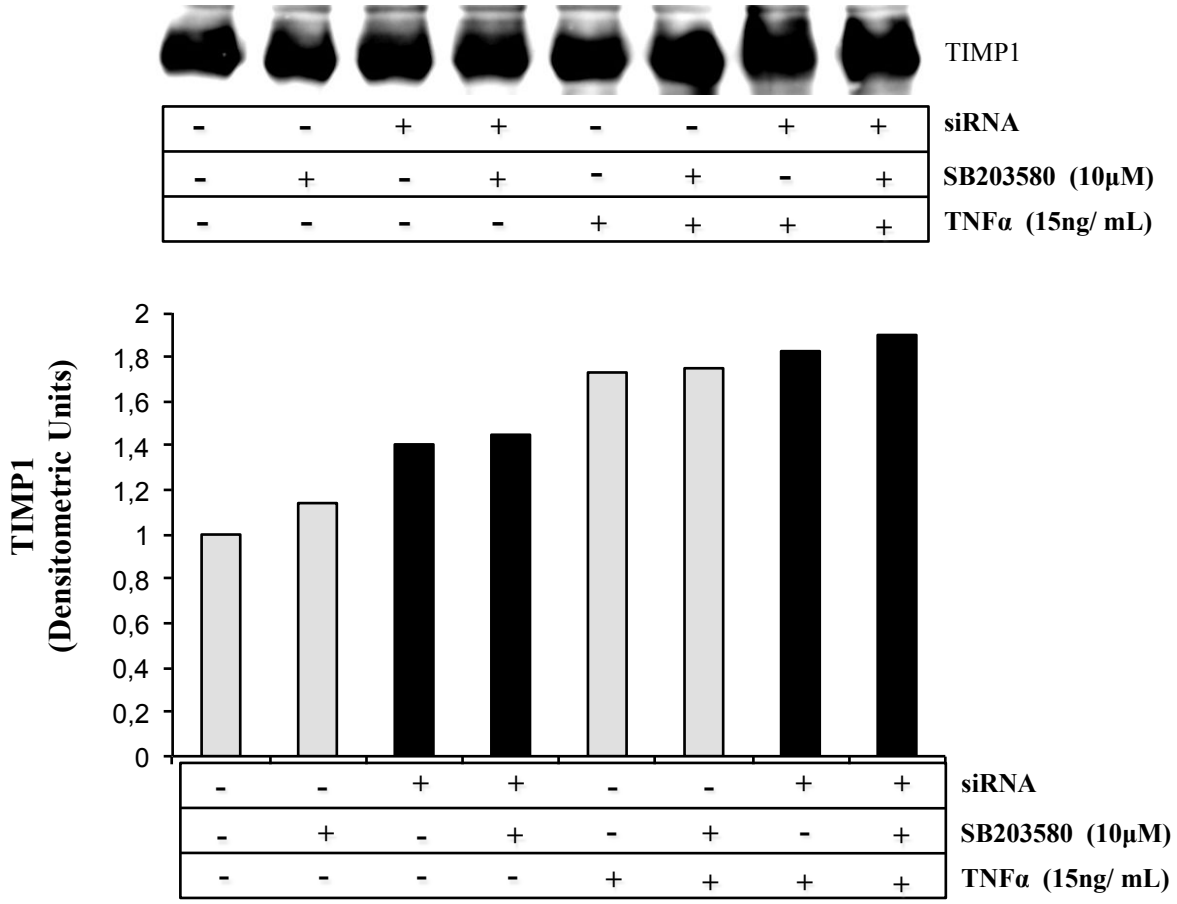

Figure 17. TIMP1 expression was not modulated by p38 pathway. 48 hours after transfection with SCR or GSK-3α and β siRNA, A549 were pre-treated with SB203580 and underwent TNFα stimulation. Western Blot analysis was performed on supernatants 48 hours after stimulation; TIMP-1 (27 KDa) expression was not influenced by treatment.

GSK-3 knock-out in murine embryonic fibroblasts (MEF) increased basal and TNFα-induced MMP-9 activity

Finally, to preliminary explore the effect of GSK-3 inhibition in fibroblasts, whose importance is rising in the pathogenesis of IPF not only as a direct mediator of fibrosis, but also as a modulator of the process itself, we used a cell line of murine embryonic fibroblast available as wild type (WT) and knock out for GSK-3β (courtesy of Prof. Woodgett). In order to investigate the mechanism through which the kinase GSK-3 could modulate MMP-9 and MMP-2 secretion and gene expression, we performed the zymographic analysis of the conditioned media collected from MEF WT and MEF KO in resting conditions or upon TNF-a stimulation at 12, 24 or 48 hours; experiments were performed in serum starvation, as previously described. Interestingly, latent MMP-9 resulted to be constitutively secreted at all time points in KO cells only (Figure 18 a). MMP-2 was constitutively secreted both in WT and KO cells; GSK-3b KO increased 7 times and 4 times, at 24 and 48 hours respectively, the levels of the secreted zymogen in resting conditions compare to WT cells ($p<0.01$) (data not shown).

Zymographic analysis also showed that TNF-a induced MMP-9 secretion both in WT and in GSK-3b KO cells as early as 12 hours after stimulation. Moreover, the zymogen levels accumulated in media collected from MEF KO were higher than in MEF WT media at each time point (*1.00 ± 0.00 versus 0.42 ± 0.16, p < 0.01 at 12 hours; 2.50 ± 0.26 versus 1.45 ± 0.30, p < 0.05 at 24 hours; 5.70 ± 1.26 versus 2.00 ± 0.37, p < 0.01 at 48 hours)* (Figure 18 b).

On the other hand, pro-MMP-2 secretion seemed to be independent by TNF-a in WT cells but significantly increased in KO MEF.

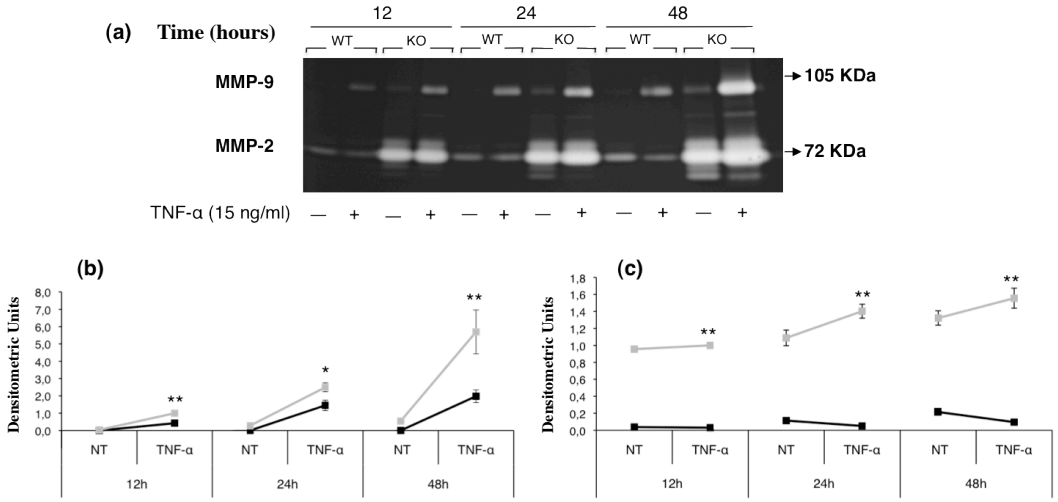

Figure 18. Zymographic analysis of MMP-2 and MMP-9 activity in supernatant of MEF WT and KO for GSK-3β under TNFα stimulation. (a) Zymographic gel representative for 3 independent trials. MEF WT and KO were plated and, once at confluence, cultered in FCS-free medium for 24 hours and then stimulated with TNF-α 15 ng/ml. *Medium* was collected after 12, 24 or 48 hours and gelatinolytic activity was assessed. **(b)** and **(c)** Densitomeric analysis for MMP-9 and MMP-2 secreted by MEF WT (black line) and KO (grey line). Results are displayed as mean ± SD of 3 independent experiments for MMP-9 **(b)** and MMP-2 **(c)** (*) p <0,05 if compared to MEF WT (**) p <0.01 if compared to MEF WT.

These results were confirmed by Western Blot and RT-PCR analysis, and using primary mouse skin-derived fibroblasts undergone TNF-α stimulation and SB216763-mediated GSK-3 α and β inhibition (data not shown).

5. DISCUSSION AND CONCLUSIONS

We previously demonstrated an anti-inflammatory and anti-fibrotic effect of GSK-3 inhibition in a mouse model of BLM-induced pulmonary fibrosis [90]. As confirmed by BAARSMA et al. [88, 99], GSK-3 may thus be considered a potential therapeutic target in pulmonary fibrosis. In the present study we further investigated the GSK-3 role in signalling pathways specifically involved in the fibrogenesis, both in early and late phases of the process. In particular, we focused our attention on ECM remodelling, which is known to play a pivotal role in IPF. MMPs and TIMPs are indeed essential in the physiological turnover of the matrix and in the repair of disrupted basal membrane (BM). Moreover, apart from type II epithelial alveolar cells, fibroblasts and immune system, it is currently believed that also fibrotic ECM is not a simple consequence of the IPF pathogenesis, but can activate a pro-fibrotic positive feedback loop able to sustain or even drive the disease progression [100]. The impairment in the ECM turnover plays a role in many pulmonary disorders, including emphysema, asthma and lung carcinoma, and in local and metastatic cancer invasiveness. The importance of MMPs in the pathogenesis of IPF is still under careful investigation, since the aberrant deposition of ECM is a hallmark of the disease, but some evidence is already available for specific MMPs [37]. Studies from different groups have shown that there are MMPs highly expressed in IPF, playing diverse roles in the fibrotic response; however, the exact mechanisms are not well characterized [47]. Increased levels of MMPs could sustain fibrosis progression by increasing ECM degradation and inducing mediators, as VEGF, which favour neo-angiogenesis and capillary permeabilitiy [101]. Moreover, *in vivo* use of the MMP inhibitor batimastat and knock-out mice for some MMPs (including MMP9 e MMP12) allowed to demonstrate that inhibition of MMPs can reduce the development of BLM-induced pulmonary fibrosis [39, 102, 103]. On the other hand, excessive levels of TIMPs could sustain an anti-collagenolytic microenvironment, thus promoting an aberrant collagen deposition; TIMP-1, for example, was found to be up-regulated in a BLM mouse model and TIMP3 resulted over-expressed in a cohort of IPF patients [101, 103]. MMP-2, MMP-9, TIMP-2 and TIMP-1 have been investigated in our study, exploring the possible role of the pleiotropic kinase GSK-3 in modulating their production and activity.

Provided that the BLM-induced mouse model of lung fibrosis is not universally accepted as a trustable IPF model, mainly due to the role of inflammation in the development of fibrosis, it is still the most used in vivo model for studies about the pathogenesis of the disease and the first model where to test potential anti-fibrotic drugs before phase I clinical trials [93, 94]. Our data clearly showed, in this model, that MMPs and TIMPs are involved in the pathogenesis of BLM-induced fibrosis. In particular, we demonstrated that MMP-2, MMP-9 and TIMP-1 levels were increased at day 7 in BALF of BLM treated mice. At this time point the process is still in the inflammatory phase and there is a consistent inflammatory infiltration of the lung. Alveolar macrophages, lymphocytes and neutrophils are recruited into the alveolar spaces and are believed to be responsible for the high levels of MMP-2, MMP-9 and TIMP-1 in the BALF. The main population infiltrating the lung parenchima was represented by iAMs which were shown by IHC analysis to strongly express MMP-2, MMP-9, TIMP-1 and -2. Noteworthy, we were able to show that not only the inflammatory cells were responsible for the release of these mediators, but also

type II epithelial alveolar cells. These cells already displayed at day 7 a significant degree of cuboidalization associated to a detectable expression of both MMPs and TIMPs, with a strong positivity for MMP-9 and TIMP-1. At day 28, when fibrosis was well established, we found in BALF an inversion in the hierarchy of MMPs; MMP-9 almost disappeared and MMP-2, which appeared less relevant in the early phases and consitutively expressed even in PBS-treated mice, became significantly increased in the BLM group, together with TIMP-1 and -2. Preliminary data from IHC analysis of lungs at day 28 confirmed this trend in type II epithelial alveolar cells.

SB216763-mediated GSK-3 inhibition significantly reduced both BLM-induced inflammation and fibrosis in our mouse model, as already shown in our previous paper [90]. The present study also suggests a possible role of the kinase GSK-3 in modulating the balance between MMPs and TIMPs in the context of pulmonary fibrosis. In vivo GSK-3 inhibition, indeed, strongly decreased MMP-9 activity and, to a lower extent, MMP-2 activity in BALF of BLM-treated mice. Moreover, SB216763 significantly reduced MMP-9, MMP-2, TIMP-1 and TIMP-2 production in iAMs and cuboidalized type II epithelial alveolar cells at day 7. At day 28 GSK-3 inhibition resulted in a reduction of both MMP-9 and MMP-2 in the BALF, restoring an almost physiological secretion. At this time point the effect was much more prominent on MMP-2, which has previously been shown to be more relevant in the fibrotic phase. Finally, the BLM-induced increase of TIMP-1 was prevented by regular administration of SB216763 during the 4 weeks before sacrifice. Even if preliminary, IHC results after GSK-3 inhbition were in line with BALF data, underlining once more the role of cuboidalized epithelial alveolar cells as main character of the play. Data from the BLM mouse model, in conclusion, showed that GSK-3 is involved, in vivo, in MMPs and TIMPs modulation following a pro-fibrotic lung injury. Nonetheless, it is not possible to assess if the effect of SB216763 is exerted directly on all the involved cell types or only indirectly through an anti-inflammatory effect.

To address this question and further understand the molecular mechanisms underlying the role of GSK-3 in MMPs modulation, we then performed the above described in vitro experiments on single cell lines, namely A549 and MEF. As already shown, the *in vitro* effect of GSK-3 silencing was the opposite of what expected on the basis of the *in vivo* results. We obtained, indeed, a significant MMP-9 induction downstream of TNFα stimulation and, in MEF knock out for GSK-3β, MMP-9 induction resulted detectable even without stimulation. Moreover, in A549 cells, GSK-3 silencing increased TNFα-dependent MMP-9 production via the NF-κB pathway, as demonstrated by an increase in p65 phosphorilation levels. The effect on MMP-9 also seemed to be dependent on the ERK1,2 pathway, since the ERK1,2 phosphorilation inhibitor PD98059 was able to prevent MMP-9 production with or without GSK-3 silencing. On the contrary, p38 was not involved in MMP-9 modulation, despite its phosphorilation resulting to be increased after GSK-3 silencing. Finally, the role of GSK-3 in MAPK SAP/JNK pathway needs to be further investigated, since GSK-3 silencing reduced JNK2 phosphorilation while increasing JNK1 phosphorilation, in our experiments. Concerning TIMP-1, which appeared to be constitutively expressed and increased after GSK-3 silencing in A549 cells, we can only say that this was not dependent on an interaction with ERK1,2 or p38 pathway.

At present, *in vitro* results are clearly in contrast with those obtained in the mouse model: the only common feature is represented by the finding that GSK-3 is involved in the modulation of MMPs and TIMPs in different cell types. The effect of this modulation, however, points at the kinase as at a positive modulator *in vivo*, while its inhibition in A549 and MEF cells results in a strong induction of MMP-9. Data concerning the prominent role of MMP-2 in the fibrotic phase of the BLM-induced process are not comparable with the present in vitro models, since they are all based on short-term cultures. Moreover, the TNFα-dependent MMP-9 strong induction in A549 cells after GSK-3 silencing suggests that GSK-3, as shown in other carcinoma-derived epithelial cell lines, could act as a regulator of Epithelial to Mesenchimal Transition (EMT) [24, 104]. EMT, which physiologically happens, for example, during embryogenesis, is believed to be a crucial pathogenic step in tumor progression, but also in IPF; in this context, in particular, it is meant to be one of the main source of fibroblasts taking part into fibroblastic foci formation and aberrant ECM deposition, as previously described. In fact, GSK-3 has been shown to be a regulator of Snail in A549 cells, which is a transcriptional repressor of E-caderine, a well known epithelial marker whose down-regulation is indeed an EMT marker [89, 105]. Thus, MMP-9 increase could be interpreted as an EMT marker itself, and this will be assessed in our future experiments.

At this point of the discussion, there are two crucial questions rising from the analysis of our results. The first one is whether A549 or MEF and, generally, single cell lines can be considered a suitable model where to study IPF pathogenic mechanisms. As extensively discussed in the previous sections, IPF pathogenesis is more than complicated and involves a plethora of different pathways. As for many other diseases, its development is not based on a single aberration but mainly on a pro-fibrotic microenvironment, in which each pathway is relevant but is unlikely to be essential. Thus, it is not surprising that many promising anti-IPF molecules, acting on single pathways (e.g. TGF-β, Endothelin) did not achieve any results in vivo. As a confirmation of these theory, the only two drugs currently approved for IPF treatment, Pirfenidone and Nintedanib, exploit a multiple targets strategy to disrupt (only partially, unfortunately) the pathogenic mechanisms and slower the disease progression [18, 35]. Moreover, A549 are a carcinoma-derived cell line and MEF an embryonic one, and this implicates a "cell mood" completely different from that found in IPF, with a different signalling background that is expected to differently react to stimulation (including TNFα or GSK-3 inhibition). A good example is represented by fibroblasts: MRC5 cells, a human lung embryonic cell line, display a significantly different behaviour and cell growth if compared with primary lung fibroblast; but the difference is even more significant when comparing normal fibroblasts with IPF fibroblasts, which present a markedly decreased cell growth rate and response to stimuli, including TGF-β. Finally, it has clearly been shown that there is not a single cell type on which IPF development is based; type II epithelial alveolar cells can be the main character of the play, maybe, but fibroblasts are also essential and definitely far from being mere executors. The importance of ECM is rising, as well, as a fundamental part of the microenvironment and also leucocytes, that have been put aside for years together with the role of inflammation in the pathogenesis of the disease, are now coming back in the main theories as modulators more than as effectors (e.g. M2 macrophages) [106]. Thus, single cell cultures are likely to be replaced by multiple cell culture systems and cell lines

must leave their place to primary cells; this is the direction of our future studies, and we are already taking part in the development of a new in vitro model, based on the association between long term 3D fibroblast culture, resembling fibroblastic foci and including a significant deposition of ECM, and epithelial alveolar cells. This will hopefully be the kind of model where definitely explore the role of GSK-3 in the modulation of ECM turnover.

The second and final question is whether GSK-3 silencing or knock-out can be the best strategy to evaluate this potentially intriguing pharmacologic target. As extensively discussed in the introduction, GSK-3 is a pleiotropic kinase, implicate in many different pathways and with a fascinating huge number of control mechanisms that allow it to manage all of its tasks in an organized fashion. The long clinical experience with lithium teach us that in vivo inhibition of this kinase is not only safe, despite the multiple implications, but also that this safety is likely due to the partial inhibition that lithium exerts on GSK-3, that may be optimal for dampening GSK-3's self-activating mechanisms in disease processes while allowing GSK-3 to fulfil, unhindered, its many other cellular actions [107]. On the basis of this idea, the pharmacologic in vivo inhibition performed in our mouse model is not only closer to the possible application in clinical practice, but also more suitable than in vitro *experiments* to really assess the role of the kinase and the actual potential of its inhibition. In addition to the potential benefit of only partial inhibition of GSK-3, in terms of future applications, the development of disease-selective inhibitors of GSK-3 will hopefully be possible, based on the awareness of the specific mechanisms that regulate GSK-3 and that depend on GSK-3 in the specific pathologic context.

In conclusion, our study gives some hints but we are still far from completely understanding the role of GSK-3 in the pathogenesis of pulmonary fibrosis and available data present some controversies [87, 88]. Due to its implications at different levels in so many pathways involved in development of fibrosis, it remains a fascinating target in the field of IPF, where the aim of the research is not to close a bad way but to disrupt a dangerous net.

6. REFERENCES

1. Selman M, King TE, Pardo A, American Thoracic S, European Respiratory S, American College of Chest P: **Idiopathic pulmonary fibrosis: prevailing and evolving hypotheses about its pathogenesis and implications for therapy.** *Ann Intern Med* 2001, **134:**136-151.
2. Raghu G, Collard HR, Egan JJ, Martinez FJ, Behr J, Brown KK, Colby TV, Cordier JF, Flaherty KR, Lasky JA, Lynch DA, Ryu JH, Swigris JJ, Wells AU, Ancochea J, Bouros D, Carvalho C, Costabel U, Ebina M, Hansell DM, Johkoh T, Kim DS, King TE, Jr., Kondoh Y, Myers J, Muller NL, Nicholson AG, Richeldi L, Selman M, Dudden RF, Griss BS, Protzko SL, Schunemann HJ, Fibrosis AEJACoIP: **An official ATS/ERS/JRS/ALAT statement: idiopathic pulmonary fibrosis: evidence-based guidelines for diagnosis and management.** *Am J Respir Crit Care Med* 2011, **183:**788-824.
3. Coultas DB, Zumwalt RE, Black WC, Sobonya RE: **The epidemiology of interstitial lung diseases.** *Am J Respir Crit Care Med* 1994, **150:**967-972.
4. Hansell A, Hollowell J, Nichols T, McNiece R, Strachan D: **Use of the General Practice Research Database (GPRD) for respiratory epidemiology: a comparison with the 4th Morbidity Survey in General Practice (MSGP4).** *Thorax* 1999, **54:**413-419.
5. Katzenstein AL, Myers JL: **Idiopathic pulmonary fibrosis: clinical relevance of pathologic classification.** *Am J Respir Crit Care Med* 1998, **157:**1301-1315.
6. Wuyts WA, Agostini C, Antoniou KM, Bouros D, Chambers RC, Cottin V, Egan JJ, Lambrecht BN, Lories R, Parfrey H, Prasse A, Robalo-Cordeiro C, Verbeken E, Verschakelen JA, Wells AU, Verleden GM: **The pathogenesis of pulmonary fibrosis: a moving target.** *Eur Respir J* 2013, **41:**1207-1218.
7. Cronkhite JT, Xing C, Raghu G, Chin KM, Torres F, Rosenblatt RL, Garcia CK: **Telomere shortening in familial and sporadic pulmonary fibrosis.** *Am J Respir Crit Care Med* 2008, **178:**729-737.
8. Garcia CK, Raghu G: **Inherited interstitial lung disease.** *Clin Chest Med* 2004, **25:**421-433, v.
9. Marshall RP, Puddicombe A, Cookson WO, Laurent GJ: **Adult familial cryptogenic fibrosing alveolitis in the United Kingdom.** *Thorax* 2000, **55:**143-146.
10. King TE, Jr., Albera C, Bradford WZ, Costabel U, Hormel P, Lancaster L, Noble PW, Sahn SA, Szwarcberg J, Thomeer M, Valeyre D, du Bois RM, Group IS: **Effect of interferon gamma-1b on survival in patients with idiopathic pulmonary fibrosis (INSPIRE): a multicentre, randomised, placebo-controlled trial.** *Lancet* 2009, **374:**222-228.
11. Raghu G, Freudenberger TD, Yang S, Curtis JR, Spada C, Hayes J, Sillery JK, Pope CE, 2nd, Pellegrini CA: **High prevalence of abnormal acid gastro-oesophageal reflux in idiopathic pulmonary fibrosis.** *Eur Respir J* 2006, **27:**136-142.
12. Nathan SD, Noble PW, Tuder RM: **Idiopathic pulmonary fibrosis and pulmonary hypertension: connecting the dots.** *Am J Respir Crit Care Med* 2007, **175:**875-880.
13. Lettieri CJ, Nathan SD, Barnett SD, Ahmad S, Shorr AF: **Prevalence and outcomes of pulmonary arterial hypertension in advanced idiopathic pulmonary fibrosis.** *Chest* 2006, **129:**746-752.
14. Nadrous HF, Pellikka PA, Krowka MJ, Swanson KL, Chaowalit N, Decker PA, Ryu JH: **Pulmonary hypertension in patients with idiopathic pulmonary fibrosis.** *Chest* 2005, **128:**2393-2399.

15. Kawut SM, O'Shea MK, Bartels MN, Wilt JS, Sonett JR, Arcasoy SM: **Exercise testing determines survival in patients with diffuse parenchymal lung disease evaluated for lung transplantation.** *Respir Med* 2005, **99:**1431-1439.
16. Nathan SD, Shlobin OA, Ahmad S, Urbanek S, Barnett SD: **Pulmonary hypertension and pulmonary function testing in idiopathic pulmonary fibrosis.** *Chest* 2007, **131:**657-663.
17. Noble PW, Albera C, Bradford WZ, Costabel U, Glassberg MK, Kardatzke D, King TE, Jr., Lancaster L, Sahn SA, Szwarcberg J, Valeyre D, du Bois RM, Group CS: **Pirfenidone in patients with idiopathic pulmonary fibrosis (CAPACITY): two randomised trials.** *Lancet* 2011, **377:**1760-1769.
18. Richeldi L, du Bois RM, Raghu G, Azuma A, Brown KK, Costabel U, Cottin V, Flaherty KR, Hansell DM, Inoue Y, Kim DS, Kolb M, Nicholson AG, Noble PW, Selman M, Taniguchi H, Brun M, Le Maulf F, Girard M, Stowasser S, Schlenker-Herceg R, Disse B, Collard HR, Investigators IT: **Efficacy and safety of nintedanib in idiopathic pulmonary fibrosis.** *N Engl J Med* 2014, **370:**2071-2082.
19. Idiopathic Pulmonary Fibrosis Clinical Research N, Martinez FJ, de Andrade JA, Anstrom KJ, King TE, Jr., Raghu G: **Randomized trial of acetylcysteine in idiopathic pulmonary fibrosis.** *N Engl J Med* 2014, **370:**2093-2101.
20. King TE, Jr., Pardo A, Selman M: **Idiopathic pulmonary fibrosis.** *Lancet* 2011, **378:**1949-1961.
21. Fernandez IE, Eickelberg O: **New cellular and molecular mechanisms of lung injury and fibrosis in idiopathic pulmonary fibrosis.** *Lancet* 2012, **380:**680-688.
22. Allen JT, Spiteri MA: **Growth factors in idiopathic pulmonary fibrosis: relative roles.** *Respir Res* 2002, **3:**13.
23. Bauman KA, Wettlaufer SH, Okunishi K, Vannella KM, Stoolman JS, Huang SK, Courey AJ, White ES, Hogaboam CM, Simon RH, Toews GB, Sisson TH, Moore BB, Peters-Golden M: **The antifibrotic effects of plasminogen activation occur via prostaglandin E2 synthesis in humans and mice.** *J Clin Invest* 2010, **120:**1950-1960.
24. Pfaff EM, Becker S, Gunther A, Konigshoff M: **Dickkopf proteins influence lung epithelial cell proliferation in idiopathic pulmonary fibrosis.** *Eur Respir J* 2011, **37:**79-87.
25. Grimminger F, Gunther A, Vancheri C: **The role of tyrosine kinases in the pathogenesis of idiopathic pulmonary fibrosis.** *Eur Respir J* 2015.
26. Inomata M, Kamio K, Azuma A, Matsuda K, Kokuho N, Miura Y, Hayashi H, Nei T, Fujita K, Saito Y, Gemma A: **Pirfenidone inhibits fibrocyte accumulation in the lungs in bleomycin-induced murine pulmonary fibrosis.** *Respir Res* 2014, **15:**16.
27. Willis BC, Borok Z: **TGF-beta-induced EMT: mechanisms and implications for fibrotic lung disease.** *Am J Physiol Lung Cell Mol Physiol* 2007, **293:**L525-534.
28. Hung C, Linn G, Chow YH, Kobayashi A, Mittelsteadt K, Altemeier WA, Gharib SA, Schnapp LM, Duffield JS: **Role of lung pericytes and resident fibroblasts in the pathogenesis of pulmonary fibrosis.** *Am J Respir Crit Care Med* 2013, **188:**820-830.
29. Bonner JC: **Regulation of PDGF and its receptors in fibrotic diseases.** *Cytokine Growth Factor Rev* 2004, **15:**255-273.
30. Zhuo Y, Zhang J, Laboy M, Lasky JA: **Modulation of PDGF-C and PDGF-D expression during bleomycin-induced lung fibrosis.** *Am J Physiol Lung Cell Mol Physiol* 2004, **286:**L182-188.
31. Aono Y, Nishioka Y, Inayama M, Ugai M, Kishi J, Uehara H, Izumi K, Sone S: **Imatinib as a novel antifibrotic agent in bleomycin-induced pulmonary fibrosis in mice.** *Am J Respir Crit Care Med* 2005, **171:**1279-1285.

32. Inoue Y, King TE, Jr., Barker E, Daniloff E, Newman LS: **Basic fibroblast growth factor and its receptors in idiopathic pulmonary fibrosis and lymphangioleiomyomatosis.** *Am J Respir Crit Care Med* 2002, **166:**765-773.
33. Hamada N, Kuwano K, Yamada M, Hagimoto N, Hiasa K, Egashira K, Nakashima N, Maeyama T, Yoshimi M, Nakanishi Y: **Anti-vascular endothelial growth factor gene therapy attenuates lung injury and fibrosis in mice.** *J Immunol* 2005, **175:**1224-1231.
34. Hostettler KE, Zhong J, Papakonstantinou E, Karakiulakis G, Tamm M, Seidel P, Sun Q, Mandal J, Lardinois D, Lambers C, Roth M: **Anti-fibrotic effects of nintedanib in lung fibroblasts derived from patients with idiopathic pulmonary fibrosis.** *Respir Res* 2014, **15:**157.
35. Cottin V: **The role of pirfenidone in the treatment of idiopathic pulmonary fibrosis.** *Respir Res* 2013, **14 Suppl 1:**S5.
36. Chakraborti S, Mandal M, Das S, Mandal A, Chakraborti T: **Regulation of matrix metalloproteinases: an overview.** *Mol Cell Biochem* 2003, **253:**269-285.
37. Pardo A, Selman M: **Role of matrix metaloproteases in idiopathic pulmonary fibrosis.** *Fibrogenesis Tissue Repair* 2012, **5:**S9.
38. Nkyimbeng T, Ruppert C, Shiomi T, Dahal B, Lang G, Seeger W, Okada Y, D'Armiento J, Gunther A: **Pivotal role of matrix metalloproteinase 13 in extracellular matrix turnover in idiopathic pulmonary fibrosis.** *PLoS One* 2013, **8:**e73279.
39. Betsuyaku T, Fukuda Y, Parks WC, Shipley JM, Senior RM: **Gelatinase B is required for alveolar bronchiolization after intratracheal bleomycin.** *Am J Pathol* 2000, **157:**525-535.
40. Yao PM, Lemjabbar H, D'Ortho MP, Maitre B, Gossett P, Wallaert B, Lafuma C: **Balance between MMP-9 and TIMP-1 expressed by human bronchial epithelial cells: relevance to asthma.** *Ann N Y Acad Sci* 1999, **878:**512-514.
41. Kelly EA, Jarjour NN: **Role of matrix metalloproteinases in asthma.** *Curr Opin Pulm Med* 2003, **9:**28-33.
42. Hrabec E, Strek M, Nowak D, Greger J, Suwalski M, Hrabec Z: **Activity of type IV collagenases (MMP-2 and MMP-9) in primary pulmonary carcinomas: a quantitative analysis.** *J Cancer Res Clin Oncol* 2002, **128:**197-204.
43. Shi M, Cao M, Song J, Liu Q, Li H, Meng F, Pan Z, Bai J, Zheng J: **PinX1 inhibits the invasion and metastasis of human breast cancer via suppressing NF-kappaB/MMP-9 signalling pathway.** *Mol Cancer* 2015, **14:**66.
44. Herrera I, Cisneros J, Maldonado M, Ramirez R, Ortiz-Quintero B, Anso E, Chandel NS, Selman M, Pardo A: **Matrix metalloproteinase (MMP)-1 induces lung alveolar epithelial cell migration and proliferation, protects from apoptosis, and represses mitochondrial oxygen consumption.** *J Biol Chem* 2013, **288:**25964-25975.
45. Selman M, Ruiz V, Cabrera S, Segura L, Ramirez R, Barrios R, Pardo A: **TIMP-1, -2, -3, and -4 in idiopathic pulmonary fibrosis. A prevailing nondegradative lung microenvironment?** *Am J Physiol Lung Cell Mol Physiol* 2000, **279:**L562-574.
46. Yamashita CM, Dolgonos L, Zemans RL, Young SK, Robertson J, Briones N, Suzuki T, Campbell MN, Gauldie J, Radisky DC, Riches DW, Yu G, Kaminski N, McCulloch CA, Downey GP: **Matrix metalloproteinase 3 is a mediator of pulmonary fibrosis.** *Am J Pathol* 2011, **179:**1733-1745.
47. Jara P, Calyeca J, Romero Y, Placido L, Yu G, Kaminski N, Maldonado V, Cisneros J, Selman M, Pardo A: **Matrix metalloproteinase (MMP)-19-deficient fibroblasts display a profibrotic phenotype.** *Am J Physiol Lung Cell Mol Physiol* 2015, **308:**L511-522.
48. Pardo A, Selman M: **Matrix metalloproteases in aberrant fibrotic tissue remodeling.** *Proc Am Thorac Soc* 2006, **3:**383-388.

49. Patel AS, Lin L, Geyer A, Haspel JA, An CH, Cao J, Rosas IO, Morse D: **Autophagy in idiopathic pulmonary fibrosis.** *PLoS One* 2012, **7:**e41394.
50. Vincenti MP, Brinckerhoff CE: **Transcriptional regulation of collagenase (MMP-1, MMP-13) genes in arthritis: integration of complex signalling pathways for the recruitment of gene-specific transcription factors.** *Arthritis Res* 2002, **4:**157-164.
51. Uchinami H, Seki E, Brenner DA, D'Armiento J: **Loss of MMP 13 attenuates murine hepatic injury and fibrosis during cholestasis.** *Hepatology* 2006, **44:**420-429.
52. Ruiz V, Ordonez RM, Berumen J, Ramirez R, Uhal B, Becerril C, Pardo A, Selman M: **Unbalanced collagenases/TIMP-1 expression and epithelial apoptosis in experimental lung fibrosis.** *Am J Physiol Lung Cell Mol Physiol* 2003, **285:**L1026-1036.
53. Zucker S, Hymowitz M, Conner C, DeClerck Y, Cao J: **TIMP-2 is released as an intact molecule following binding to MT1-MMP on the cell surface.** *Exp Cell Res* 2004, **293:**164-174.
54. Nguyen M, Arkell J, Jackson CJ: **Thrombin rapidly and efficiently activates gelatinase A in human microvascular endothelial cells via a mechanism independent of active MT1 matrix metalloproteinase.** *Lab Invest* 1999, **79:**467-475.
55. Zhong J, Gencay MM, Bubendorf L, Burgess JK, Parson H, Robinson BW, Tamm M, Black JL, Roth M: **ERK1/2 and p38 MAP kinase control MMP-2, MT1-MMP, and TIMP action and affect cell migration: a comparison between mesothelioma and mesothelial cells.** *J Cell Physiol* 2006, **207:**540-552.
56. Pardo A, Selman M, Kaminski N: **Approaching the degradome in idiopathic pulmonary fibrosis.** *Int J Biochem Cell Biol* 2008, **40:**1141-1155.
57. Kolb M, Bonniaud P, Galt T, Sime PJ, Kelly MM, Margetts PJ, Gauldie J: **Differences in the fibrogenic response after transfer of active transforming growth factor-beta1 gene to lungs of "fibrosis-prone" and "fibrosis-resistant" mouse strains.** *Am J Respir Cell Mol Biol* 2002, **27:**141-150.
58. Cabrera S, Gaxiola M, Arreola JL, Ramirez R, Jara P, D'Armiento J, Richards T, Selman M, Pardo A: **Overexpression of MMP9 in macrophages attenuates pulmonary fibrosis induced by bleomycin.** *Int J Biochem Cell Biol* 2007, **39:**2324-2338.
59. Lemjabbar H, Gosset P, Lechapt-Zalcman E, Franco-Montoya ML, Wallaert B, Harf A, Lafuma C: **Overexpression of alveolar macrophage gelatinase B (MMP-9) in patients with idiopathic pulmonary fibrosis: effects of steroid and immunosuppressive treatment.** *Am J Respir Cell Mol Biol* 1999, **20:**903-913.
60. Atkinson JJ, Senior RM: **Matrix metalloproteinase-9 in lung remodeling.** *Am J Respir Cell Mol Biol* 2003, **28:**12-24.
61. Legrand C, Gilles C, Zahm JM, Polette M, Buisson AC, Kaplan H, Birembaut P, Tournier JM: **Airway epithelial cell migration dynamics. MMP-9 role in cell-extracellular matrix remodeling.** *J Cell Biol* 1999, **146:**517-529.
62. Woodgett JR: **Judging a protein by more than its name: GSK-3.** *Sci STKE* 2001, **2001:**re12.
63. Grimes CA, Jope RS: **The multifaceted roles of glycogen synthase kinase 3beta in cellular signalling.** *Prog Neurobiol* 2001, **65:**391-426.
64. Hanger DP, Hughes K, Woodgett JR, Brion JP, Anderton BH: **Glycogen synthase kinase-3 induces Alzheimer's disease-like phosphorylation of tau: generation of paired helical filament epitopes and neuronal localisation of the kinase.** *Neurosci Lett* 1992, **147:**58-62.
65. Stambolic V, Ruel L, Woodgett JR: **Lithium inhibits glycogen synthase kinase-3 activity and mimics wingless signalling in intact cells.** *Curr Biol* 1996, **6:**1664-1668.
66. Eldar-Finkelman H, Martinez A: **GSK-3 Inhibitors: Preclinical and Clinical Focus on CNS.** *Front Mol Neurosci* 2011, **4:**32.

67. Linding R, Jensen LJ, Ostheimer GJ, van Vugt MA, Jorgensen C, Miron IM, Diella F, Colwill K, Taylor L, Elder K, Metalnikov P, Nguyen V, Pasculescu A, Jin J, Park JG, Samson LD, Woodgett JR, Russell RB, Bork P, Yaffe MB, Pawson T: **Systematic discovery of in vivo phosphorylation networks.** *Cell* 2007, **129:**1415-1426.
68. Farghaian H, Turnley AM, Sutherland C, Cole AR: **Bioinformatic prediction and confirmation of beta-adducin as a novel substrate of glycogen synthase kinase 3.** *J Biol Chem* 2011, **286:**25274-25283.
69. Jope RS, Johnson GV: **The glamour and gloom of glycogen synthase kinase-3.** *Trends Biochem Sci* 2004, **29:**95-102.
70. Stamos JL, Chu ML, Enos MD, Shah N, Weis WI: **Structural basis of GSK-3 inhibition by N-terminal phosphorylation and by the Wnt receptor LRP6.** *Elife* 2014, **3:**e01998.
71. Beurel E, Grieco SF, Jope RS: **Glycogen synthase kinase-3 (GSK-3): regulation, actions, and diseases.** *Pharmacol Ther* 2015, **148:**114-131.
72. Frame S, Cohen P: **GSK-3 takes centre stage more than 20 years after its discovery.** *Biochem J* 2001, **359:**1-16.
73. Suzuki T, Bridges D, Nakada D, Skiniotis G, Morrison SJ, Lin JD, Saltiel AR, Inoki K: **Inhibition of AMPK catabolic action by GSK-3.** *Mol Cell* 2013, **50:**407-419.
74. Kandasamy AD, Schulz R: **Glycogen synthase kinase-3beta is activated by matrix metalloproteinase-2 mediated proteolysis in cardiomyoblasts.** *Cardiovasc Res* 2009, **83:**698-706.
75. Ougolkov AV, Bone ND, Fernandez-Zapico ME, Kay NE, Billadeau DD: **Inhibition of glycogen synthase kinase-3 activity leads to epigenetic silencing of nuclear factor kappaB target genes and induction of apoptosis in chronic lymphocytic leukemia B cells.** *Blood* 2007, **110:**735-742.
76. Kaidanovich-Beilin O, Woodgett JR: **GSK-3: Functional Insights from Cell Biology and Animal Models.** *Front Mol Neurosci* 2011, **4:**40.
77. Beurel E, Yeh WI, Michalek SM, Harrington LE, Jope RS: **Glycogen synthase kinase-3 is an early determinant in the differentiation of pathogenic Th17 cells.** *J Immunol* 2011, **186:**1391-1398.
78. Lo Monte F, Kramer T, Gu J, Anumala UR, Marinelli L, La Pietra V, Novellino E, Franco B, Demedts D, Van Leuven F, Fuertes A, Dominguez JM, Plotkin B, Eldar-Finkelman H, Schmidt B: **Identification of glycogen synthase kinase-3 inhibitors with a selective sting for glycogen synthase kinase-3alpha.** *J Med Chem* 2012, **55:**4407-4424.
79. King MK, Pardo M, Cheng Y, Downey K, Jope RS, Beurel E: **Glycogen synthase kinase-3 inhibitors: Rescuers of cognitive impairments.** *Pharmacol Ther* 2014, **141:**1-12.
80. Forlenza OV, de Paula VJ, Machado-Vieira R, Diniz BS, Gattaz WF: **Does lithium prevent Alzheimer's disease?** *Drugs Aging* 2012, **29:**335-342.
81. Jope RS, Yuskaitis CJ, Beurel E: **Glycogen synthase kinase-3 (GSK-3): inflammation, diseases, and therapeutics.** *Neurochem Res* 2007, **32:**577-595.
82. Martin M, Rehani K, Jope RS, Michalek SM: **Toll-like receptor-mediated cytokine production is differentially regulated by glycogen synthase kinase 3.** *Nat Immunol* 2005, **6:**777-784.
83. Vincent EE, Elder DJ, O'Flaherty L, Pardo OE, Dzien P, Phillips L, Morgan C, Pawade J, May MT, Sohail M, Hetzel MR, Seckl MJ, Tavare JM: **Glycogen synthase kinase 3 protein kinase activity is frequently elevated in human non-small cell lung carcinoma and supports tumour cell proliferation.** *PLoS One* 2014, **9:**e114725.
84. Cheng H, Woodgett J, Maamari M, Force T: **Targeting GSK-3 family members in the heart: a very sharp double-edged sword.** *J Mol Cell Cardiol* 2011, **51:**607-613.
85. Meijer L, Flajolet M, Greengard P: **Pharmacological inhibitors of glycogen synthase kinase 3.** *Trends Pharmacol Sci* 2004, **25:**471-480.

86. Coghlan MP, Culbert AA, Cross DA, Corcoran SL, Yates JW, Pearce NJ, Rausch OL, Murphy GJ, Carter PS, Roxbee Cox L, Mills D, Brown MJ, Haigh D, Ward RW, Smith DG, Murray KJ, Reith AD, Holder JC: **Selective small molecule inhibitors of glycogen synthase kinase-3 modulate glycogen metabolism and gene transcription.** *Chem Biol* 2000, **7:**793-803.
87. Caraci F, Gili E, Calafiore M, Failla M, La Rosa C, Crimi N, Sortino MA, Nicoletti F, Copani A, Vancheri C: **TGF-beta1 targets the GSK-3beta/beta-catenin pathway via ERK activation in the transition of human lung fibroblasts into myofibroblasts.** *Pharmacol Res* 2008, **57:**274-282.
88. Baarsma HA, Engelbertink LH, van Hees LJ, Menzen MH, Meurs H, Timens W, Postma DS, Kerstjens HA, Gosens R: **Glycogen synthase kinase-3 (GSK-3) regulates TGF-beta(1)-induced differentiation of pulmonary fibroblasts.** *Br J Pharmacol* 2013, **169:**590-603.
89. Kim EY, Kim A, Kim SK, Kim HJ, Chang J, Ahn CM, Chang YS: **Inhibition of mTORC1 induces loss of E-cadherin through AKT/GSK-3beta signalling-mediated upregulation of E-cadherin repressor complexes in non-small cell lung cancer cells.** *Respir Res* 2014, **15:**26.
90. Gurrieri C, Piazza F, Gnoato M, Montini B, Biasutto L, Gattazzo C, Brunetta E, Cabrelle A, Cinetto F, Niero R, Facco M, Garbisa S, Calabrese F, Semenzato G, Agostini C: **3-(2,4-dichlorophenyl)-4-(1-methyl-1H-indol-3-yl)-1H-pyrrole-2,5-dione (SB216763), a glycogen synthase kinase-3 inhibitor, displays therapeutic properties in a mouse model of pulmonary inflammation and fibrosis.** *J Pharmacol Exp Ther* 2010, **332:**785-794.
91. Moeller A, Ask K, Warburton D, Gauldie J, Kolb M: **The bleomycin animal model: a useful tool to investigate treatment options for idiopathic pulmonary fibrosis?** *Int J Biochem Cell Biol* 2008, **40:**362-382.
92. Moore BB, Hogaboam CM: **Murine models of pulmonary fibrosis.** *Am J Physiol Lung Cell Mol Physiol* 2008, **294:**L152-160.
93. Scotton CJ, Chambers RC: **Bleomycin revisited: towards a more representative model of IPF?** *Am J Physiol Lung Cell Mol Physiol* 2010, **299:**L439-441.
94. Scotton CJ, Hayes B, Alexander R, Datta A, Forty EJ, Mercer PF, Blanchard A, Chambers RC: **Ex vivo micro-computed tomography analysis of bleomycin-induced lung fibrosis for preclinical drug evaluation.** *Eur Respir J* 2013, **42:**1633-1645.
95. Umezawa H, Maeda K, Takeuchi T, Okami Y: **New antibiotics, bleomycin A and B.** *J Antibiot (Tokyo)* 1966, **19:**200-209.
96. Razonable RR, Henault M, Paya CV: **Stimulation of toll-like receptor 2 with bleomycin results in cellular activation and secretion of pro-inflammatory cytokines and chemokines.** *Toxicol Appl Pharmacol* 2006, **210:**181-189.
97. Dunsmore SE, Shapiro SD: **The bone marrow leaves its scar: new concepts in pulmonary fibrosis.** *J Clin Invest* 2004, **113:**180-182.
98. Smith DG, Buffet M, Fenwick AE, Haigh D, Ife RJ, Saunders M, Slingsby BP, Stacey R, Ward RW: **3-Anilino-4-arylmaleimides: potent and selective inhibitors of glycogen synthase kinase-3 (GSK-3).** *Bioorg Med Chem Lett* 2001, **11:**635-639.
99. Baarsma HA, Bos S, Meurs H, Visser KH, Smit M, Schols AM, Langen RC, Kerstjens HA, Gosens R: **Pharmacological inhibition of GSK-3 in a guinea pig model of LPS-induced pulmonary inflammation: I. Effects on lung remodeling and pathology.** *Respir Res* 2013, **14:**113.
100. Parker MW, Rossi D, Peterson M, Smith K, Sikstrom K, White ES, Connett JE, Henke CA, Larsson O, Bitterman PB: **Fibrotic extracellular matrix activates a profibrotic positive feedback loop.** *J Clin Invest* 2014, **124:**1622-1635.

101. Garcia-Alvarez J, Ramirez R, Checa M, Nuttall RK, Sampieri CL, Edwards DR, Selman M, Pardo A: **Tissue inhibitor of metalloproteinase-3 is up-regulated by transforming growth factor-beta1 in vitro and expressed in fibroblastic foci in vivo in idiopathic pulmonary fibrosis.** *Exp Lung Res* 2006, **32:**201-214.
102. Corbel M, Caulet-Maugendre S, Germain N, Molet S, Lagente V, Boichot E: **Inhibition of bleomycin-induced pulmonary fibrosis in mice by the matrix metalloproteinase inhibitor batimastat.** *J Pathol* 2001, **193:**538-545.
103. Manoury B, Nenan S, Guenon I, Lagente V, Boichot E: **Influence of early neutrophil depletion on MMPs/TIMP-1 balance in bleomycin-induced lung fibrosis.** *Int Immunopharmacol* 2007, **7:**900-911.
104. Wang H, Wang HS, Zhou BH, Li CL, Zhang F, Wang XF, Zhang G, Bu XZ, Cai SH, Du J: **Epithelial-mesenchymal transition (EMT) induced by TNF-alpha requires AKT/GSK-3beta-mediated stabilization of snail in colorectal cancer.** *PLoS One*, **8:**e56664.
105. Doble BW, Woodgett JR: **Role of glycogen synthase kinase-3 in cell fate and epithelial-mesenchymal transitions.** *Cells Tissues Organs* 2007, **185:**73-84.
106. Stahl M, Schupp J, Jager B, Schmid M, Zissel G, Muller-Quernheim J, Prasse A: **Lung collagens perpetuate pulmonary fibrosis via CD204 and M2 macrophage activation.** *PLoS One* 2013, **8:**e81382.
107. Garcia-de-Alba C, Becerril C, Ruiz V, Gonzalez Y, Reyes S, Garcia-Alvarez J, Selman M, Pardo A: **Expression of matrix metalloproteases by fibrocytes: possible role in migration and homing.** *Am J Respir Crit Care Med* 2010, **182:**1144-1152.